NASA TECHNICAL MEMORANDUM NASA TM-77498

ELECTRONIC STRUCTURE AND PROPERTIES OF MAGNETIC DEFECTS IN $Co_{(1+x)}Al_{(1-x)}$ AND $Fe_{(1+x)}Al_{(1-x)}$ ALLOYS

D. Abbé

Translation of "Structure électronique et propriétés des défaults magnétiques des alliages $Co_{1+x}Al_{1-x}$ et $Fe_{1+x}Al_{1-x}$", Office National d'Etudes et de Recherches Aérospatiales, Paris (France), ONERA-NT-1976-5 (PhD Thesis, University of Paris), July 1976, pp. 1-73.

NATIONAL AERONAUTICS AND SPACE ADMINISTRATION
WASHINGTON, D.C. 20546 JULY 1984

STANDARD TITLE PAGE

1. Report No. NASA TM-77498	2. Government Accession No.	3. Recipient's Catalog No.
4. Title and Subtitle ELECTRONIC STRUCTURE AND PROPERTIES OF MAGNETIC DEFECTS IN $CO_{(1+x)}$ $AL_{(1-x)}$ AND $(Fe_{1+x})AL_{(1-x)}$ ALLOYS		5. Report Date JULY 1984 6. Performing Organization Code
7. Author(s) D. Abbé, University of Paris, France		8. Performing Organization Report No. 10. Work Unit No.
9. Performing Organization Name and Address Leo Kanner Associates, Redwood City, California 94063		11. Contract or Grant No. NASw-3541 13. Type of Report and Period Covered Translation
12. Sponsoring Agency Name and Address National Aeronautics and Space Administration, Washington, D.C. 20546		14. Sponsoring Agency Code

15. Supplementary Notes

Translation of "Structure électronique et propriétés des défauts magnétiques des alliages Co_{1+x} Al_{1-x} et Fe_{1+x} Al_{1-x}", Office National d'Etudes et de Recherches Aerospatiales, Paris (France), ONERA-NT-1976-5 (PhD Thesis, University of Paris), July 1976, pp. 1-73 (N77-21977)

16. Abstract

The study of CoAl and FeAl compounds has been developed along two directions. It is shown that results on magnetic susceptibility and specific heat at low temperature on (NiCo) Al and (CoFe)Al ternary alloys are in good agreement with band calculations obtained by various authors. Results on magnetization and specific heat under field at low temperature on non-stoichiometric compounds show clearly the importance of the nearest neighbor effects. In the case of CoAl, the isolated cobalt atoms substituting aluminum are characterized by a Kondo behavior, and, for FeAl, the isolated extra iron atoms are magnetic and polarize the matrix. Moreover, for the two compounds, clusters of higher order play a considerable part in the magnetic properties for CoAl, these clusters also seem to be characterized by a Kondo behavior, for FeAl, these clusters whose moment is higher than in the case of isolated atoms, could be constituted of excess parts of iron atoms.

17. Key Words (Selected by Author(s))	18. Distribution Statement
	Unlimited-Unclassified

19. Security Classif. (of this report)	20. Security Classif. (of this page)	21. No. of Pages	22.
Unclassified	Unclassified	91	

TABLE OF CONTENTS

ELECTRONIC STRUCTURE AND PROPERTIES OF MAGNETIC DEFECTS IN $CO_{(1+x)}$ $AL_{(1-x)}$ AND $FE_{(1+x)}$ $Al_{(1-x)}$ ALLOYS

Daniel Abbé
University of Paris

Summary

/2*

The study of CoAl and FeAl compounds has been developed along two directions:
-on the one hand, it is shown that results on magnetic susceptibility and specific heat at low temperature on (NiCo)Al and (CoFe)Al ternary alloys are in good agreement with band calculations obtained by various authors;
-on the other hand, our results on magnetization and specific heat under field at low temperature on non-stoichiometric compounds show clearly the importance of the nearest neighbor effects. In case of CoAl, the isolated cobalt atoms substituted to aluminum are characterized by a Kondo behavior ($T_k \simeq 1.7$ K) and for FeAl, the isolated extra iron atoms are magnetic andpolarize the matrix. Moreover, for the two compounds, clusters of higher order play a considerable part in the magnetic properties: for CoAl, these clusters also seem to be characterized by a Kondo behavior ($T_k \simeq 0.1$ K); for FeAl, these clusters, whose moment is higher than in the case of isolated atoms, could be constituted of excess pairs of iron atoms.

Introduction

/3

CoAl and FeAl are ordered isomorphic compounds of simple cubic structure of type B_2 isotypes of CsCL, miscible in any proportions. These compounds have largely been studied within the last few years, the interest which they have aroused resulting principally from their behavior on the plane of magnetic properties. These are indeed nonmagnetic when they are stoichiometric. Very strong magnetic susceptibilities ($\simeq 10^{-4}$ uem/mole) are on the same order as for transition metals. When we substitute extra transition atoms for aluminum atoms, recent experiments demonstrate that these atoms surrounded by nearest neighbors of the same nature are carriers of a moment, and that moreover they polarize their immediate surroundings. The study of magnetic properties of extra atoms is thus of the same nature as the study of an impurity in a transition metal.

This work presents a study of these standardized compounds which was developed following two directions:
-study of the properties connected to the structure of bands of stoichiometric compounds;

*Numbers in the margin indicate pagination in the foreign text.

-study of the properties conncected to the magnetic behavior of the extra transition atoms.

In both cases, our contribution includes measurements of specific heat at low temperature supported by measurements of magnetization.

The experimental studies conducted on these compounds demonstrates the quasi-permenent presence of defects of crystallographic structure which, as we are going to see, have considerable significance on the physical properties. It is, from this fact, very difficult to have precise data on the structure of bands. Nevertheless, analysis of the specific heat and magnetic susceptibility results allow us to provide some data. Our study on ternary alloys $Ni_{1-x}Co_xAl$ and $Fe_{1-x}Co_xAl$ demonstrate that the results obtained for such a method are well expalined from the structure of bands of TRAl compounds (TR=Ni, Co, Fe) calculated by Connoly-Johnson [1] and Moruzzi-Williams-Janak [2].

The pinpoint defects which occur in these compounds are either from transition atoms by substitution on the aluminum sub-lattice or from transition gaps. The presence of such defects has been clearly demonstrated experimentally by joint measurements of lattice and density parameters [3] and [4]. The existence of these defects can result in intrinsic disordering, which primarily depends on the thermal history of the sample, either from discrepancies in stoichiometry or from both at once. The magnetic characteristics of extra transition atoms are explained by the effects of local surroundings: the electronic sturcture at the level of a specific atom depends primarily on the nature of its nearest neighbors, which principally is made to occur from interactions at short distance between atoms. For the CoAl alloy, we have clearly demonstrated Kondo type behavior for the extra isolated cobalt atoms. Our measurements have demonstrated moreover the particular behavior of higher order clusters, certain of which at least appear to also have Kondo behavior. For FeAl alloys, the results are simpler: our measurements demonstrate the establishment of gigantic moments around the iron atoms isolated by substitution. Analysis of our experimental results for this alloy do not exclude the presence of higher order clusters, but the precision of our measurements do not allow us to characterize them very precisely.

Chapter 1 /4

Experimental Techniques

In order to accomplish this work, we have used two techniques: calorimetry at low temperature with and without field, and measurements of magnetization with weak and strong field. We will stress most particularly in this section the installation for magnetization in strong field which we have constructed. The other devices will be described more concisely.

I.1. Calorimetry At Low Temperature Without Field

For our measurements, we have used a calorimeter which covers a range of temperatures going from approximately 1.5°K to 18°K. This apparatus can receive samples of several cm^3 in order to obtain good precision on the measurements. We give in this section its description and the calibration method.

I.1.A. Description (figure 1)

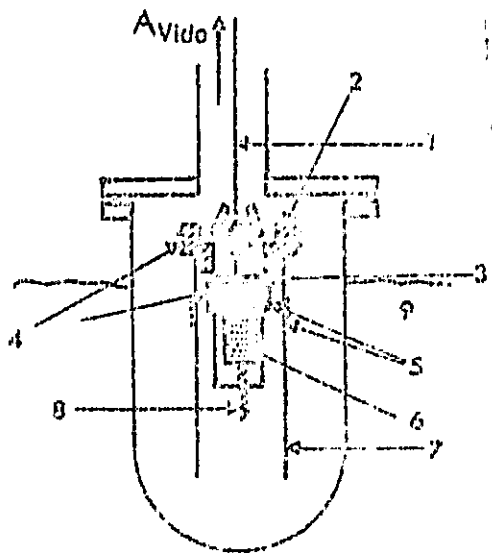

Figure 1. Diagram of principle of calorimetry with field.

1-Mechanical contact; 2-Support screen; 3-Ge probe; 4-Thermocouple; 5-Heating resistors; 6-Sample; 7-Screen; 8-Screw; 9-Liquid helium.

Key: A -Vacuum

It concerns an adiabatic calorimeter. The thermically isolated sample is cooled beforehand to the temperature of the helium bath through the intermediary of a mechanical contact. We measure the increase of temperature (approximately 0.1°K) which produces a localized energy flux with time.

The sample, thermometer, and heating device are interconnected with a copper sample-holder. The sample is placed in thermal contact with the sample-holder through the intermediary of a molybdenum screw of low specific heat. This arrangement allows good reproducibility /5
of the calorific capacity of these accessories which it will be necessary to measure in order to obtain the specific heat of the sample.

The essential points for good functionning of the apparatus are thus: thermal isolation, measurement of the temperature and energy flux.

a) Thermal Isolation

The perturbation of heat fluxes on the sample correspond to ...

three types of processes: α) gaseous convection and conduction, β) radiation, and γ) solid conduction. It is thus a question of minimizing them or compensating for them.

α) Gaseous Convection and Conduction

In order to overcome gaseous convection, it suffices to arrange in a chamber whose water-tightness is very accurately ensured for the portion submerged in the helium bath-the loss from leakage increases very notably when the helium becomes superfluid. This chamber is evacuated by an auxiliary pump equipped with a liquid nitrogen trap, which allows us to attain a vacuum of approximately 10^{-6} when the calorimeter is at ambient temperature.

β) Radiation

In the realm of temperature explored, transfers by radiation between the sample and its close surroundings are low. Only actually of importance are the fluxes originating from the portions at higher temperatures or close to ambient. The calorimeter is equipped to this end with a radiation trap which intercepts the flux originating from the draining by pumping of the chamber.

γ) Conduction

We will distinguish the transfers which are produced with the heated portions from those which are produced with the cooled portions. Indeed, for these last, the thermal flux which depends on the temperature of the sample produces different drifts before and after heating. This effect thus affects the precision of the extrapolations. In order to minimize the conduction originating from heated portions, the measurement wires which descend the length of the draining by pumping are coiled on copper rods interconnected with the radiation trap.

The measurement wires are then wound on a thermal mass whose temperature is controlled in a fashion to maintain it at a value very slightly lower than that of the sample, which allows us to compensate for the effects which could lead to heating of this. In order to detect the deviation in temperature, we use a Ag-AuFe differential thermocouple (sensitivity: $5\mu V/°K$). A low noise amplifier ($0.01\ \mu V$) allows us to obtain a signal of sufficient level in order to be used by a regulation cable; this last sends a current into a winding arranged on the thermal mass.

It is possible, by slightly lowering the temperature of the thermal mass in relation to that of the sample, to compensate the residual effects of conduction by measurement wires whose end is at ambient temperature.

It is possible to adapt, on the thermal mass, a thermal screen which even reduces transfers by convection or radiation between the sample and chamber, which is at the temperature of the bath.

b) Measurement of Temperature

If we seek a precision greater than 10^{-2} on the measurements of specific heat, it is necessary to be able to measure the increase of temperature ($\simeq 0.1°K$ associated with the heat flux with the same precision, a precision of approximately $3 \cdot 10^{-4}°K$ on the measurement of temperature. The method used is determination of the resistance of a germanium probe attached on the sample-holder. Germanium has been preferred to carbon because it is insensitive to thermal cycling between the temperature of helium and ambient temperature. Calibration of the probe is thus made once for all of them. This calibration, if it must be made by direct methods (determination of vapor pressures of helium, or gas thermometer) was very delicate at the level of precision sought: it is necessary that the relative error on the temperature be less than $0.5 \cdot 10^{-2}$. The resistance of the probe is measured by a standard potentiometric method (measurement of the pressure of the limits of the probe, and at the limits of a sample resistor mounted in series). These measurements are made at a relatively low level on a Hewlett-Packard digital voltmeter (precision: 2 μV) in a fashion to reduce the current which travels through the thermometer (beyond a certain level the dispersions produce a difference of temperature between the probe and sample). /6

c) Production and Measurement of the Heating Flux

The heating winding, in constantan wire, is coiled on the sample holder. It is fed by a continuous 4V source. A resistor arranged in series allows us to vary the current and a 100 Ω shunt ensures the measurement of it. The measurement of pressure is ensured by two wires connected to the end of the winding. The flux dissipated is thus determined as the product of the current by the pressure and by the heating time.

d) Cooling

Cooling is carried out in two stages. On the one hand, cooling with liquid nitrogen, then after having expelled the nitrogen, cooling with helium. In order to bring the sample to the desired temperature, we temporarily disrupt its thermal isolation by forming the mechanical contact connecting the sample to the thermal mass. This is permanently connected to the pieces in contact with the bath by a braid and three colonnettes constituted by stainless steel tubes of low thickness.

I.1.B. Calibration

Calibration of the thermometer is very delicate to accomplish for the installations of measurement of specific heat. Indeed, in order to commit a relative error less than 10^{-2} on the measurement of specific heat, it is necessary that the calibration error committed on the temperature did not vary more than $0.5 \cdot 10^{-3}$°K between two temperatures separated by 0.1°K (deviation of temperature associated with the heating time) and that the relative error on the absolute temperature is lower than $0.5 \cdot 10^{-2}$°K. in order to obtain this realm of precision, the simplest method consists of using as calibration measurement the measurement of specific heat of a sample which is very well known. Calibration has been based principally on nickel which possesses a high specific heat, which improves the reproducibility. For this substance, the most precise and most recent experimental data published to date are those of Dixon et al. [5] reinterpreted by Bower et al. [6] and which lead to a specific heat of the type:

$$C=\gamma T+\beta T^3+\alpha T^{3/2}$$

$$\alpha=0.029 \text{ mJ/K}^{5/2}\text{mole}$$
$$\beta=0.01848 \text{ mJ/K}^4\text{mole}$$
$$\gamma=7.024 \text{ mJ/K}^2\text{mole}$$

Unfortunatley, Dixon et al. limited themselves to temperatures included between 1.2 and 4.2°K, while nickel can not furnish us with calibration in the higher range of temperature (4.2-18°K). Another calibration was necessary for these temperatures: we are making use of the copper sample of the 1965 calorimetry conference [7].

These calibrations allow us to determine a function of thermometric error $\varphi(\theta)$ where Θ is the measured temperature, and to thus go up to the true specific heat $C(\theta)$ for the temperature θ through the expression:

$$C_{measured}(\theta)=C(\theta)[1+\varphi(\theta)]$$

I.2. Calorimetry Under Magnetic Field

A supplementary study by calorimetry under field was necessary for certain of our alloys. We have used a calorimeter designed to function with a supercoating coil furnishing magnetic fields attaining 65 kOe. The solutions to the problems which are posed by the perfecting of this apparatus are identical (with some close variations to which we will return) to those of the calorimeter previously described. Other problems specific to the apparatus will be developed in this paragraph: the self-sufficiency of the coil, the problem of bulkiness connected to the low diameter of the coil, the magnetoresistance of the thermometers and the extraneous electromotive forces induced within the circuits of measurement of vibration within the field of the coil. /7

α) Problem of Self-Sufficiency in Helium of the Coil

We have at first a compromise to make for the dimensions of the current leads of the coil. If their cross-section is too low, they casue evaporation of the helium bath by Joule effect in the opposite case, this by solid conduction since the surroundings reheat the bath. However, the measurement at temperatures lower than 4.2°K which, before the manipulation, require a preliminary pumping time and placement of the sample in thermal equilibrium, must be carried out in a simple phase, since new siphoning would produce resumption of these operations. We have been induced to adopt the arrangement represented in figure 2: the calorimeter is cooled by conduction, by a small interior bath, with extremely reduced consumption since all the walls which surround it are thermalized by the helium bath of the coil. The measurement wires cross the interior bath, which eliminates the problems of conduction from the surroundings.

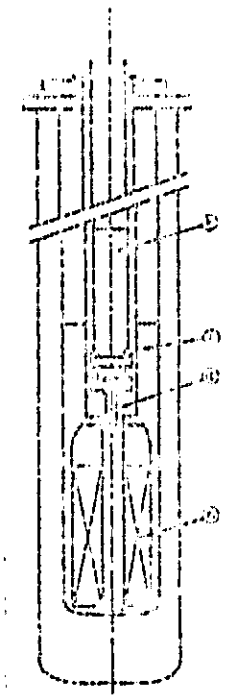

Figure 2. Diagram of the calorimeter under field.

a-superconducting coil;b-interior bath;c-exterior bath (coil);d-laboratory chamber.

β) Bulkiness

Since we have investigated high fields with this apparatus, which leads to reduced useful spaces (interior diamter of the coil equal to 40 mm), we have omitted the screen, by compensating for radiation and gaseous conduction originating from cooled portions through modification of the discrepancy of temperature between the sample and the thermal mass of the screen. This last continues to exist, and its temperature is reduced to that of the sample as we described in I.1A (γ).

γ) Perturbation of Measurements by the Field

We have had to take into account displacement of the measurement wires, particularly those of the thermocouple, screen regulation, and thermometers, in the field of the coil. These displacements would induce extraneous electromotive forces which we could reduce by suspending the calorimeter by flexible connections and by adopting a stretched out arrangement for the sample-holder. Despite these precautions, there continued to exist unacceptable noise levels on the screen regulation. We have been able to reduce them by twisting the thermocouple and filtering the signal before amplification.

Analogous effects occur within the thermometric circuits connected to ambient noises of the laboratory. It has been possible to neutralize them by selecting a sufficiently low operating frequency (20 Hz) for the detector of the measurement bridge of temperature which in this apparatus functions in altaernating current. /8

δ) Calibration

The effects of magnetoresistance under 55 kOe attained for germanium have the value at 1.2 K: $\left(\frac{\Delta R}{R}\simeq 200\%\right)$ [8]. This effect is not reproducible since it depends on the relative orientation of the pick-up and the field. We have thus preferred carbon thermometers (Allen-Bradley resistors) which are clearly less sensitive $\left(\frac{\Delta R}{R}\simeq 10\%\right.$ with the same conditions) [9]. However, for these thermometers, which are sensitive to thermal cycling between the surroundings and low temperatures, it is necessary to proceed with calibration after each cooling. Fortunately, these thermometers not being sensitive to thermal cyclings at low temperature, we have used the following procedure:

1) Calibrations carried out on the sample of known specific heat, independent of the magnetic field, have the function of determining on the one hand the calibration errors in zero field of the germanium thermometer (same procedure as for the previously described calorimeter), and on the other hand, the value as a function of the field and the temperature of the coefficient of magnetoresistance of the carbon thermometer. The standard which we have selected is zirconium [10]: this non-magnetic material is currently manufactured for the needs of the nuclear industry with a very good level of purity and offers a very high electronic specific heat ($\gamma=2.8$ mJ/K^2 mole; $\beta=7.88$ mJ/K^4 mole).

2) At the start of each experiment, the two thermometers are compared during the measurement of specific heat in zero field. The experiments under field are made with the assistance of the carbon thermometer, by making use of the values of the coefficient of magnetoresistance obtained from calibration measurements which we assume are reproducible.

I.3. Measurements of Magnetization

Measurements of magnetization as a function of temperature have been carried out with the assistance of two types of apparatus; the first uses medium fields (H<10 kOe), the second allows us to carry out measurements under very intense fields (H≈55 kOe).

I.3.A. Apparatus for Measurements Using Fields Lower than 10 kOe [11]

This apparatus allows us to maeasure magnetizations by the Curie-Faraday method, for fields lower than 10 kOe and for a range of temperature included between 2 and 300°K. We use a Varian electro-magnet, whose polar pieces have been cut in fashion so that the square gradient of the field $(2H\frac{dH}{dz})$ is constant with a volume on the order of 1 cm^3. It is thus not possible to vary independently H and $\frac{dH}{dz}$. We verify, by displacing a sample following Oz, that the force is constant over approximately 2 cm for a separation of polar pieces of 36±2 mm (figure 3). The characteristics of $H\frac{dH}{dz}$ are given on the same figure.

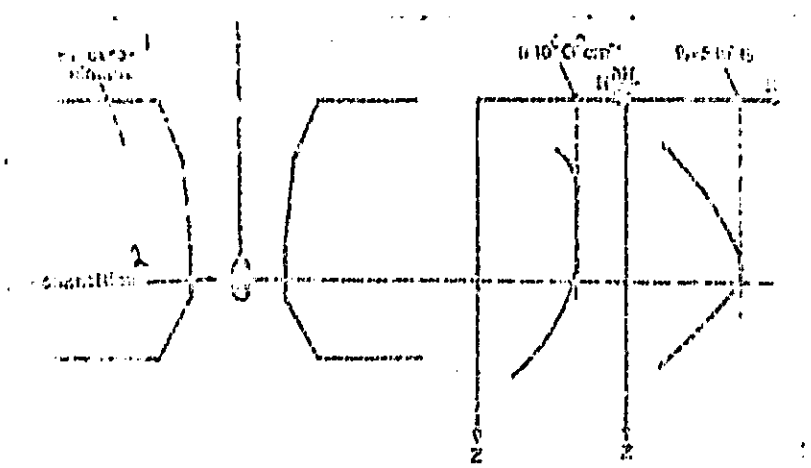

Figure 3. Variation of $H\frac{dH}{dz}$ with the side z.

Key: 1-Electromagnet;2-Sample.

The force sustained by the sample is measured with the assistance of an electronic microbalance (Sartorius type) which allows us to measure under vacuum variations of weight of 1 microgram with a maxiumu load of 2 g. The functional principle of this balance is the following: the beam is interconnected with a coil B_1 placed in the clearance of a permanent magnetization. Two coils B_2 and B_3

very close to B_1 and run through by a high frequency current served by detectors of imbalance, this being translated by a variation of impedance. This signal is transmitted to an electronic assembly which sends the current I into B_1, inducing an intense torque and reestablishing the balance. The current I is proportional to the force inducing the imbalance. We can then directly read the apparent weight of the sample on an amperemeter graduated in μg. This is summarized by block diagram 4.

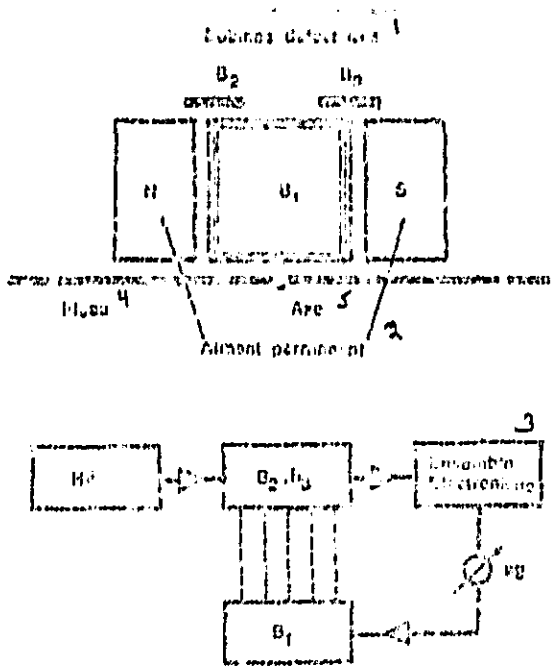

Figure 4. Diagram of the balance.

Key: 1-Detector coils;2-Permanent magnet;3-Electronic assembly;4-Beam;5-Axis.

The cryostat (helium-nitrogen) used is a whetstone cryostat (figure 5), the volume of liquid nitrogen in the whetsone has been replaced by a copper screen. Finally a regulation cable serves to obtain the intermediate temperatures between the fixed points (liquid helium: 4.2°K; liquid nitrogen: 77°K, and ambient temperature). This regulation is obtained by heating of a constantan winding ($R \simeq 1$ KΩ). The power dispensed is reduced to the temperature reading through the intermediary of a cable including a MECI recorder and a proportional-integral-differential servo-control. /10

This apparatus, being easy to use and having a low consumption of cryogenic liquids has allowed us to rapidly accomplish the measurements for T>20°K, and the preliminary stages of the measurements for T<20°K.

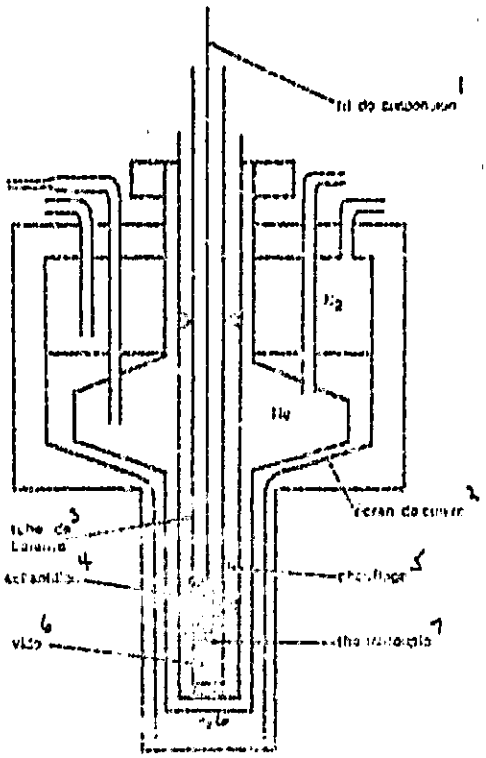

Figure 5. Diagram of the cryostat of the apparatus in weak field.

Key: 1-Suspension wire;2-Copper screen;3-Balance tube;4-Sample;5-Heating;6-Vacuum;7-Thermocouple.

I.3.B. Apparatus for Magnetization Measurements Under Fields H<55 kOe

This apparatus allows us to measure magnetization by the Curie-Faraday method for fields furnished by a superconducting coil going up to 55 kOe and from temperatures included between 1.6 and 20°K. In this paragraph, we first describe the characteristics of coils producing the field and the field gradient, then we give a technical description of the apparatus and its different accessories (balance, cryostats, temperature regulation device, ...) and finally, we end with the different calibrations.

a) Superconducting Coil

In contrast to the apparatus in weak field, the magnetic field and the field gradient are furnished here by independent coils. This arrangement allows us in particular to preserve sufficient sensitivity in the measurements with weak field.

The assembly of superconductor elements has been designed in a fasihion to occupy a reduced volume in order to have, on the one hand, low consumption of cryogenic liquids, and on the other hand, a suspension wire for the sample of reasonable length (≃125 mm). The windings have been constructed with a $Nb_{0.6}Ti_{0.4}$ multistrand superconductor wire (ϕ=0.375 mm).

α) Limitations

It is to be feared that the coil does not relay during the manipulation, that is to say that it is no longer superconducting. This phenomenon can lead to complete destruction of the coil if at one point the superconductor substance returns to normal. It then produces local overheating, which propagates itself step by step, the assembly of the coil transits into an avalanche pehnomenon, and the totality of accumulated energy (approximately 3KJ) is dissipated in a very short time, producing immediate deterioration of the coil if no safety device is provided.

This change of state can be due either to an increase of temperature, as we are going to see, or to modification of the magnetic field. Indeed, a sufficiently strong magnetic field has the effect of destroying the superconductivity. The threshold, or critical value, of the magnetic field is a function of the temperature. At the critical temperature, the critical field is zero. The variation of the critical field as a function of temperature is represented in figure 6 for several superconductor elements [12]. These threshold curves separate the superconductor state, at lower left, from the normal state (at upper right). We will give in paragraph δ the calculation of the critical intensity connected to the critical field.

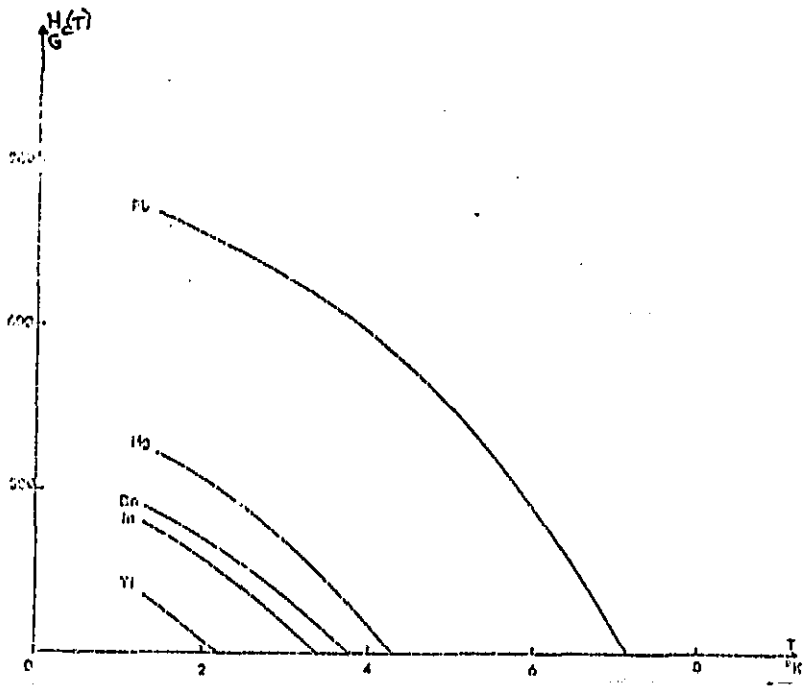

/11

Figure 6. Curves of threshold of critical field.

Other parameters can lead to relay of the coil, particularly electrodynamic stresses. Unddr the influence of these stresses, the spirals can displace individually in a fashion to minimize the electromagentic energy of the system. The excess of energy in relation to the initial situation induces local elevation of temperature which leads to change of state of the material.

β) Technical Characteristics

The geometry of the coil of principal field must create a magnetic field such that the center of the coil is in a position of stable equilibrium for a paramagnetic sample (If indeed the sample came to press against the walls of the coil, friction forces would render measurements impossible). For these we use a coil composed of two half-coils and separated by a distance e (figure 7). The field then offers a minimum along the axis of the coil to the central point, thus a maximum radially (the buckling being zero: appendix 2) (figure 8) [The calculations of H have been carried out on the computer following standard methods (H. Zijlstra: "Measurements of magnetic quantities", Wiley-New York). These calculations and the plan of the coil have been furnished to us by the Electronic Structure of Solids Laboratory of the University of Strasbourg].

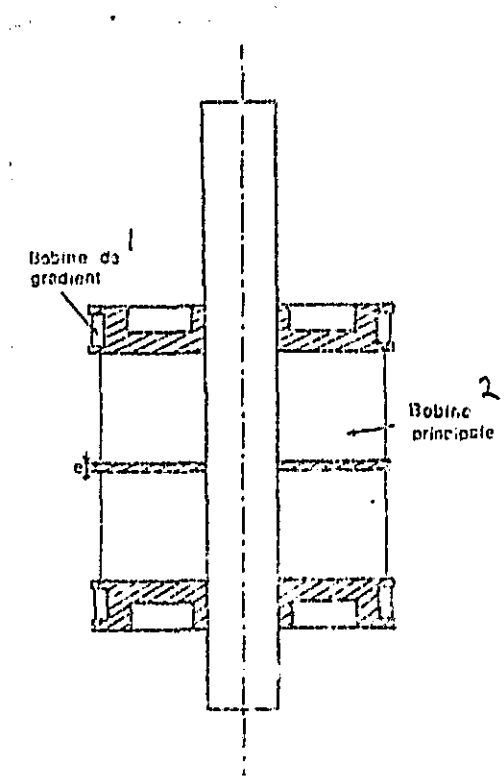

Figure 7. Diagram of the superconducting coil.

Key: 1-Gradient coil; 2-Principal coil.

Great regularity in the winding is required in order to ensure that the field gradient only provides gradient coils and not a defect of construction of the principal coil.

Moreover, we have been devoted to constructing a coil having the greatest compactness possible in order to avoid that it does not relay at the time of placement under pressure, the spirals being able to displace themselves under the influence of electrodynamic stresses. This regularity is indispensable if we want to obtain intense fields.

Although, we have retained a safety margin of approximately 20% on the maximum intensity of the field coil, we have introduced a system designed to protect the coil from effects of possible relays. For this, the two half-coils have been enclosed in a Wheatsone bridge, as well as two 100 Ω resistors. Once the pressure at the boundaries of one or another arm of the bridge, constituted by an assembly: half-coil 100 Ω resistor, exceeds 5 mV, an electronic system cuts the supply to the field coil. This system includes a pressure amplifier which actuates the relays cutting the supply to the coil once a relay effect is detected. The energy of the coil is released into a discharge resistor placed in parallel with the coil (diagram 9). /13

/12

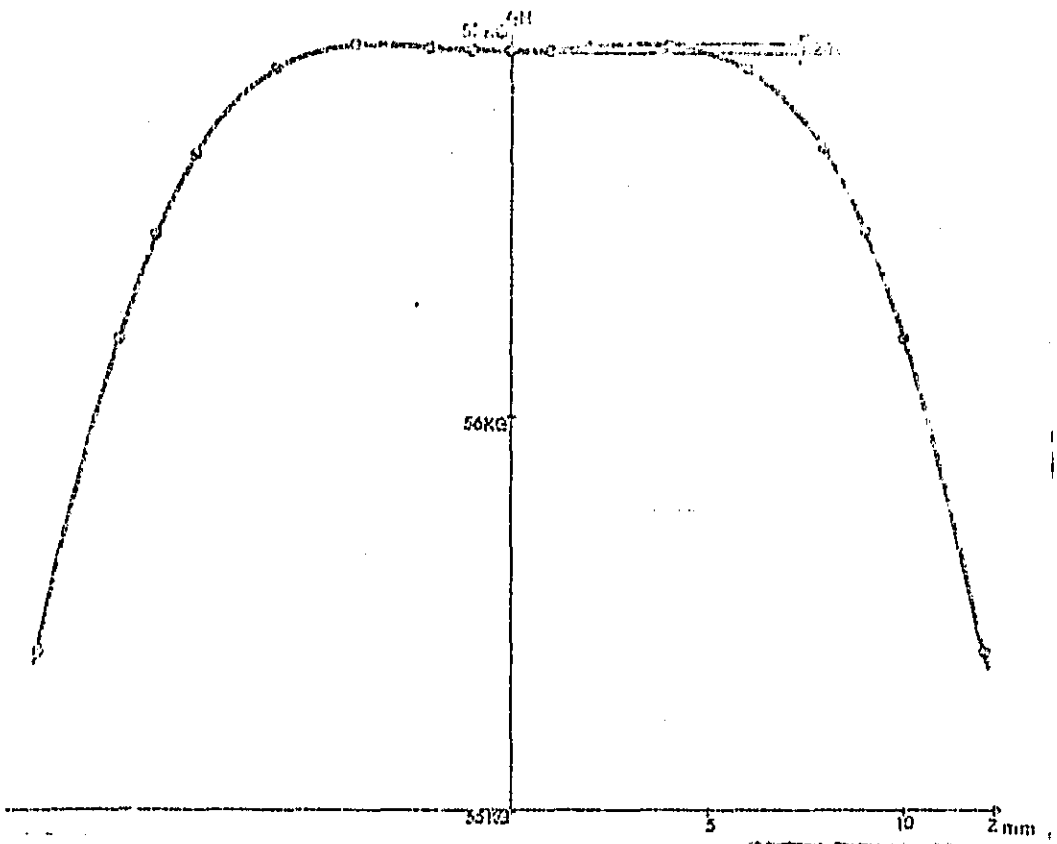

Figure 8. Variation of the principal field on the Oz axis of the superconducting coil.

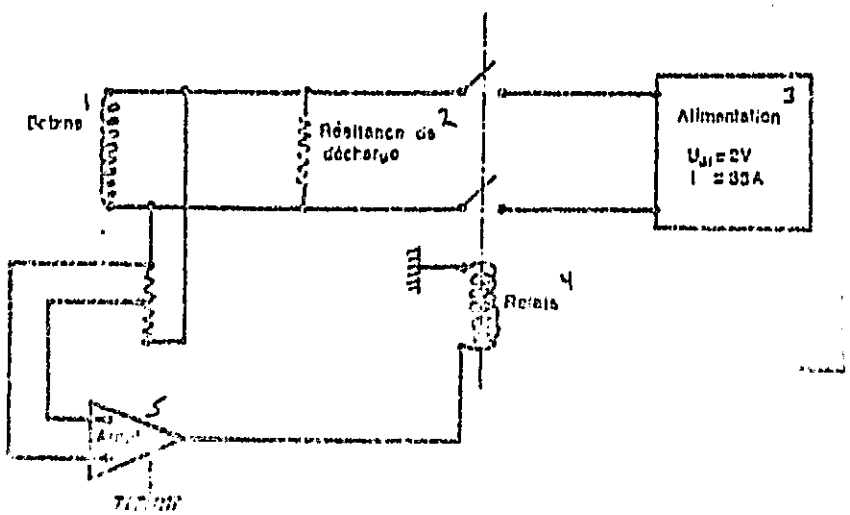

Figure 9. System for protection of the field coil.

Key: 1-Coil;2-Discharge resistor;3-Supply;4-Relays; 5-Amplifier.

γ) Gradient Coils

The field gradient is produced by two antiparallel coils situated on the z axis, on both sides of the principal coil (figure 7). The gradient calculated at the center can vary from 0 to 235 Oe/cm for currents comprised between 0 and 20 amperes.

δ) Performances

Dimensions

The field coil includes 12000 spirals. The gradient coil, twisted in opposition, include the same number of spirals (210).

Determination of the Functional Limit Point

We arrange for the superconductor material of the function f= g(H) (figure 10) which gives the maximum current travelling through the wire considered in the presence of a magnetic field H without producing return to the normal state. This function is furnished by the manufacturer, and it is desirable to remain considerably below this limit, very optimistically.

We can therefore calcualte the field at the interior of the solenoid at a point of the axis situated at the distance x from the center [13]: /14

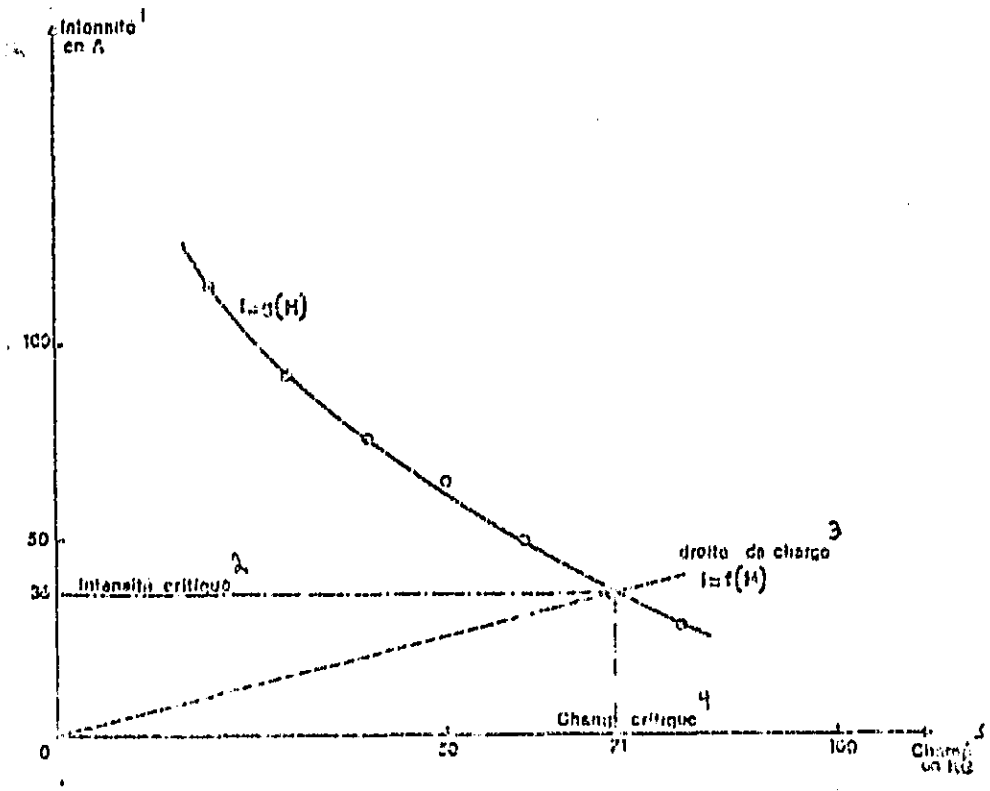

Figure 10. Critical intensity as a function of the magnetic field.

Key: 1-Intensity in A;2-Critical Intensity;3-Load line;4-Critical field;5-Field in KG.

$$Hoz = \frac{4\pi nl}{10}\left[\frac{l+z}{2(a-b)}\,\mathrm{Log}\,\frac{a+s_1}{b+s_1}+\frac{l-z}{2(a-b)}\,\mathrm{Log}\,\frac{a+r_2}{b+r_2}\right]$$

with l: half-length $\quad r_1^2=b^2+(1-z)^2 \quad s_1^2=b^2+(1+z)^2$

a: internal radius $\quad r_2^2=a^2+(1+z)^2 \quad s_2^2=a^2+(1+z)^2$

b: external radius

If n represents the number of turns in cm and if all the lengths are expressed in cm, Hoz will be expressed in Oersteds.

At the center of the solenoid, this expression becomes:

$$Hoz=\frac{4\pi ni}{10}\,\frac{l}{a-b}\,\mathrm{Log}\,\frac{a+s_2}{b+s_1}$$

In our case, for i=1 A, we have: Hoz=1945 KOe.

If we report this value of H in the relationship i=f(H), we determine the critical intensity which it is desirable not to exceed. We discover i=36 A for n=12000 (figure 10). We will be limited to i=26.5 A, with a maximum field of approximately 55 kOe.

The inductance coil is on the order of 6 Henrys, thus allowing us to attain the maximum field in approximately one minute for a pressure rise of 1 V.

ε) Use of the Coil

After winding, the spirals of the coil are not always in the most stable equilibrium position. In order to avoid the relay effects due to displacement of the spirals, we construct a series of relays for more and more intense currents so that the system gradually assumes a more stable position. Thus, starting from an intensity close to zero, we can attain the intensity for use without risk of deteriorating the superconducting coil (training phenomenon).

b) Technical Description of the Apparatus

α) Measurement of the Force

We use a "Sartorius" electronic balance allowing us to measure under vacuum variations of weight of 1 microgram with a maximum lofad of 2 g (see description in paragraph A).

β) Cryostat and its Accessories (Figure 11)

The measurements are carried out in a range of temperatures included between 1.6 and 20°K. We attain for the sample the temperature of the helium bath (4.2°K) by injecting exchange gas (gaseous helium) under low pressure ($\simeq 10^{-3}$ Torr) into chambers A and B (we select a low pressure in a fashion to reduce the heat influx due to convection or gaseous conduction). A lower temperature is attained by pumping over the helium bath (1.6°K).

In order to decrease overheating by radiation from the liquid helium bath, we have placed screens which serve to reflect the energy originating from the top of the installation, but also to ensure good use of the negative kilocalories originating from the evaporated helium, particularly during cooling of the installation.

In order to limit solid conduction, the cross-section of measurement wires is reduced to a minimum ($\phi \simeq 5/100^4$ mm). These wires, as well as those of the supply of the principal coil and gradient coils, are either directly in contact with the helium bath, or indirectly through the intermediary of exchange gas. It is notable that chambers A and B are constituted of stainless steel tubes of very low thickness.

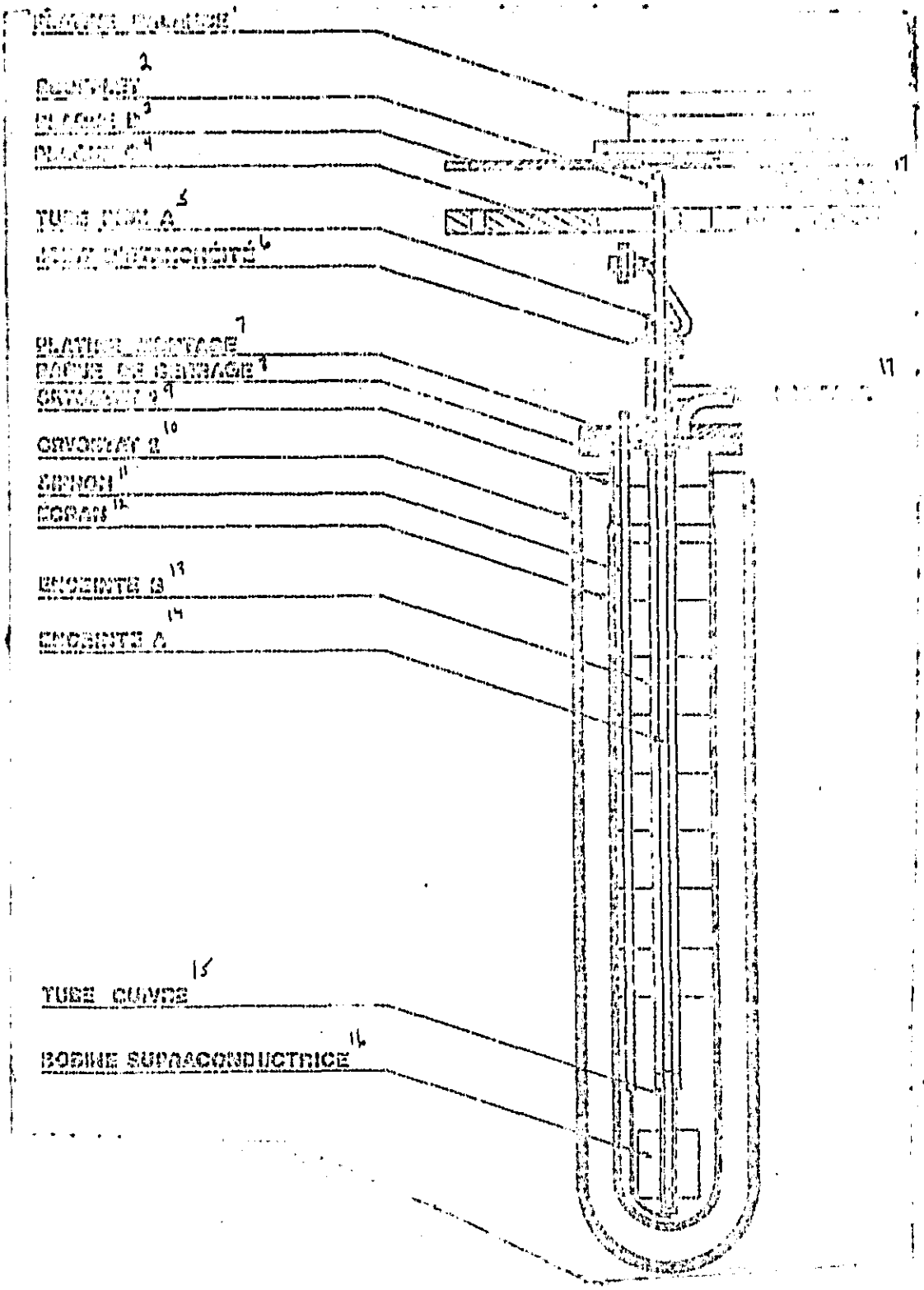

Figure 11. Diagram of the apparatus in a strong field.

Key: 1-Balance plate; 2-Bellows; 3-Plate D; 4-Plate C; 5-Stainless steel tube A; 6-Watertight joint; 7-Installation plate; 8-Clamping ring; 9-Cryostat 1; 10-Cryostat 2; 11-Siphon; 12-Screen; 13-Chamber B; 14-Chamber A; 15-Copper tube; 16-Superconducting coil; 17-Pumping.

γ) Temperature Regulation

Temperature regulation is ensured on the one hand by the intermediate chamber B situated between experimental chamber A and the helium bath; this contains gaseous helium whose pressure can be adjusted in a fashion to ensure variable influx of negative kilocalories originating from the bath; on the other hand, through a heating coil, of constantan wire of 0.05 mm diameter, two-threaded coil on chamber A. This last is controlled by an electronic regulation device. This device limits the heating power to the temperature of a thermocouple close to the sample through the intermediary of a cable constituted of an MECI recorder and a proportional-integral-differential regulator. /1

The Au-Fe-Chromel thermocouple, whose sensitivity is approximately 18 μV per degree in the temperature interval 4.2-20°K, is wound on chamber A. This system allows us to regulate the temperature to nearly 0.2 degree between 4.2 and 20°K.

We observe that the measurement of temperature here is delicate. Indeed, it is not a question of measuring the temperature on the sample itself, which would imply contact, thus an error in the measurement of the force. We have thus wound the thermocouple on chamber A by replacing, at the level of the sample, the stainless steel tube by a copper tube. This tube allows at the same time a good distribution of the heat furnished by the heating winding.

δ) Problems of Vibrations and Positionning of the Sample in Relation to the Coil

The sensitivity of the balance induces us to provide a system which allows us to eliminate vibrations (pumps, ground, ...). For this, the whole installation is conncected to a massive plate (C) which itself is suspended by flexible bonds to the installation framework. This device allows us to elinminate low frequencies (less than 4 Hz) which are at the origin of all perturbatory vibrations.

Moreover, it has been necessary to provide adjustment of positionning of the sample in relation to the center of the coil and to its axis. In order to carry out the first adjustment, we have mounted the balance plate on four screws in order to have vertical displacement of the sample. The second adjustment is more delicate a priori, since the sample is suspended by a very fine copper wire of approximately 125 mm length, and as we have seen, it is important to place the sample within the axis of the coil. We have been induced to place the balance plate on an intermediate plate (D) which supports the mounting assembly and which rests by three screws on the plate (C). This device allows very precise adjustment of the sample in relation to the axis of the coil.

c) Calibration

Calibration of this apparatus includes two parts: calibration of the force which will be described in paragraph α and that of temperature which will appear in paragraph β. Finally, we will introduce in the last part the correction which we must apply to our measurements.

α) Calibration of the Force

The forces which we measure are conneected to the magnetization M by $F=mM\frac{dH}{dz}$ (m: mass of the sample). If $M=\chi H$ (χ: magnetic susceptibility), the preceding expression becomes $F=m\chi H\frac{dH}{dz}$. We determine on the one hand the product $H\frac{dH}{dz}$ by measurement of susceptibility and on the other hand the field gradient $\frac{dH}{dz}$.

The first measurement is obtained by comparison with a sample of supposedly known susceptibility. Unfortunatley, even for very pure substances, the dispersion of results in the literature is such that we can not hope to reduce the imprecision below 1% on the absolute values of susceptibility. Finally, we have selected vanadium as a standard [14].

If we designate by the index e the quantities relative to the standard, the force measured for a same value of $H\frac{dH}{dz}$ and for a sample of unknown susceptibility is given by the expression:

$$F=F_e\frac{M\chi}{m_e\chi_e}$$

Since $\chi=A\frac{F}{m}$, with $A=\frac{m_e\chi_e}{F_e}$, which is a known constant. Knowledge of A thus allows us to attain the product $H\frac{dH}{dz}$.

Determination of $\frac{dH}{dz}$ can be obtained by two methods:
-from the product $H\frac{dH}{dz}$ and the calculated value of H (curve 12)(We will note that there exists limits to the linearity on this figure incumbent with non-knowledge of the magnetic field of the principal coil. In order to determine the field, we have arbitrarily relied on the maximum calculated value of the field and we have deduced from it the actual values of the field at the interior of the coil. The fact of selecting H_{max} cal. introduced only an indefinteless on the order of 1% on the magnetization value). /17
-or from a measurement on an easily saturatable substance (gadolinium or iron sulfate) for which we know the magnetization value at saturation. The force measured can then be shown in the form:

$$F=M_{sat}\frac{dH}{dz}$$

β) Calibration of Temperature

We have used the same thermocouple as for the installation of susceptibility at weak field. This has been calibrated with gadolinium sulfate powder which perfectly follows a Curie law $\chi=C/T$ up to 1°K. Investigation of $\chi T'$ as a function of T', where T' is the measured temperature, allows us to know the error $\Delta T=T'-T$. This is low near fixed points ($\Delta T=\pm 0.2°$) but reaches 20°K toward 150-200°K. We have taken into account this discrepancy which is reproducible if the conditions of pressure within the laboratory chamber are constant. For temperatures less than 4.2°K, we measure the pressure on the helium bath which gives the temperature at the level of the sample. /18

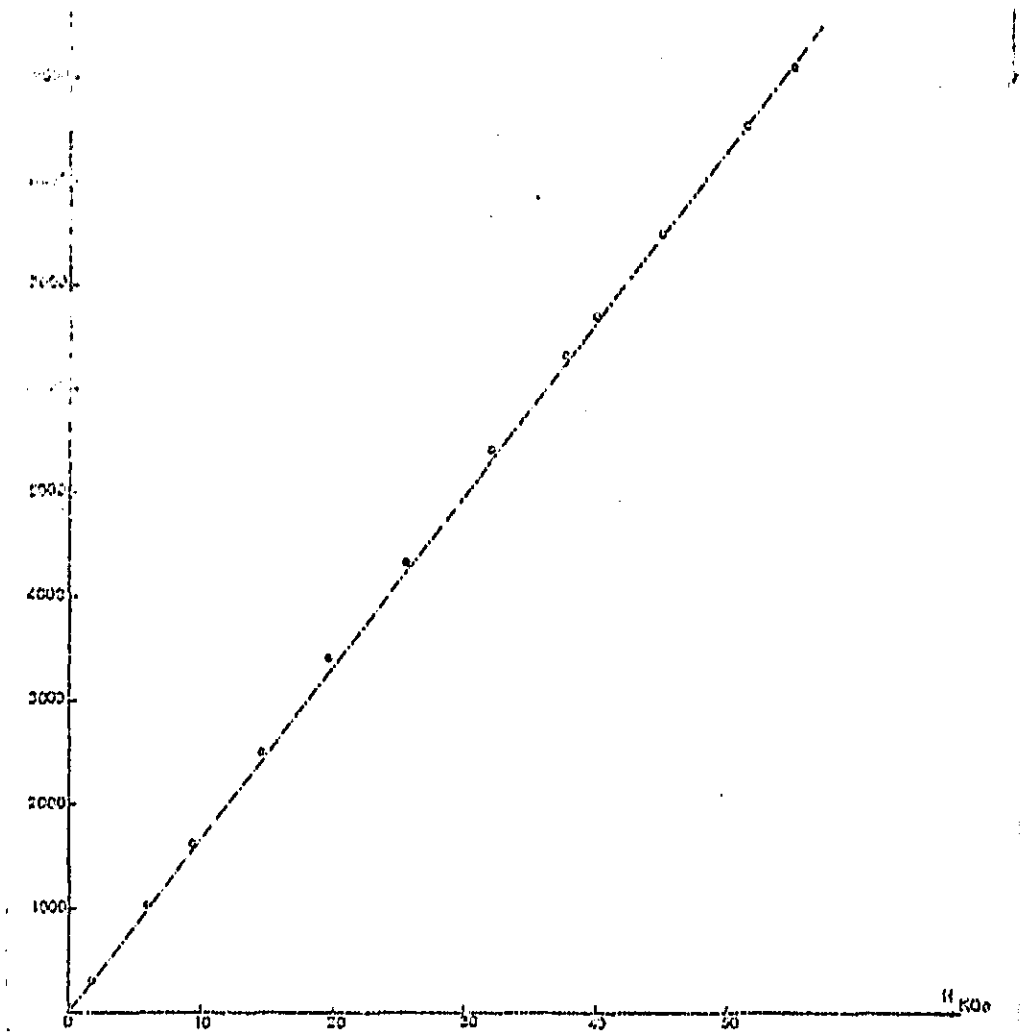

Figure 12. Vanadium calibration.

γ) Correction Due to Sample-Holder

The sample, on the order of a mg, is placed into a capsule of approximately 0.06 g which is suspended by a copper wire of 0.05 mm diameter to the beam of the balance. The assembly being relatively light, we have been induced to use a weight to tighten the wire. Our selection rested on a copper tare, a material whose magnetic properties are well known. If we take the precaution of well dessicating the capsules under vacuum, the measurements of susceptibility made on the assembly: copper-capsule-wire, demonstrate that this has a reproducible diamagnetism little dependent on temperature, which we have taken into account in our measurements.

I.4. Preparation of NiAl, CoAl, FeAl Alloys and Ternary Compounds (NiCo)Al and (CoFe)Al

Our study relates to monophasic and homogeneous alloys. All the samples have been prepared by arc fusion under argon atmosphere then by high frequency furnace fusion in aluminum oxide crucible. The different alloys have then undergone different thermal treatments according to their degree of homogenization. We describe in this paragraph the different stages of production of these compounds.

α) NiAl Alloys

We have used "Mond" nickel (99.97%) whose impurities are (ppm by weight): 110 of carbon, 110 or iron, 13 of copper, and 15 of sulfur. Arc fusion of the nickel-aluminum assemblage (99.997% purity) has then been accomplished under approximately one atmosphere of argon.

β) CoAl Alloys (Figure 13)

These alloys have been obtained from aluminum sheet metals and "Ugine-Kuhlmann" cobalt granules with 99.7% purity whose principal impurities are nickel (0.18%) and iron (0.09%). These granules have been melted by electronic bombardment in order to eliminate impurities and imprisonned gases. The alloy thus divided undergoes two arc fusions on copper base plate and under argon atmosphere. We verify the homogeneity of the alloy obtained through measurements of magnetic susceptibility on various amounts of the same sample. According to the result, we may or may not carry out an additional fusion in high frequency furnace in an aluminum oxide crucible under argon atmosphere.

γ) FeAl Alloys (Figure 14)

The alloys have been prepared from aluminum sheet metal and "Ores and Metals" iron with 99.93% purity (manganese 0.03%, carbon 0.03%).

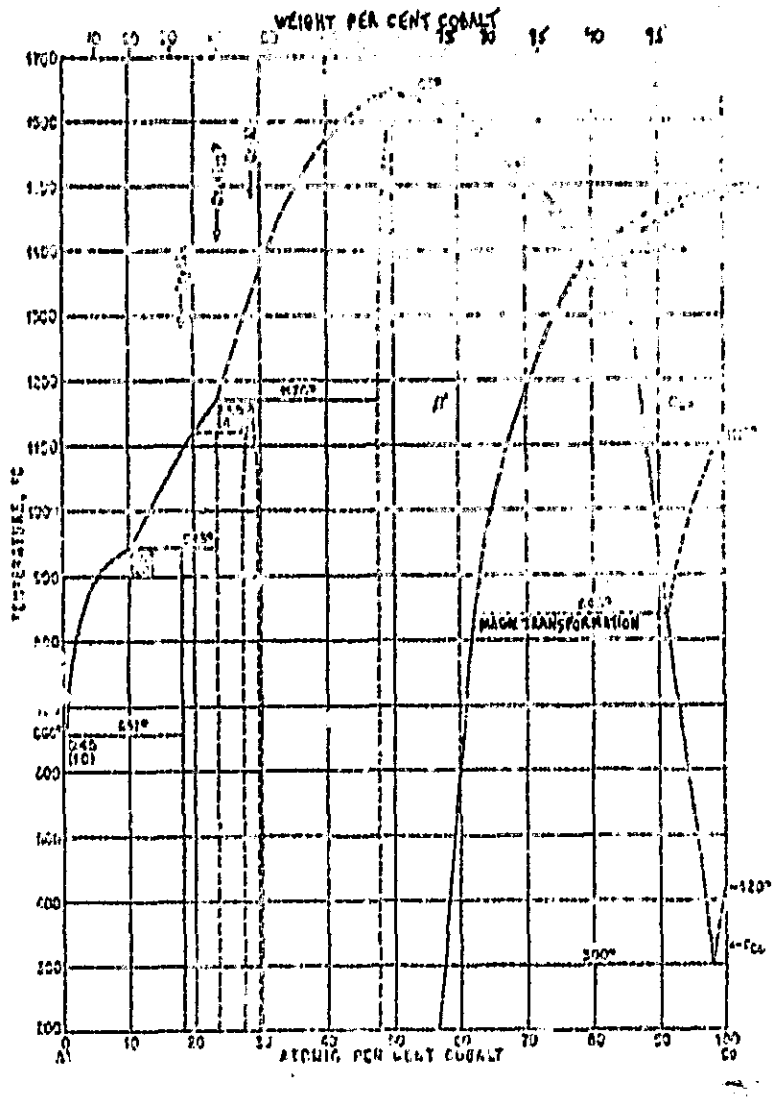

Figure 13. Phase diagram of CoAl.

In order to obtain an alloy in which the iron concentration on the aluminum sites is the lowest possible, it would have been desirable to provide an excess of aluminum. But this has been in part prohibited due to the fact of the low extension toward aluminum of the realm of existence of the FeAl compound. For the same reasons, we have been forced to guard against major segregation which occur through the appearance of a second phase rich in aluminum (phase ζ) and which are connected to the particular topology of the diagram. Indeed, with the difference from NiAl and CoAl, FeAl does not give congruent fusion at a slightly higher fusion temperature and slightly different from the temperature of of appearance of the phases more concentrated in aluminum (phases ε and ζ). After arc fusion and high frequency furnace fusion, these samples have received reheating for homogenization for 135 h at 900°C. According to the heterogeneity obtained after micrography, we carry out a new series of re-

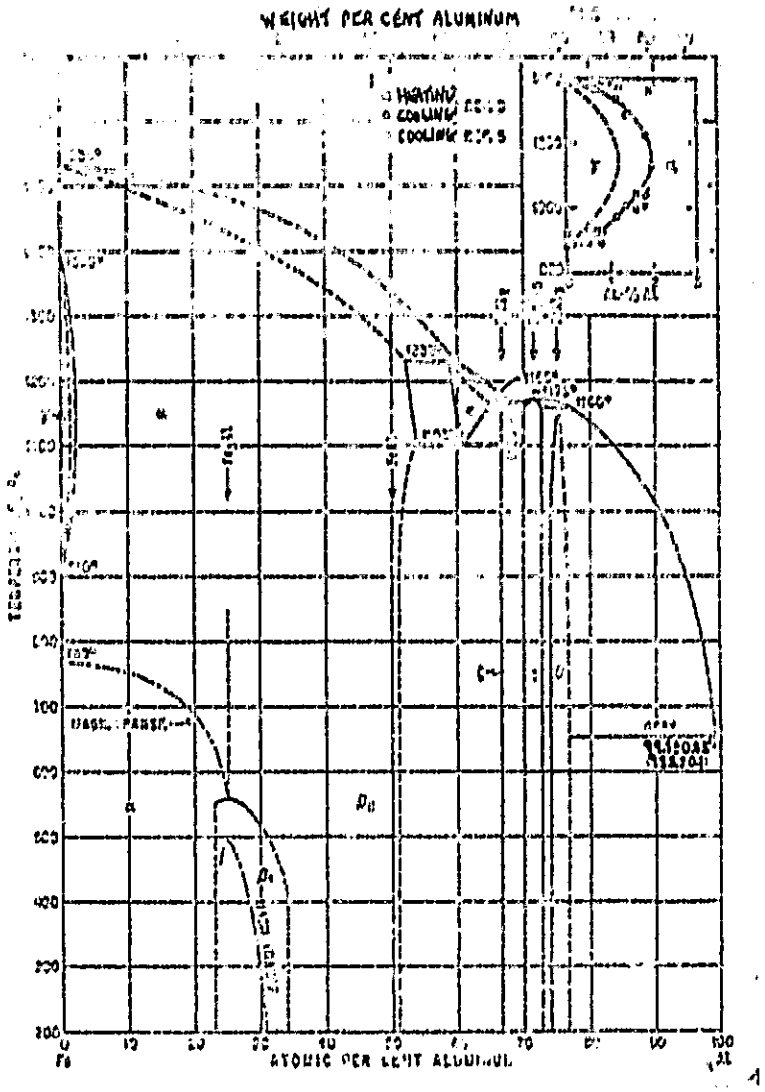

Figure 14. Phase diagram of FeAl.

heatings extending from 2 to 4 days for a temperature comprised between 1100 and 1200°C. In order to vary the iron concentration on the aluminum sites, certain of these samples have undergone tempering from variable temperatures.

δ) Ternary Compounds (NiCo)Al, (CoFe)Al

Besides, we have undertaken the manufacture of alloys of $(Ni_{1-x}Co_x)_{1+y}Al_{1-y}$ and $(Co_{1-x}Fe_x)_{1+x}Al_{1-y}$ with x varying from 0 to 1 and y very near zero for lower values ($y \simeq -0.01$). These compounds have undergone the same treatments as the preceding alloys, with for the alloys rich in iron precautions analogous to those which we have described for FeAl. For these last, in case of heterogeneity revealed by microprobe, reheatings from 2 to 4 days at 1300°C have been carried out.

Appendix 1. Significance of Axial Centering

/21

At the center of the coil, the Maxwell expressions expressing the con ervation of flux and the Ampere theory become:

$$\overrightarrow{\text{div}}\ \vec{B}=0 \text{ and } \overrightarrow{\text{rot}}\ \vec{B}=\vec{0} \text{ (no current)}$$

where $\overrightarrow{\text{rot}}\ (\overrightarrow{\text{rot}}\ \vec{B})=\vec{0}$. This implies $\nabla^2\vec{B}=0$ (1) (in vacuum $\nabla^2\vec{H}=0$).

If the field given by the coil is following z (the components following x and y will be negligible) expression (1) becomes:

$$\frac{\partial^2 Hz}{\partial x^2}+\frac{\partial^2 Hz}{\partial y^2}+\frac{\partial^2 Hz}{\partial z^2}=0 \quad (2)$$

At the center of the coil, Hz is maximum, thus $\frac{\partial^2 Hz}{\partial z^2}$ is negative. So that expression (2) is moderate, it is necessary that $\frac{\partial^2 Hz}{\partial x^2}$ and $\frac{\partial^2 Hz}{\partial y^2}$ is positive. That is to say that we will have a minimum as a function of $r=(x^2+y^2)^{1/2}$. For a paramagnetic sample, the central point of the coil is in an unstable position radially and the sample will have a tendency to adhere against the walls.

In order to avoid this disadvantage, we remove some spirals in the coil at the level of the sample. With these conditions, Hz is minimum at the center and we will have this time a maximum following r. The axial position is then a position of stable equilibrium.

Chapter II.

/22

Structure of Bands of Transition Metals and TRAl Intermetallic Compounds (TR=Ni, Co, Fe)

We will concern ourselves in this chapter with the structure of bands of stoichiometric TRAl intermetallic compounds (TR=Ni, Co, Fe). After a report on the model for bands of transition metals (paragraph 1), we give two theoretical descriptions of calculations for bands (rigid bands, approximation of the cohe·ent potential) for concentrated alloys (paragraph 2). Finally in paragraph 3 we summarize and discuss several calculations for bands on the TRAl compounds defined (TR=Ni, Co, Fe), before testing in 4 the studies which we have accomplished on the proerties connected to the structure of bands of these compounds.

II.1 Model of Bands of Transition Metals

II.1.A. Non-Magnetic Metals: Model With One Electron

Transition atoms are characterized by the existence of nd layers which are progressively filled when the atomic number increases. These d states have very different properties from those of other valence states ((n+1)s) (figures 15 and 16).

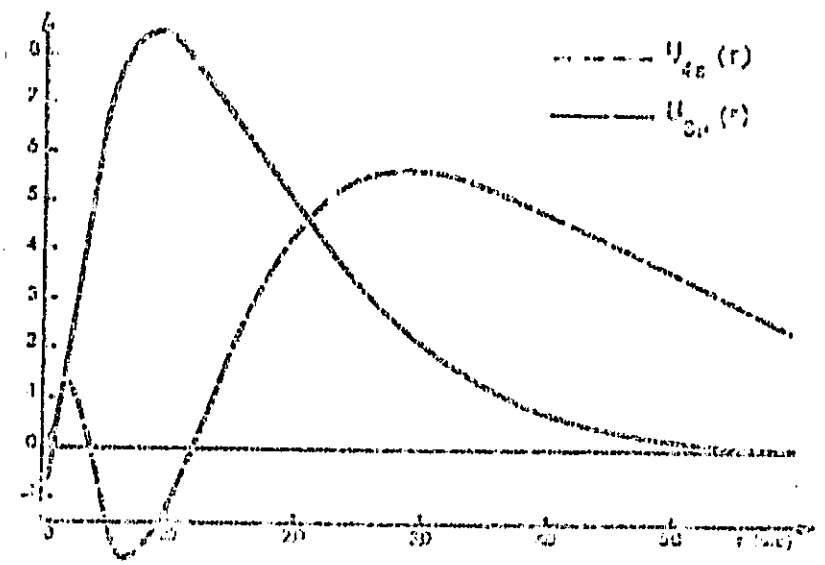

Figure 15. Wave functions $\Psi(3d)$ and $\Psi(4s)$ for vanadium: the 4s electron density oscillates strongly in the region where the 3d layer has its maximum (orthogonalization).

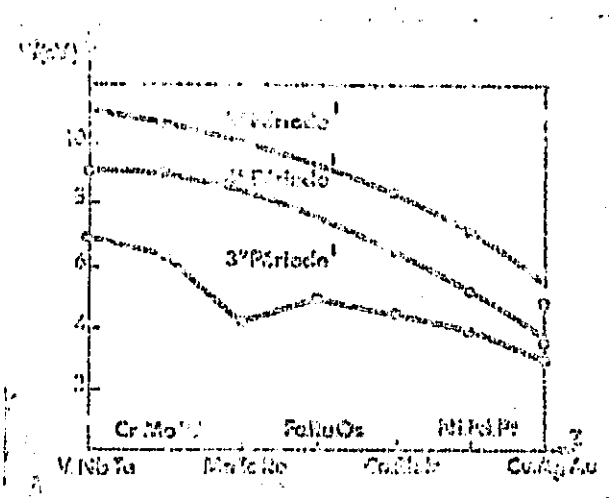

Figure 16. Size of "d" bands for transition metals (after [17]). Key: 1-Period.

a) The d orbitals are of low extent (~0.5 Å) in comparison with those of the s electrons. The d layers present their maximum of electron density in a region where the potential of the lattice is strongly attractive: they are thus very stable.

b) When we increase the atomic number through a same series (Ti→Ni), the potential becomes more and more attractive such that the d layers become more and more stable, while their extent becomes lower and lower. /23

c) When we shift from one series to another (Ni→Pd→Pt) the number of modes increases such that the wave functions become more and more extensive and less and less stable.

When the atoms are placed in contact to form a solid, the atomic wave functions partially recover: there can be circulation of an electron from one atom to another, the atomic orbitals cease to be of natural soid states. We can form new natural states by linear combinations of atomic orbitals centered on all the lattice sites.

When we neglect the mixture of s and d states, the solid can be described with the simplified Mott-Slater model [15] [16] by two bands of different symmetry overlapping at the Fermi level (figure 17):
-the s band whose size is comparable to that of normal metals (on the order of 10 eV);
-the d bands, much narrower (3 to 6 eV), because they are constructed from more compact atomic orbitals, thus with greater overlap than s orbitals [17] (figure 16).

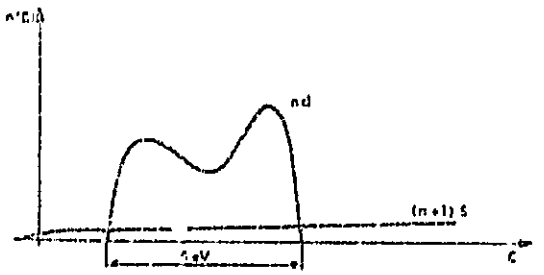

Figure 17. Density of states per unit of energy n(ε) for a transition metal.

In the theoretical calculations, the s and d bands are often treated independently. The s bands are treated with the approximation of nearby free electrons or by orthogonalized planar waves (OPW), while the d bands are treated by strong bands [18] [19] [20] or by KKR or APW. The calculations made with the approximation of planar waves increased, demonstrating that the s-d hybridization only affects localized regions of the reciprocal space and whose energy is distant from the Fermi energy [21] [22] [23]. Consequently this hybridization does not enter into consideration for the properties which follow from excitations in the vicinity of the Fermi surface: particularly paramagnetic susceptibility, electronic specific heat (results of Mat-

theiss [24]).

This simplified model resting particularly on a description in terms of states of an electron, however still accounts for a great number of experimental properties in satisfactory fashion. We have thus been able to clearly demonstrate the existence of narrow and incompletely filled d bands, as the electronic specific heat and Pauli susceptibility very clearly demonstrate, which are direct measurements of the density of states at the Fermi Level: /24

$$\gamma = \frac{\pi^2 k_B^2}{3} n(E_F)$$

$$\chi_p = \mu_B^2 n(E_F)$$

The values of γ (figure 18) are indeed, on the average, well hgiher than those obtained for normal methods. This represents the existence of a d band with high density in incompletely filled states. Moreover, these values are very fluctuating, this represents the existence of peaks of density of states (Van Hove eccentricities). Finally, these fluctuations reproduce almost identically when we pass from one series to another.

Figure 18. Electronic specific heats in the three transition series. (___: first series; __.__: second series; ---: third series)

Nevertheless, we observe high values of susceptibility in agreement with a great density of states $n(E_f)$, as well as rapid variation of the susceptibility with temperature, which also represents the existence of peaks of density of states.

II.1.B. Magnetic Metals

/25

The magnetism of transition metals can not be correctly included within the framework of this model with one electron. The discrepancies between the measured susceptibility and the Pauli susceptibility particularly point out modifications induced by electron-electron effects.

It is necessary to substitute within the Hamiltonian of bands Ho a Hamiltonian taking into account interactions between electrons. We will obtain a simple model where we neglect the orbital multiplicity of the d band and electron interactions other than inter-atomic. Only the matrix element U representing the intra-band coulomb interaction is taken into acoount [25] [26].

The Hamiltonian of interaction for an atom then takes the form: $H_1=Un_{i\uparrow}+n_{i\downarrow}$, when $n_{i\sigma}$ is the number per atom of electrons of spin σ.

The total Hamiltonian for the band has the following form (Hubbard Hamiltonian) [27]:

$$H=H_0+\sum_i H_i$$

with

$$H_0=\sum_{k,\sigma,m} E_k n_{k,\sigma}$$

where σ denotes the spin, k the wave vector, E_k is the relation of dispersion of the metal without electron interactions, and $n_{k,\sigma}$ the number of electrons of spin σ of wave vector k in the band.

Even with this simplified model, we have a problem with N substances, and in order to discuss them, we will obtain them with the Hartree-Fock approximation.

II.1.C. Stoner Model [28]

In this model we consider that an electron is subjected to a mean potential due to the effect of all the other electrons, including the transfer effects. This mean potential is assumed to be spatially uniform. This has taken a form approaching the Hubbard Hamiltonian:

$$H_{Stoner}=H_0+U\sum_i(n_{i\uparrow}\langle n_{i\downarrow}\rangle+\langle n_{i\uparrow}\rangle n_{i\downarrow})$$

where $\langle n_0\rangle$ is the mean number of electrons per atom with spin σ cal-

culated in autocoherent form. This corresponds to the Hartree-Fock approximation where we separate in the wave function the contribution of spin from that of the variables of space. With these conditions, the Hamiltonian becomes separatable into a sum of terms with one electron.

The initial success of the model is to predict instability of the paramagentic state in relation to the ferromagnetic state, even more pronounced when the density of states at the Fermi level is more sinnificant. We obtain the criteria of instability by departing from the fundamental paramagnetic state of Hartree-Fock, by considering the total amount of energy when we create a small ferromagnetic polarization. This polarization is obtained by transferring one layer (of thickness δE) of electrons of spin $\downarrow$ below the Fermi level toward the states of spin $\uparrow$ (figure 19).

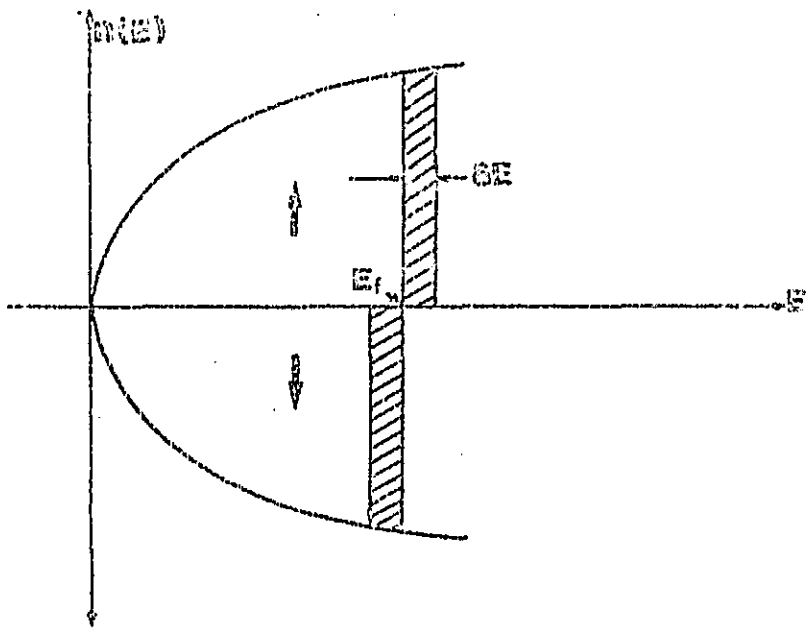

/26

Figure 19. Density of states for electrons of spin $\uparrow$ and $\downarrow$.

The transfer of kinetic energy is:

$$\Delta T = n(E_F)\,\delta E^2$$

where n(E) is the density of states per atom and direction of spin.

The variation of interaction energy is:

$$\Delta E_{int} = U\left[\frac{n}{2} + n(E_F)\,\delta E\right]\left[\frac{n}{2} - n(E_F)\,\delta E\right] - \frac{Un^2}{4} = -Un^2(E_F)\,\delta E^2$$

and the total variation of energy E is:

$$\Delta E = n(E_F)\,\delta E^2[1-Un(E_F)]$$

In these conditions, we will have ferromagnetism when $Un(E_F)>1$ (Stoner criteria).

When the non-magnetic state is stable, we can calculate the static stability χ per atom. In the presence of a field H_0, the energies with one electron $E_{k\sigma}$ are (figure 20):

$$\begin{cases} E_{k\uparrow} = E_k + (n_\downarrow - \dots)H_0 \\ E_{k\downarrow} = E_k + (n_\uparrow + \dots)H_0 \end{cases}.$$

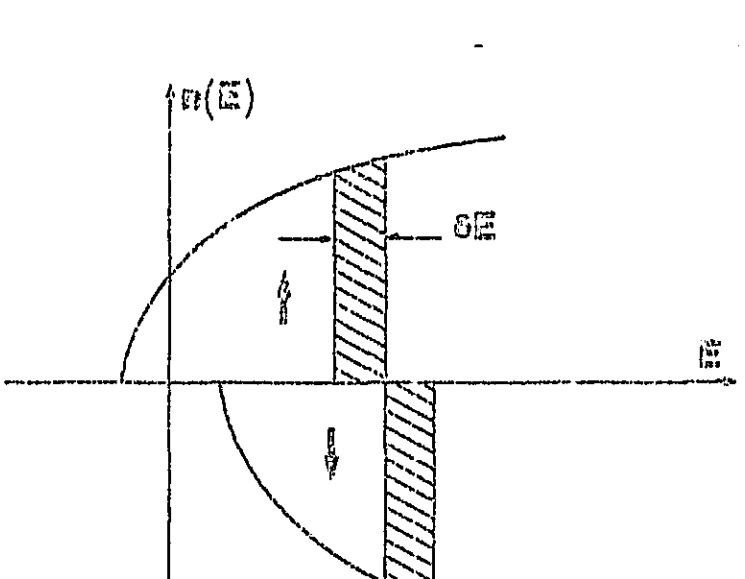

Figure 20. Calculation of susceptibility.

The energy δE which shifted bands $\uparrow$ and the quantity $(n\uparrow - n\downarrow)$ are connected by the relationships: /27

$$\begin{cases} \delta E = \mu_B H_0 + U(n_\uparrow - n_\downarrow) \\ n_\uparrow - n_\downarrow = 2\delta E\, n(\varepsilon_F) \end{cases}$$

where:
$$n_\uparrow - n_\downarrow = \frac{2\mu_B H_0 n(\varepsilon_F)}{1 - Un(\varepsilon_F)}$$

that is to say:
$$\chi = \frac{M}{H_0} = \frac{2\mu_B^2 n(\varepsilon_F)}{1 - Un(\varepsilon_F)} .$$

At non-zero temperature, we would discover:
$$\chi(T) = \frac{\chi_0(T)}{1 - \frac{U\chi_0(T)}{2\mu_B^2}} .$$

The numerator is the Pauli susceptibility of the system without interaction.

The Stoner model for bands allows us to explain, for the ferromagnetic metals Fe, Co, Ni, the moments at fractional saturation which could only be complete in a Heisenberg model where the moments are localized on the atoms. On the other hand, this theory allows us to explain the disagreement which exists between the value of the magnetic moment calculated from the paramagnetic susceptibility at high temperature, and that which we determine at low temperature from magnetization at saturation. Also, the Stater-Pauling curves (c.f. §II.2.A), which give the variation of the mean moment $\bar{\mu}$ of an Mx alloy with the concentration c of impurities x, for alloys of nickel and cobalt, have been interpreted with this model. Nevertheless, it is necessary to remark that the Stoner model does not allow us to explain the Curie-Weiss law for ferromagnetic substances above T_c. Although this result constitutes the most obvious defect of the theory of band magnetism, there does not exist at the present time a more satisfactory expression. On the other hand, this model only takes into account individual electron excitations; it can not interpret the law of demagnetization by $T^{3/2}$ of Block at low temperature which results from collective excitations of the wind of electrons (spin waves).

However, despite these criticisms, the Stoner model allows us to understand the strong susceptibility of materials such as palladium or platinum for which $Un(E_F)$ is near unity, and also to interpret the variations of χ with temperature from variations of χ_0. Such materials are called materials with reinforced or even nearly-magnetic materials. The magnetic impurities presently give rise in these materials to gigantic moments. We will see later that FeAl falls into this category.

II.2. Concentrated Alloys

The study of concentrated alloys has not been marked by real progress until very recently. The only cases treated were where the atomic potentials on the various atoms present in the alloy are close together (approximation of rigid bands) or on the contrary very different (split band limit). In the first case everything occurs as if the substitution of an atom B into a matrix A simply modified the

filling of states of bands of the matrix, without deformation of this band. In the second, on the contrary, the levels of impurity lead to a band separated from the valence band of the matrix. The intermediate case of a difference of potential on the order to the sizes of bands give rise to a common band whose upper limit is greater than that of the bands of separation. This situation is well described by approximation of the coherent potential (paragraph B). The results of the model of rigid bands which we will use for certain of our alloys are reported in A.

II.2.A. Model for Rigid Bands [29] [30]

We will observe in the diluted band, such that we neglect the interaction between impurities. The simplest method to describe the /28
structure of bands of alloy is to consider that the density of states $n(E,c)$ corresponding to the concentration c is deduced from the density of states of pure metal $n(E,0)$, without change of form, by a simple displacement of energy:

$$n(E,c)=n(E,0)-c\frac{\delta n}{\delta E}(E,0)\Delta E$$

In this expression, we have assumed, besides, that with the limit of weak concentrations, the displacement of energy was proportional to the concentration c, the impurity introducing only a displacement of the assemblage equal to the mean of the perturbator potential $V_p(r)$. This hypothesis constitutes the model for rigid bands. This model can be justified in relatively restrictive cases by a method of perturbation of the first order when the displacement of energy $E(k)$ of each Bloch function $\Phi(k,r)$: $\Delta E(k)=\langle\Phi(k,r)/V_p(r)/\Phi(k,r)\rangle$ is independent of the wave vector k. This condition is satisfied when the lattice potential is very strong (strong bands) or very weak (free electrons).

The very significant result follows that the screen with charge Z introduced by the impurity is furnished primarily by d electrons; indeed, the number of additional states introduced into the s and d bands is respectively $n_s(E_F)\Delta E$ and $n_d(E_F)\Delta E$; since $n_s(E_F)\ll n_d(E_F)$, the screen charge due to the s electrons is negligible in relation to that which is due to the d electrons.

This result has been particularly used ([29] [30]) for the study of ferromagnetic or paramagnetic alloys. Thus if we dissolve neighboring elements (Co, Fe, Mn) into the nickel or iron or nickel into the cobalt, the additional electrons fill the d band and reduce the mean magnetic moment μ according to the law: $\mu=\mu_m-cZ\mu_B$ (μ_m: moment of the matrix; c: concentration of impurities). We observe well such behavior experimentally (Slater-Pauling curve) (figure 21). The same type of explanation is used to take into account the decrease of paramegnetism of palladium when we dissolve silver into it (figure 22).

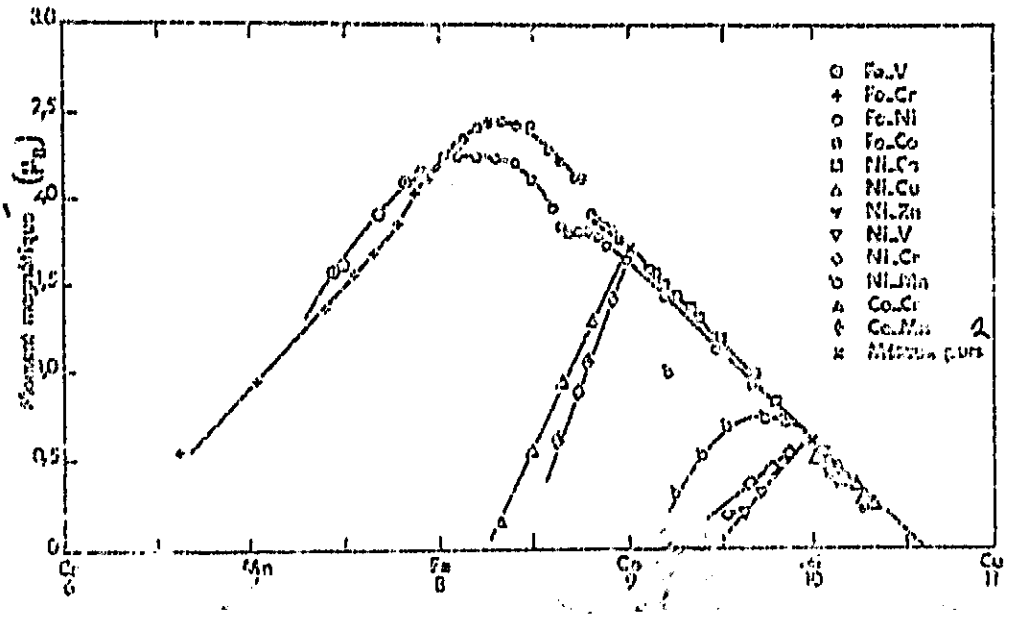

Figure 21. Mean magnetic moments $\bar{\mu}(c)$ for elements of the first transition series.

Key: 1-Magnetic moment; 2-Pure metals.

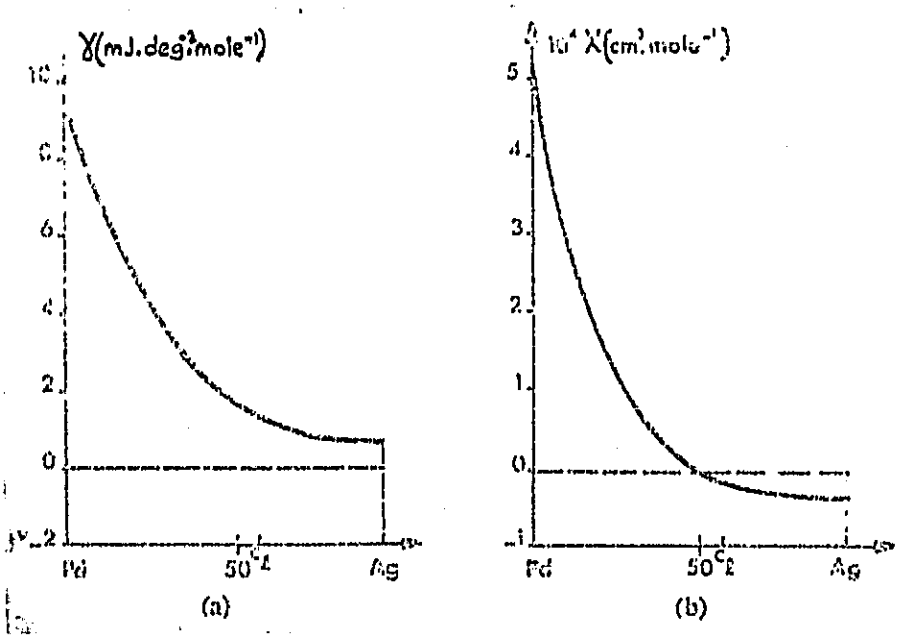

Figure 22. Electronic specific heat γT and magnetic susceptibility χ of PdAg alloys: γ and χ (proportional to $n(E_F)$ remain constant for $c>c_1\simeq 0.6$, concentration from which the "d" band is full.

II.2.B. Method for Approximation of Coherent Potential (CPA) /29

This method has been introduced by Soven [31], Onodera and Toyozawa [32] and Velicky et al. [33]. It is essentially based on a method of a mean field and replaces the real potential by a periodic potential defined in such a fashion that the diffusion of electrons into the mean surroundings obtained by attributing to the A and B atoms probabilities p_A and p_B equal to the concentrations (for a homogeneous alloy), is on the average zero. It is then possible to calculate the densities of partial states on each type of atom. The CPA method is especially used when the A and B bands can be treated as strong bands, as in the case of base alloys of nickel (Willliams and Faulkner, 1971) and NiFe (Kanamori, 1971). In the simplest form, the CPA method is an approximation at one site. It is thus existent at the first order of c_2 and $_3$ can not involve local fluctuations of environment which are of c^2, c^3, ... (c.f. §III.3.A). These fluctuations can be approximately taken into account using certain developments of the method. Tsukade [34] and Brouers et al. [35] have provided such a development by considering not only an atom alone, but a cluster constituted by a central atom A (or B) surrounded by its Z nearest neighbors A (or B), in the mean environment (NiRh and PdRh alloys).

II.3. Structure of Bands of Defined Intermetallic Compounds NiAl, CoAl and FeAl

Connolly and Johnson [1] have calculated the structure of bands of NiAl by the method of increasing planar waves (APW). This calculation is clearly useful for CoAl and FeAl in a model for rigid bands, the compounds being isomorphic. The results of these calculations are given in figure 23. On the other hand, Moruzzi-Williams and Janak [2] have calculated by the method of Korring, Kohr and Rostoker (KKR) the structure of bands of six intermetallic compounds of structure B_2 of NiAl and CoAl. The results are given in figures 24 and 25.

/30

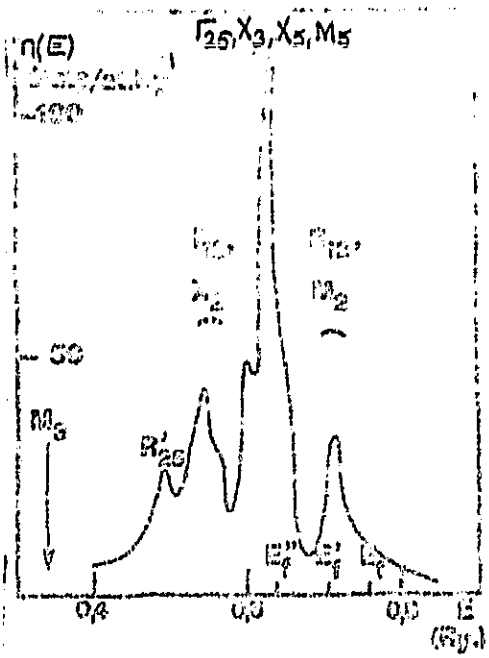

Figure 23. Density of electronic states for NiAl, according to Connolly and Johnson [1]. E_F indicates the Fermi level of NiAl, E'_F and E''_F those of CoAl and FeAl.

Key: 1-States/at.Ry.

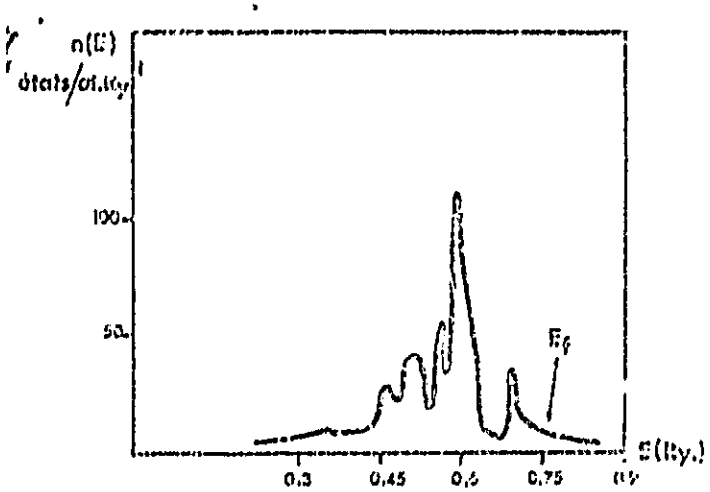

Figure 24. Density of electronic states for NiAl after [2].
Key: 1-States/at.Ry.

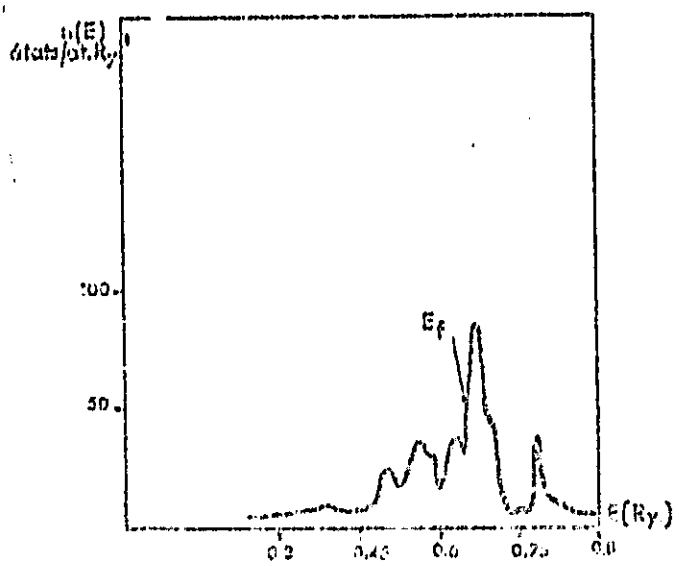

Figure 25. Density of electronic states for CoAl after [2].
Key: 1-States/at.Ry.

These figures demonstrate the presence of a narrow band of 3d character between 0.4 and 0.8 Rydbergs. We see that the two types of calculations result in the same structure of bands for NiAl and confirm the approximative validity of the model for rigid bands for CoAl. Moreover, as is generally the case for the d bands, this is marked for all of a series of structures. In more precise fashion, we see on figure 23, that for NiAl, the 3d band is nearly planar and that peaks appeared below the FermiLevel: /31

-a peak between the Fermi levels for NiAl and CoAl;
-a narrower peak at the perpendicularity of the Fermi level for FeAl;
-finally, a central peak at approximately 0.5 Ry.

By making use of the diagrams given on figures 26 and 27, we can discover the VanHove anomalies associated with these peaks, most particularly interesting to us are those which correspond to symmetries of d type (Γ_{12}, Γ_{25}, X_2, X_3, X_5, M_5, M_2 and R_{12}) [36] (the atomic orbitals leading to the corresponding Bloch states are given as an illustrative example on figure 28).

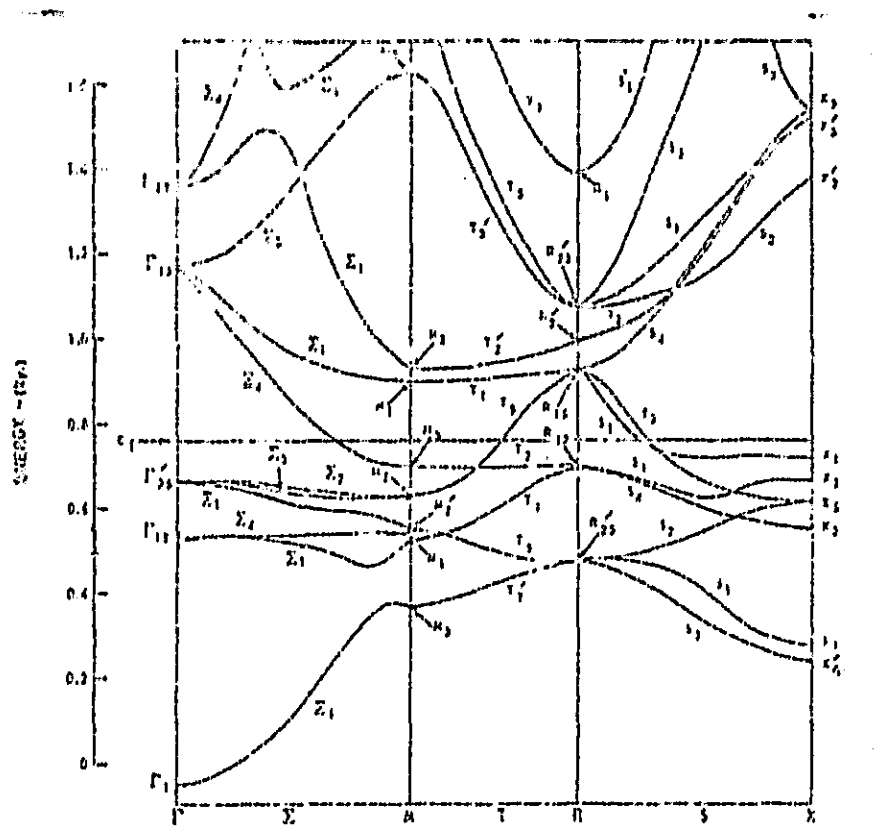

Figure 26. Relationships of dispersion for NiAl along directions Σ, T, and M, calculated by APW method according to [1].

We see that the peak which appeared between the Fermi Levels of NiAl and CoAl undoubtedly correspond mainly to the M_2 and R_{12} states of symmetry, thus of the e.g. "anti-bonded" type in the description of Goodenough [37]. The narrower and sharper peak which appeared for lower energies at the perpendicularity of the Fermi level for FeAl, correspond to Γ_{25}, X_3, X_5, and M_3 states of symmetry which are of t_{2g} type. It is noteworthy that the t_{2g} states (M_3 and R_{25}), of more

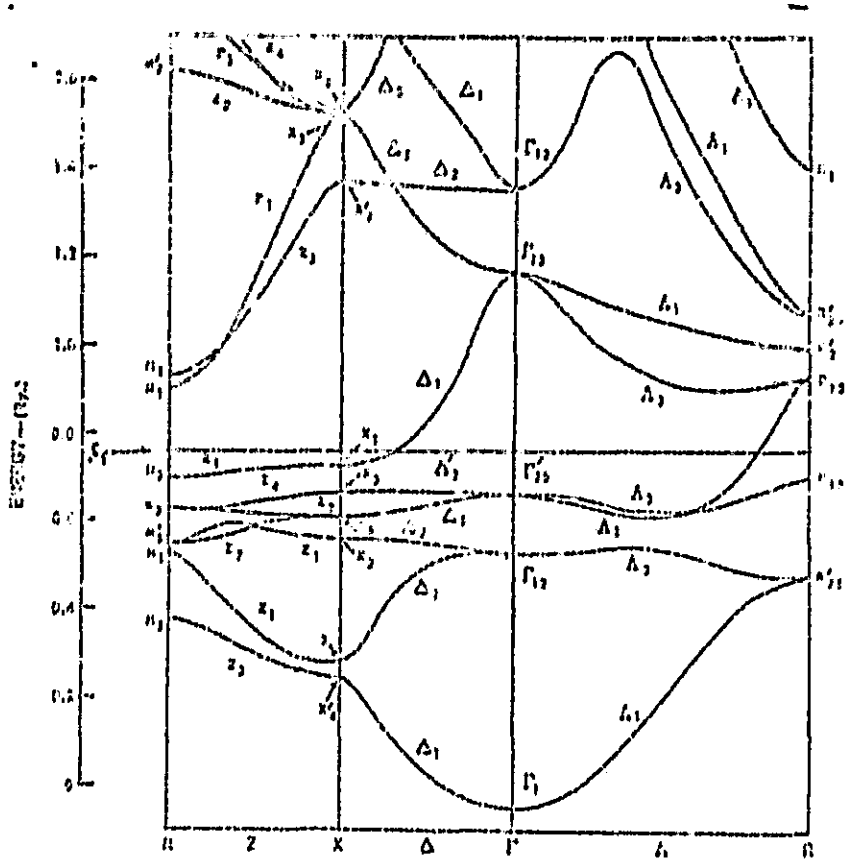

Figure 27. Relationships of dispersions for NiAl along directions z, Δ and Λ, calculated by the APW method according to [1].

bound nature than the other states, appeared for lower energies (0.45-0.5 Ry). Nevertheless, the essential part of t_{2g} states appears to be contained in the peak situated at 0.63 Ry whose size does not exceed 1 eV. This result demonstrates that as a first approximation, the enlargement due to the effects of bands does not exceed for the states (d, t_{2g}) that which we obtained with a description of resonant type on isolated d levels (d-d interactions between small transition atoms in relation to d-s and d-p interactions). For the opposite states (d, e_g) , the d-d effects are dominant (the e_g orbitals have an orientation which favors overlapping between neighboring atoms). As we have seen, the R_{12} and M_2 states correspond to "anti-bonded" energy states, while Γ_{12} and χ_2 states are primarily "bonded" energy states.

II.4. Study of Properties Connected to the Structure of Bands of Stoichiometric Compounds

An effective method to study experimentally the structure of bands of a compound, with the model for rigid bands, is the study of

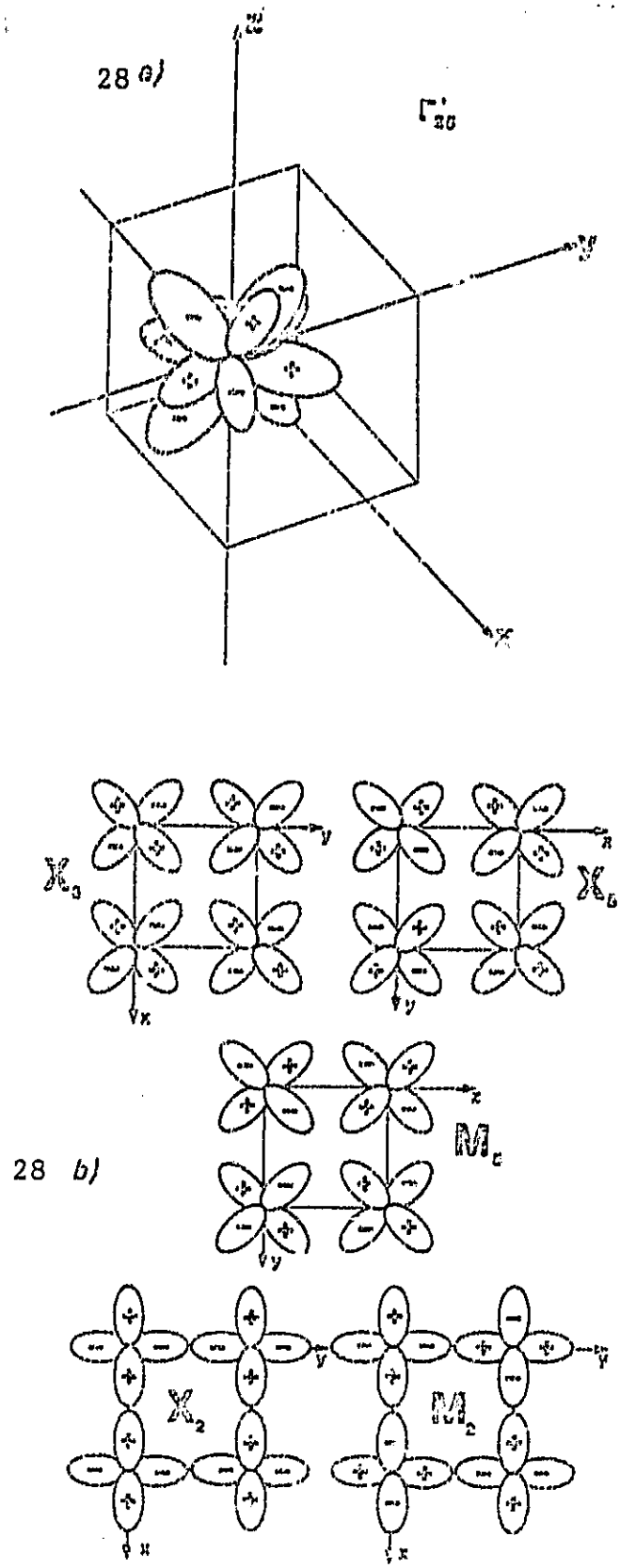

Figure 28. a) atomic orbitals connected to the d: Γ_{25} symmetry state b) atomic orbitals corresponding to d (X_3, X_5, M_5, X_2 and M_2 symmetry states).

the electronic specific heat and the Pauli susceptibility. Indeed, these quantities are proportional to the density of states at the Fermi level. It is then possible to describe the general aspect of the structure of bands by a study of concentration.

II.4.A. Study of Compounds $(Ni_{1-x}Co_x)_{1+y}Al_{1-y}$

Our study has related to samples of composition $(Ni_{1-x}Co_x)_{1+y}$ /34
Al_{1-y}, x varying from 0 to 1 and y very close to zero for lower values ($y \simeq -0.01$) in a fashion to avoid the problems connected with magnetism of cobalt atoms occupying aluminum sites (c.f. §III.5) (the substitutional nickel atoms are not negative [38]).

Figure 29 gives the magnetic susceptibility of various samples as a function of temperature. It appears that the dependence on T of the susceptibility had two distinct origins:

a) Presence of a significant Curie-Weiss term at low temperature:

$$\chi_{CW} = \frac{C}{T+\theta} \quad (T<77°K) \text{ with } \theta \simeq 0 \text{ and C small}$$

This term is undoubtedly associated with transition atoms substituted for aluminum, whose behavior can be magnetic (see later §III.5). Also for $y<0$, such atoms exist in small quantity, either where the thermodynamic equilibrium induces this effect at 900°C, temperature of reheating of the samples, or where, in less probable fashion, the equilibrium has not reached this temperature.

b)Slow variation with temperature of the Pauli (or Van Vleck) susceptibility. This effect predominates above 77°K.

If we define from the susceptibility an estimated term χ_{CW}, and which we extrapolate at 0°K, we obtain a value χ_p which is given on figure 30.

We will note that χ_p is even larger for samples which correspond as much to large values of x (CoAL, $Ni_{0.25}Co_{0.75}Al$) as to small x. For CoAl, we find $\chi_p \simeq 2.3\ \chi_o$, where χ_o is the value of Pauli susceptibility calculated from γ; for NiAl, on the contrary $\chi_p \simeq \chi_o$. This reinforcement of the susceptibility in the case of cobalt can have two origins:

a) significant Stoner reinforcement (§II.1.C) undoubtedly associated with a greater value of the intra-atomic energy transfer U. Such a result would result from the fact that the extra cobalt atoms are magnetic in CoAl, whereas the nickel is not magnetic in NiAl.

b) notable contribution, for CoAl with the susceptibility, of the Van Vleck term $(d)^1$, which was very low for NiAl since the d band is nearly full in this last case.

---

[1] In the case of transition metals, the orbital paramagnetic susceptibility χ_{orb} (Van Vleck paramagnetism) is significant and can occur in the form for a k band:

$$\chi_{orb} = 2\mu_B^2 \sum_{n,m} \left[\int \frac{d^3k}{(2\pi)^3} \frac{f(E_{nk}) - f(E_{mk})}{E_{mk} - E_{nk}} \times |\langle n,k|Lz|m,k\rangle|^2 \right]$$

where: n and m are indices of decay; $f(e_{nk})$ represents the function of Fermi distribution; Lx is component following z (direction of field applied) or orbital magnetic moment operator.

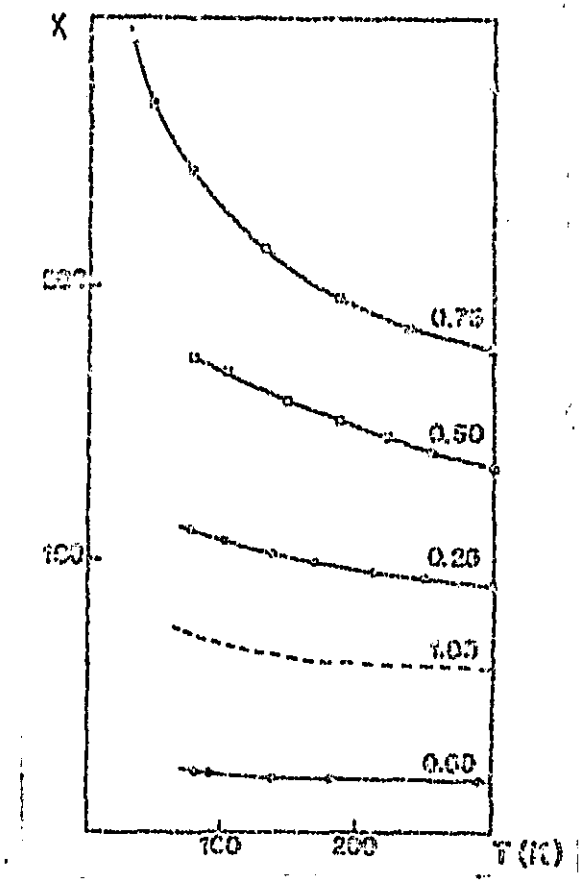

Figure 29. Negative susceptibility of $Ni_{1-x}Co_xAl$ alloys as a function temperature x=0.00; 0.25; 0.50; 0.75; 1.00 (units: 10^{-6} uem/mole).

/35

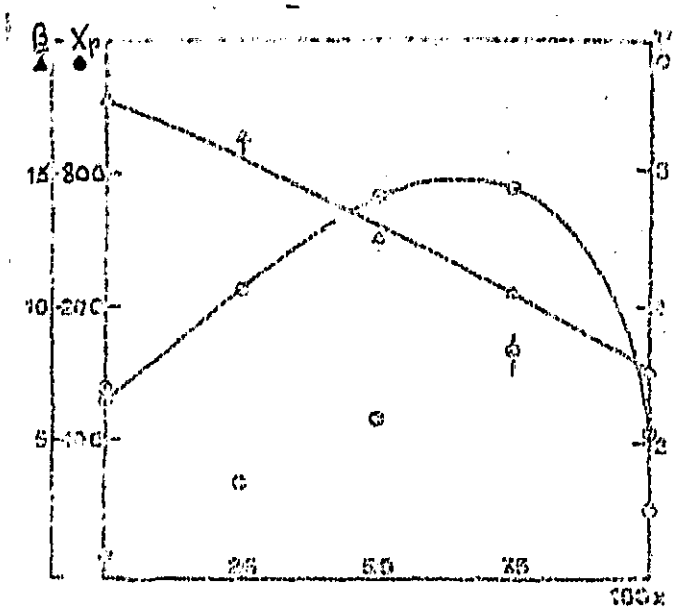

Figure 30. χ_p: estimated value of susceptibility at 0 K (units: 10^{-6} uem/ mole); γ: coefficient of electronic specific heat (units: 10^{-3} J/K^2 mole); β: coefficient of phonons of specific heat at low temperature (units: 10^{-6}/K^4 at.-gram).

The variation of the Pauli susceptibility χ_p, given in figure 30, for this family of alloys, appears to confirm the existence of the peak of density of states which appeared between the Fermi levels for NiAl and CoAl.

On the other hand, we have recapitulated in the table 31 and figure 30 the results of specific heats. As this figure demonstrates, the electronic term γ presents for $x \simeq 0.5$ a maximum which should correspond to the peak of the 3d band. These two results thus appear to confirm the model of rigid bands given earlier. /36

Nevertheless, we can be surprised at the validity of such a model since the displacement of bands between CoAL and NiAl, which is on the order of an electron-volt, is on the same order of magnitude as the size of the peak situated between the Fermi levels of these two substances. This remark leads us to believe that the effects connected to the disordered distribution of the nickel and cobalt atoms must be significant.

We note however that the experimental results are not completely explained by leaving the opposite extreme case (split band limit). The Fermi level must have kept in this case a nearly constant position in relation to each of the densities of partial states and consequently vary nearly linearly when the cobalt level varies.

x	y	γ (mJ/K^2 mole)	β (10^{-6} J/K^4 at.g)	θ_D (K)
0	0,01	2,64	17,8	473
0	0,02	2,82	17,9	477
0,25	0,01	4,30	16,2	493
0,50	0,01	5,72	12,7	535
0,75	0,01	6,63	10,8	564
1	0,01	2,22	7,75	630

Figure 31. γ is given per mole of compound, β per atom-gram of metal that is to say for a mass 2 times lower.

We can thus believe that the real physical situation, although it increases from the intermediate case, and assume, in order to be well understood, a CPA type approach, remains close enough to the model of rigid bands, but with a very rough agreement: for the reasons that we are going to state on the one hand, and on the other hand, because the peak considered corresponds to Van Hove eccentricity, which loses its strict significance when the invariance by translation is abolished from the fact of the atomic disorder. We therefore observe that the maximum of γ and χ_p is much less sharp than the peak of the structure of bands of NiAl.

II.4.B. Study of Compounds $(Co_{1-x}Fe_x)_{1+y}Al_{1-y}$ (with y Negative and Close to Zero for the Same Resons as in A)

The results are a little more complicated to interpret. Figure 32 demonstrates the specific heats of alloys of the family. A physical analysis of the results given in paragraph III.5 for FeAl indicate that it is possible to separate a magnetic term form an electronic term, proportional to the temperature and largely predominant above 8 K.

We do not attempt to make a detailed analysis for the mixed compounds of iron and cobalt, but we can make appear with certainty a considerable increase of the electronic term when we vary x from 0 to 1. This result, as well as the high values of γ for FeAl (table 33), is in agreement with the description of rigid bands given earlier. /38

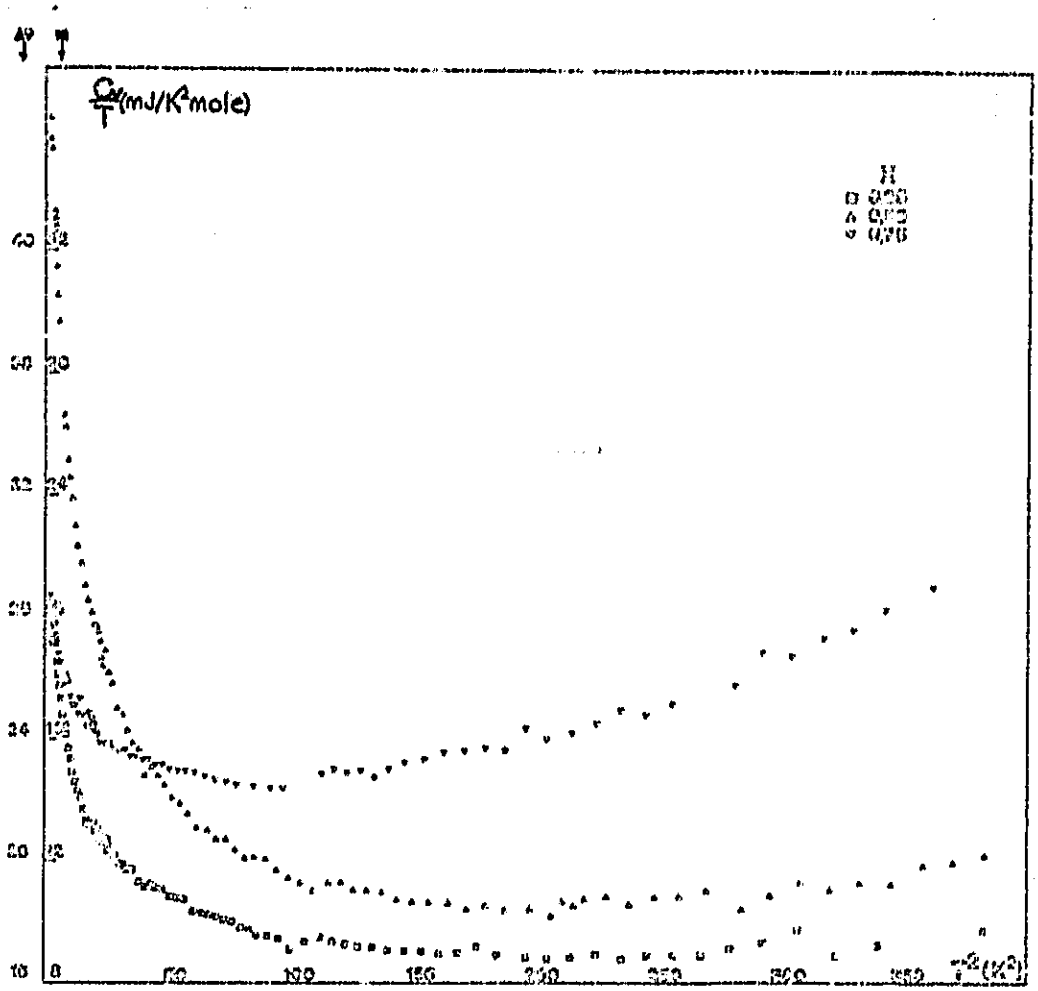

/37

Figure 32. Specific heat of alloys $(Co_{1-x}Fe_x)Al$. A same term of phonons βT^3 (β=7 10^{-5} mJ/K^4 mole) has been deduced from the results.

Moreover, if we analyze the susceptibilities of figure 34 in a fashion to separate a Curie-Weiss term from the Pauli and Van Vleck terms, we are obliged to admit for FeAl a very high coefficient of Stoner reinforcement: we have, indeed, a very strong χ_p susceptibility, analogous to that of platinum or palladium [39], much higher than the already large value of χ_0 deduced from the density of states calculated from the specific heat ($\chi_p \simeq 3.8\ \chi_0$). FeAl is thus a matrix

X	0,25	0,5	0,75	1
γ (mJ/K² .at)	0,5	17	20,0	20,46
χ (10^{-6} uem/mole)	130	235	600-700	907

Figure 33. Electronic specific heat and magnetic susceptibility of alloys $(Co_{1-x}Fe_x)Al$.

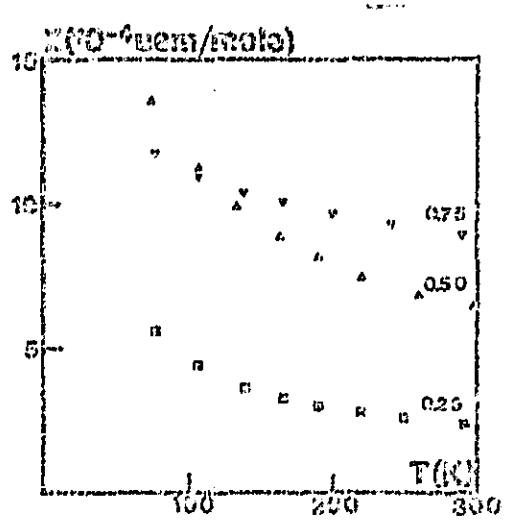

Figure 34. Magnetic susceptibility of alloys $(Co_{1-x}Fe_x)Al$.

with high density of states, almost magnetic. We thus see a gradation appear between the three compounds:

NiAl: does not present any tendency to magnetism. The d character of the states of bands of Fermi level is certainly low.

CoAl: has a behavior typical of transition metals with an already notable Stoner Coefficient.

FeAl: compares to a transition metal, very close to conditions for appearance of magnetism.

These differences occur again later when we will study transition atoms which from the fact of non-stoichiometry, are substituted for aluminum.

Chapter III

/39

First Part: Impurities in the Transition Matrices: Readjustments

Second Part: Effects of Impurities in CoAl and FeAl

In this chapter, we study most particularly the effect of impurities in the defined compounds CoAl and FeAl. In the first part, after a general study on the impurities within a normal and transition matrix (paragraph 1), we will consider the problem of magnetism of isolated impurities (Kondo effect) (paragraph 2). In paragraph 3, we consider the effects of interactions between impurities on the physical properties observed. The problem of impurities within the matrices with reinforced susceptibilities is treated in paragraph 4. These considerations are applied in the second part to the effects of impurities (extra transition atoms) in CoAl and FeAl.

III.1. Problems of Dilute Alloys Within a Transition Matrix

The problem of the electronic structure of transition impurities within a normal matrix has been resolved for approximately twenty years [40], and it can be considered henceforth as well understood from the study of the diffusion of planar waves (we assume that the electronic states of the matrix depend on the approximation of free electrons) through a central potential (coulomb potential centered on the site of impurity corresponding to a charge Z equal to the difference of valence between the matrix and the impurity).

If we call $\chi_l(r)$ the radial part of the component $\Phi_{lm}(r)$ of the diffused wave: $\Phi_{lm}(r)=\chi_l(r)\gamma_{lm}(\theta,\varphi)$ (γ_{lm}: spherical harmonic), we demonstrate that $\chi_l(r)$, for the extensive states of positive energy, that is to say for the non-bound states with the perturbator atom and where the wave function does not decrease exponentially with the distance r, is at great distance of the form:

$$\chi_l(r,k) \frac{C_l}{r}\sin\left(kr-\frac{l\pi}{2}+\delta_l(k)\right)$$

the wave number k being considered to the energy E by the relationship, valid for planar waves, $E=\frac{h^2k^2}{2m}$. The phase displacement δ_l is thus a function of E, which gives information directly on the variation of density of states n(E), for each direction of spin, through the relationship:

$$\Delta n(E) = \frac{1}{\pi}\sum_{l=0}^{\infty}(2l+1)\frac{d\delta_l}{dE}$$

These phase displacements verify moreover the rule of Friedel:

$$\int_{-\infty}^{E_F}\Delta n(E)\,dE = \frac{1}{\pi}\sum_l (2l+1)\delta_l(E_F) = Z$$

which expresses that the screen is perfect (equality between Z and the total charge displaced). This phase charge presents at great distance an aymptotic behavior given by the oscillating law:

$$\Delta\rho(r) \underset{r\to\infty}{\sim} \sum_l (2l+1)\left(\frac{-1}{\Delta\cdot r}\right)^{(l)} \sin\delta_l(E_F)\cdot\cos(2k_F r + \delta_l(E_F))$$

The component of type l=2 gives us information on the charge displaced having a d character, which is of central interest in the case of transition metals. The corresponding phase displacement δ_2 generally passes from the value 0 to the value π over a very narrow energy interval, on the order of 0.5 eV, while 5 additional states of d character, for the direction of spin considered, find themselves concentrated in a peak of density of states corresponding to a virtual bound level: the denomination derives from the fact that this density of states can be considered as originating from the resonance between atomic states d centered on the impurity whose energy is positive, that is to say greater than the energy of the base of the band of the matrix, with the states of this last of close energy. /40

These concepts can be transported without trouble to the case of alloys whose matrix is a ferromagnetic transition metal strong in relation to the states of majority spin. Indeed, we know that the subband d↑ corresponding to these states is full and that the density of states at the Fermi level is zero. The situation is thus analogous to that of a noble metal concerning these states. It is thus possible to extend this concept of virtual band level described earlier to the description of states ↑ of the impurity.For the states of minority spin (↓) on the contrary, the density of states at the Fermi level is nonzero and generally high, while the d-d effects prevail over the effects of s-d mixture. The treatment is then more complex, but we currently have satisfactory techniques at our disposal [41]. We can especially introduce a generalized phase displacement:

$$\delta(E_F) = \mathrm{Arc\,tg}\left(\frac{-\pi V n(E_F)}{1 - VF(E_F)}\right)$$

where $n(E_F)$ is the density of states of the matrix and F(E) its Hilbert transformation.

$$F(E) = \mathcal{P}\int_{-\infty}^{+\infty} \frac{n(\varepsilon)\,d\varepsilon}{E-\varepsilon}$$

the density of additional states remains connected to the phase displacements by the same relationship.

III.2. Problem of Magnetism of Isolated Impurities

In paragraph 1, we describe the critieria which govern, for a given matrix-impurity couplet, the appearance of a localized magnetic moment. Friedel [42] was the first to define these criteria, and we give them here in the Hartree-Fock approximation. In paragraph 2, we will concern ourselves with experimental studies of specific heat, susceptibility, electrical resistivity, and thermoelectrical force, and we will demonstrate that these magnitudes can present anomalies

at a characteristic temperature (Kondo temperature) which are connected to the effect of compensation for the localized moment by the conduction electrons.

III.2.A. Condition for Apearance of the Local Magnetic Moment in the Approximation of Hartree-Fock

With the Hartree-Fock approximation, we clearly take into account the Pauli principle, such that in the atom, two electrons of parallel spins can not occupy a same bound state. On the other hand, two electrons of anti-parallel spins can occupy it; they interact with each other through Coulomb interaction U.

So that a localized magnetic moment exists, it suffices that the non-magnetic state be unstable in relation to the appearance of an infinitesimal local magnetic moment $\langle m_1 \rangle$. We obtain this condition by generalizing the reasoning used in paragraph II.1 for the study of magnetism of transition metals.

The variation of energy ΔE obtained from the non-magnetic state by transferring $\langle m_1 \rangle/2$ electrons from the state of spin $\downarrow$ toward the state of spin $\uparrow$ is the sum of two terms: the increase of energy ΔE_c ($\Delta E_c \alpha 1/n_1(E_F)$) where $n_1(E_F)$ is the density of states at the Fermi level which is due to the resonant states alone) on the one hand, the decrease of energy of electron-electron interaction ΔE_θ ($\Delta E_\theta \alpha(-U)$) on the other hand. The condition of instability of the paramagnetic state in relation to an infinitesimal magnetization is then:

$$U_{n_1}(E_F) > 1$$

A magnetic state appeared even more easily when the interaction energy U and the density of states at the Fermi level $n_1(E_F)$ are greater. We observe that, with such a model, the transition between magnetic state and non-magnetic state is sudden. Nevertheless, when we take into account electron-electron interactions in more detailled fashion, the transition occurs more continuously. /41

III.2.B. s-d Transfer Model: Kondo Effect

Experimental study of the magnetic susceptibility of impurities of transition within a noble or transition metal demonstrate that the susceptibility varies more or less rapidly according to the type of impurity and the realm of temperature considered. The behavior observed is intermediate between Pauli paramagnetism and Curie law ($\chi \alpha (T^{-1})$). In practice, an impurity is considered as magnetic within a specific realm of temperature, when its contribution to the susceptibility varies strongly with temperature. It thus appeared that the distinction between magnetic state and non-magentic state is poorly defined, or rather that it only has direction for a specific realm of temperature.

Experimental studies generally demonstrate that for a given magnetic impurity, there exists a characteristic temperature θ independent of the concentration c-in the regime of isolated impurities-and that, for temperatures very much greater than θ, the initial susceptibility obeys a Curie-Weiss law of the form:

$$\chi(T)=\frac{C\mu^2}{3k_B(T+\theta)} \qquad (T>>\theta)$$

where μ is the magnetic moment of the impurity. For temperatures near θ, $\chi(T)$ varies less rapidly than the preceding law predicts, and becomes practically constant for temperatures very much lower than θ (figure 35). We thus see that the magnetic moment of the impurity is characterized by the transition from a non-magnetic state at low temperature ($T<<\theta$) to a magnetic state at high temperature ($T>>\theta$).

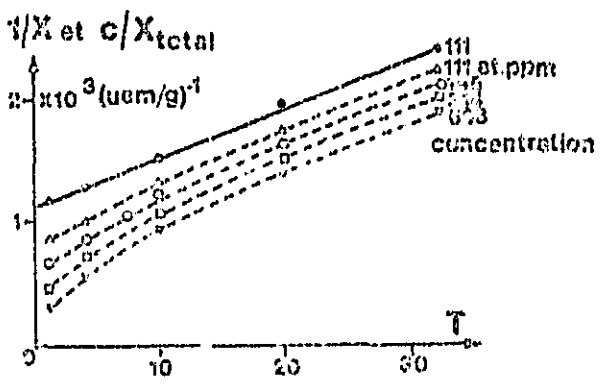

Figure 35. Initial susceptibility of CuFe by iron impurity after [43].

For these alloys, the resistivity presents in general a minimum at a temperature T_m which varies little with c (figure 36), instead of following a law of the form AT^2 over the entire interval of low temperatures.

The thermoelectrical force within these alloys is very strongly negative; it is minimum for a temperature T_k PE which varies little with the concentration (figure 37).

The specific heat also presents a peak in the vicinity of a temperature T_K which varies little with the concentration (figure 38).

In conclusion, we can note that the physical properties of localized moments isolated within normal metals present anomalies at a characteristic temperature, which can vary from 1 to 5 according to the physical magnitude considered. These anomalies can be explained in the "s-d" model of interaction trasfer proposed originally by Kondo [47].

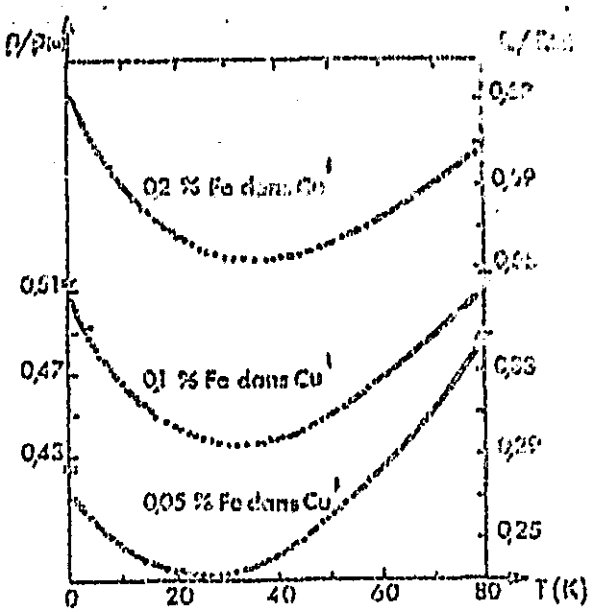

Figure 36. Minimum of resistivity observed in copper with iron impurities after [44]. /42

Key: 1-In Cu.

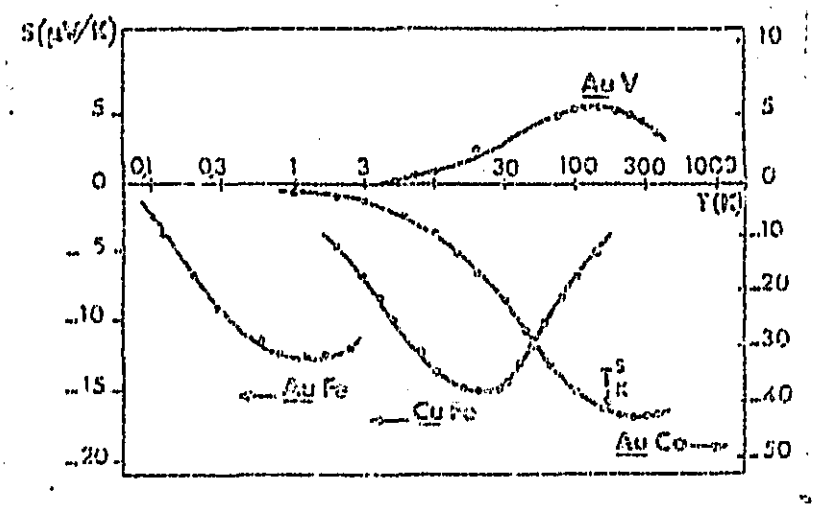

Figure 37. Variation of thermoelectrical force with temperature for certain transition impurities in the copper and gold.

The transfer interaction model allows us to qualitatively explain certain properties of resistivity of magnetization which can not be explained with the Hartree-Fock approximation. This model assumes a transfer interaction between the spin $\vec{S}$ of the impurity, and that of the conduction electrons $\vec{s}$. The Hamiltonian for transfer between a conduction electron and the impurity will be written in the form: /43

$$h_{sd}=-J\vec{S}\cdot\vec{s}\delta(r)$$

where J is the integral of atomic transfer which can be positive or negative, and $\delta(r)$ represents the fact that the interaction only took place when the s electron is on the site of the impurity. The Hamiltonian of interaction between all the conduction electrons and the impurity will be obtained by summing the preceding Hamiltonians relative to each electron of the crystal:

$$\kappa_{sd}=\Sigma h_{sd}(i)=-J\vec{S}\cdot\Sigma\vec{s}_i\delta(r_1)$$

By developing the scalar product $\vec{s}\cdot\vec{S}$, we demonstrate that the interaction energy between an electron and the impurity can be separated into two parts:

$$h_{sd}=h_{\parallel}+h_{\perp}$$

The interaction $h_{\parallel}=-JS_z s_z\delta(r)$ maintains the components of the spins of the impurity and of the conduction electron according to the quantification axis z. It is the effect of $h_{\parallel}$ which we discover with correct treatment of the diffusion of the conduction electrons through the impurity with the Hartree-Fock approximation.

The interaction $h_{\perp}=-J\delta(r)(S_x s_x+S_y s_y)$ describes the mutual reversing of the spins of the conduction electron and the impurity ("spin flip"). It is this transversal part of the interaction, which was not introduced into the Hartree-Fock approximation and which is at the origin of the effects observed.

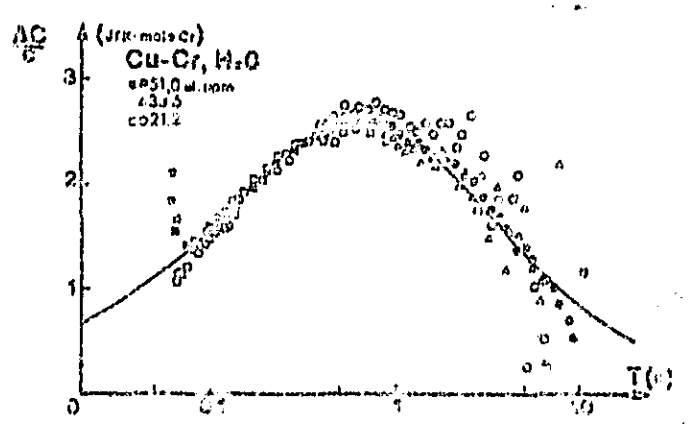

Figure 38. Magnetic contribution to the specific heat of diluted CuCr alloys after [45]. The continuous line represents the Bloomfield-Hamann theory [46].

Indeed, the treatment by perturbation of this transversal part leads to a minimum of resistivity for antiferromagnetic treatment of the s-d interaction ($J<0$) and a susceptibiilty which can be approached by a Curie-Weiss law for $T>>T_K$ (T_K: Kondo temperature, with $\theta\simeq 4.5\ T_K$).

Nevertheless, the transfer model is very difficult to study for low temperatures ($T<<T_K$), that is to say fro temperatures where the development by perturbation does not converge. Nevertheless, Bloomfield and Hamann [46] have calculated the specific heat associated with the Kondo effect in the temperature interval $10^{-4}<T/T_K<10^2$. Their numerical results give a general-purpose curve for the specific heat as a function of T/T_K, with a maximum at $T\simeq T_K/3$ (curve 38). With this curve is associated a variation of entropy which is equal to $R_c Log(2S+1)$ where S is the spin of the impurity. This suggests at low temperature antiferromagnetic coupling between the conduction electron and the moment of impurity (state of compensated spin). We will note also that the Kondo specific heat only slightly depends on the magnetic field; at $T<<T_K$ the theory predicts a variation of:

$$[1-3(\frac{\mu_B H}{k_B T_K})^2] \quad [48]$$

We observe that the behavior which we have described only appeared if the alloys are sufficiently diluted so that the interaction effects between impurities are negligible. It is generally necessary to attain concentrations lower than $3\cdot10^{-4}$. However, when the matrix is a non-magnetic transition metal, the phenomenon extends up to higher concentrations than in the case of normal or noble matrices: the mean free distance covered by electrons being reduced, the noble behavior is preserved for more significant levels of impurities [49] [50].

Finally we note to conclude that this theory allows us to include in a single diagram non-magentic impurities (high Kondo temperature) and magnetic impurities (low Kondo temeprature). Consequently, the following denominations will be suitable:
-Non-magnetic impurities: impurities whose Kondo temperature is situated above the temperature interval where the experiments are carried out. The susceptibility of these impurities is then independent of the temperature.
-Nearly magnetic impurities: impurities whose Kondo temperature is contained in the experimental interval.
-Magnetic impurities: impurities whose Kondo temperature is situated below the experimental interval, whose magnetization will be able to be situated in strong field at low temperature.

III.3. Effects of Interactions Between Impurities /44

If we desire to improve the analysis of susceptibility and specific heat, we are obliged to interest ourselves, even for diluted alloys, in magnetic atoms which are found within a particular environment. The effects connected to the interactions between impurities are not negligible and the physical properties observed depend strongly on the distance between these interactions. This is itself conneted to free distance covered by conduction electrons [51]. We can thus consider two limiting cases:

i) alloys where the mean free distance covered is low, that is to say on the order of the interatomic distance, for which the interac-

tions at short distance are the most significant. These interactions at short separation distance are the most significant, for which the interactions at long distance are dominant.

ii) alloys where the mean free distance covered is significant, for which the interactions at long distance are dominant.

Such a distinction only implies that the interactions are necessarily of different nature; it simply establishes a difference, on the one hand between the case where the perturbation is not extensive and where impurities are close (on the order of one atomic distance) and on the other hand, that where the local perturbation introduced by the impurity is very extensive and where the impurities are on the average distant from each other.

II.3.A. Effects Due to Clusters

For alloys where the interactions at long distance are negligible the physical properties observed are relatively simple to deduce. With these alloys, the isolated impurity often has a characteristic temperature θ_1 which can be very great and can also be considered as non-magnetic. If we introduce other impurities, the probability of existence of serveral nearest neighbor impurities is no longer negligible and the interaction effects begin to manifest themselves. This interaction can modify in very perceptible fashion the electronic structure of the impurities. Thus the atoms of impurity which have one or several other atoms of impurity within their neighbors see their Kondo temerature lower. The Kondo temperature of an impurity is then a function of its surroundings [52], while many non-magnetic diluted alloys due to the fact of a Kondo compensation become magnetic for stronger concentrations. Most often, the phenomena which are the center could be described as interactions between organized moments.

Within the limit of weak concentrations ($c \to 0$) and by assuming that the chemical disorder is perfect, neighboring pairs of impurities (distant from R) and isolated (c.a.d. separated from other impurities by distances $r \gg R$) would appear with a probability proportional to c^2. Isolated triplets would appear also with a probability proportional to c^3 ... These clusters would have qualitatively properties similar to those of isolated impurities, but the interactions between impurities would occur through modification of the parameters interfering with the susceptibility, specific heat, ... Thus an isolated pair of impurities (it is noteworthy that these pairs treated are not necessarily nearest neighbor pairs of atoms) situated at a distance R from each other will have an effective magnetic moment $\mu_2(R) \neq 2\mu_1$ (where μ_1 is the moment of an isolated impurity) and a temperature $\theta_2(R) \neq \theta_1$. These clusters can play a significant role also when the concentration is low (mean distance between "large" impurities). Thus when $\theta_2(R) \ll \theta_1$, the susceptibility of an isolated pair, $\mu_2^2(R)/3k_B(T+\theta_2(R))$ is much greater than that of two isolated impurities (c.a.d. $2\mu_1^2/3k_B(T+\theta_1)$) for $T \sim \theta_2(R)$. The contribution of pairs can even be amplified if the interaction between remote impurities is sufficiently strong so that the condition $\theta_2(R) \ll \theta_1$ is satisfied for a large number of values of R. It is thus necessary to be very cau-

tious in the interpretation of experimental results and to analyze these as a function of the concentration: thus the magnetization M(H,T) of the impurities will be separated by its contributions of isolated impurities M_1, of pairs M_2, etc. ...:

$$M(H,T)=cM_1(H,T)+c^2M_2(H,T)+...$$

These effects have been observed particularly in alloys CuFe, AuFe [53] (figure 39).

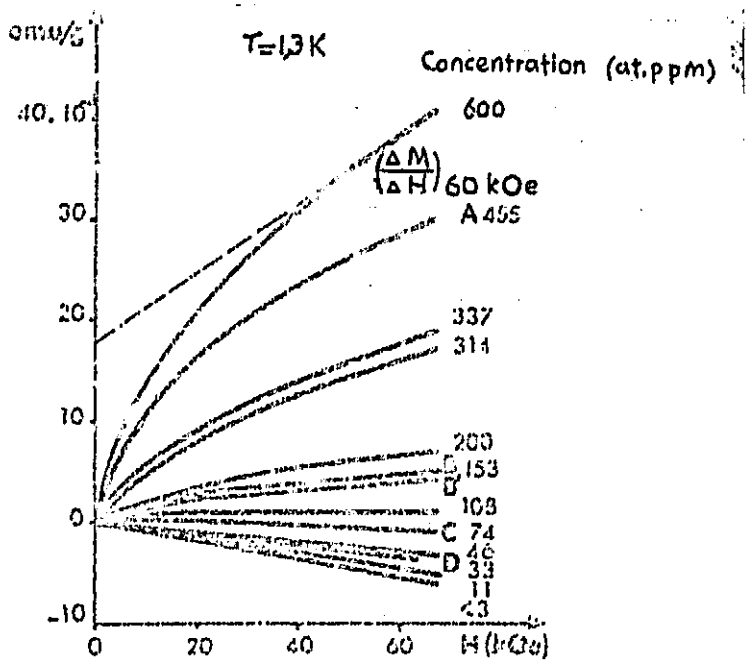

/45

Figure 39. Magnetization of alloys CuFe: for sufficiently strong concentrations, magnetization is not proportional to the field; this then results from contributions of isolated impurities and pairs.

III.3.B. Order at Great Distance Between Isolated Impurities

When the concentration c of impurities increases, a given impurity interacts with a large number of other impurities distributed at random. At the level of impurity considered, this assemblage of interactions can be expressed by a perfectly defined molecular field, but whose intensity and orientation varies with the impurity. This molecular field is thus random and on average zero by reason of the oscillating character of the interaction (R.K.K.Y.), if however we have not perturbed the distribution by an exterior magnetic field. If the temperature of the experiment is largely greater than the Kondo temperature of the alloy so that the existence of moments is ensured, particualr characteristics would appear according to the

concentration regime. We will roughly distinguish three types of regime before the transition toward ferromagnetism:

i) glass regime of spins where the effects of magnetism are negligible.

ii) mictomagnetic regime and superparamagnetic regime where the interaction effects at long distance and those of magnetization are comparable; these last becoming preponderant in the vicinity of the paramagnetic-ferromagnetic transition (We will speak a little of the superparamagnetic regime in relation to PdFe alloys in the following paragraph).

α) Glass Regime of Spins or Magnetic Glass

At sufficiently strong concentrations so that the couplings are dominant but sufficiently weak so that the effects of clusters are negligible, the experiments clearly demonstrate the properties deriving from coupling between impurities; we summarize them below:

1) Curie-Weiss susceptibility for high temperatures:

$$\chi = \frac{C}{3k_B(T+\theta)}$$

with, in the majority of cases, θ negative (anti-ferromagnetism). This negative paramagnetic temperature is also proportional to the concentration.

2) Maximum of susceptibility for a temperature T_M proportional to c which is also more pronounced than the measurements carried out in weak field (figure 40).

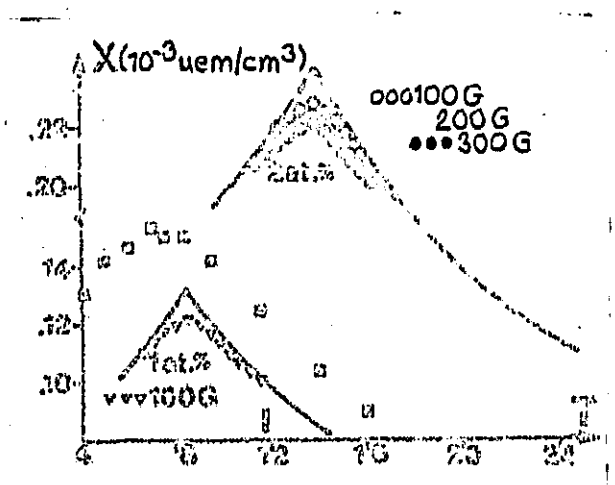

Figure 40. Variation of susceptibility as a function of temperature after [54] for the AuFe system. /46

3) At low temperature, a magnetic susceptibility in zero field $(\chi = \left.\frac{dM}{dH}\right|_{H=0})$ independent of the concentration (figure 41).

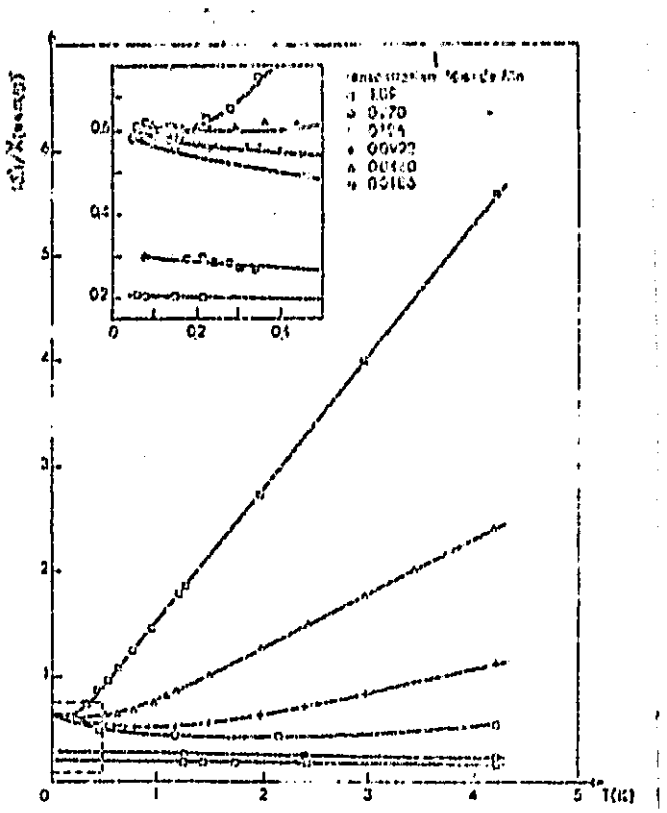

Figure 41. Inverse of initial susceptibility $\chi = \left.\frac{dM}{dH}\right|_{H=0}$ as a function of temperature for alloys CuMn: at low temperature, is independent of the concentration [51].

Key: 1-Concentration % at of Mn.

4) specific heat proportional to T and independent of c when T→0 K and presenting a maximum (figure 42). /47

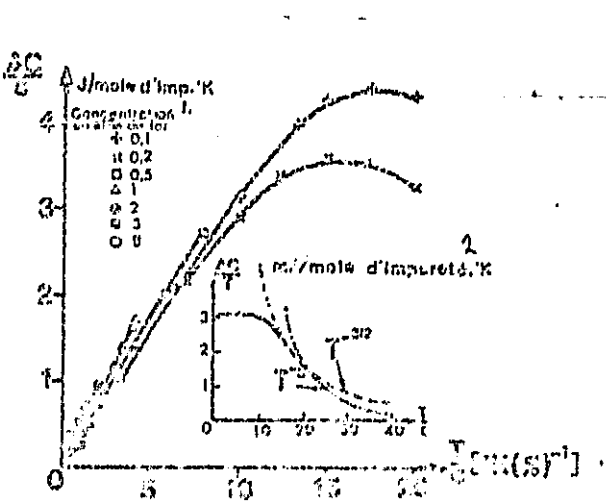

Figure 42. Specific heat of alloys AuFe through iron impurity between 1.2 and 4.2°K [51].

Key: 1-Concentration in al % of iron; 2-mJ/mole of impurity °K.

We owe Blandin [26] and Marshall [55] the idea of an aleatory molecular field H distributed according to a probablity p (H, T, H_e) (H_e being the field applied), in order to explain on the basis of interactions R.K.K.Y. (that is to say oscillating and varying by $1/r^3$) the behavior of the magnetization and the specific heat as a function of the data H_e, T and c at low temperature. Indeed, from these hypotheses, we demonstrate ([26] [51]) the relationship, with T=0 and H_e=0:

$$c'p(\frac{Hc'}{c},c')=cp(H,c)$$

The number of impurities which cross the field H (with $\alpha=\frac{c'}{c}$) for the concentration that is equal to the number of impurities which cross the field H for the concentration c. With these conditions, the physical properties should not change if we also multiply by α the temperature T and the exterior magnetic field H_e, energetic parameters describing the action of the outside world on the system. It is thus that we arrive at the laws of scales governing the specific heat:

$$\frac{C}{c}=f(\frac{He}{c},\frac{T}{c})$$

and the magnetic moment:

$$\frac{M}{c}=g(\frac{He}{c},\frac{T}{c})$$

where f and g are functions common to all the alloys of a same family. Besides, we demonstrate well within the limit of low temperatures, that the magnetic susceptibility tends toward a finite value at T=0 and that the specific heat is proportional to T.

Certain points nevertheless remain obscure, particularly the fact that Blandin and Marshall make use of an Ising model (and not a Heiseinberg model) and the discrepancy which exists between the maxima of susceptibility and specific heat. Other models have been developed recently [56] [57] in order to overcome these difficulties, but without definite success.

Although experimentally it is difficult to obtain distinct isolated impurity-coupled impurity regimes, the properties which we are going to describe have been well verified for two alloys: gold-iron [43] and copper-manganese.

β) Mictomagnetic Regime

When the concentration of impurities increases in an alloy or the interactions at long distance are dominant, the effects connected to clusters become significant; the system is then characterized by the coexistence of interactions at long distance and interactions at short distance; these last becoming more and more significant when c increases.

The experimental characteristics observed are approximately the same as those of glass-magnetic alloys, but the scale law is no longer represented. These experimental results can be interpreted by the existence of a great number of moments which are not oriented at random due to interactions of nearest neighbors whcih are either ferromagnetic or antiferromagnetic, even if the impurities are distributed at random within the alloy. We then observe properties which lead to a mixture of ferromagnetic and antiferromagnetic properties more complex than the "magnetic' glass state.

Given the complexity of the problem, little theoretical work has been carried out on this subject. Kouvel [58] has given a model based on the mutual interactions between ferromagnetic and antiferromagnetic realms in order to interpret the magnetic properties (maximum susceptibility at a temperature T_M: temperature at which the anisotropism of the antiferromagnetic realms disappeared) of CuMn and AgMn alloys.

III.4. Problem of Impurities Within Matrices With Reinforced Susceptibility /48

Up to now, our discussion has been confined to problems of impurities within normal and non-magnetic transition matrices. We have seen that the physical properties of such systems would depend on the type of impurity and realm of temperature considered. If any of the systems which we have to treat are not magnetic, we have seen that one of them (FeAl) was indeed nearly magnetic. It is thus necessary for us to study the particular case of alloys for which the susceptibility of the matrix is reinforced by transfer in a significant fashion. We will interest ourselves, in the rest of this paragraph, with Pd-Ni alloys on the one hand, and Pd-Fe on the other hand, which present great resemblance with the FeAl alloy.

Chouteau, Tournier and Mollard [59] have studied, through measurements of magnetization, the effects of interactions within Pd-Ni alloys and have demonstrated that isolated atoms and pairs are not magnetic. These results demonstrate that the transition toward the magnetic state is made within Pd-Ni alloys in non-homogeneous fashion.

PdFe alloys have been studied by numerous methods [60], including by the Mossbauer effect and by diffusion of neutrons, techniques giving the distribution of magnetization within the space. Thanks to these techniques, we possess a very clear view of the problem: the local moment on an iron atom polarizes the matrix in its vicinity such that the gigantic moments which result from it being coupled in order to produce ferromagnetic order of long distance between on very low concentrations of iron (for 0.5% at. of iron, the Curie temperature has already reached 15°K). There exist several evidences which at very low concentrations of such gigantic moments are coupled in indirect fashion through interactions of R.K.K.Y. type, producing lenses of spins [61]. Trousdale, Longworth and Kitchens [62] have demonstrated that measurements of diffusion of neutrons are in agreement with the measurements of Mossbauer effect on the order of magnitude of

the transfer interaction (α: from 6 to 6.5 Å). The diameter of the sphere of polarization α of an iron atom, given by Mossbauer effect, is determined from the hyperfine field histogram, where the transfer field is Gaussian ($J\alpha\exp(\bar{r}^2/2\sigma^2)$, where $\bar{r}$ is the mean distance between first neighbor iron and an iron atom at the origin). Clark and Meads [63] have made, through Mossbauer effect, measurements of hyperfine field within an applied magnetic field (45 kOe). In order to analyze their results, they have taken a hyperfine field He of the form:

$$He=H_{sat}B_J(y)$$

where H_{sat} is the hyperfine field at 0°K and $B_J(y)$ a Brillouin function with $y=\frac{g\mu_B J}{k_B T}\kappa$.

J is the spin associated with the cluster and κ is the real molecular field in a certain state of polarization. This field can be put in the form:

$$\kappa=H+\lambda\sigma_0\frac{He}{H_{sat}}$$

where H is the exterior field applied and $\lambda\sigma_0$ the molecular field which is connected to the Curie temperature T_c:

$$\lambda\sigma_0=\frac{3k_BT_c}{g\mu_B(J+1)}.$$

These relationships assume a homogeneous approach to the problem.

In fact the temperature T_c deduced by this method are in disagreement with the usual magnetic measurements of Curie temperature. This divergence underlines the non-homogeneous nature of the transition toward the magnetic state of the alloy. Measurements of magnetization as a function of the concentration were thus necessary.

This general problem of non-homogeneous transition toward ferromagnetism assumes detailled analysis of concentration of the physical properties studied, both for diluted and concentrated alloys. It is with this pathway that the study was made for our alloys.

III.5. Study of Magnetism of Non-Stoichiometric Compounds

III.5.A. Study of Alloys $Co_{1+x}AL_{1-x}$

α) Introduction

The studies carried out by various authors on the CoAl compounds have generally been developed in parallel with those of the CoGa system which presents similar properties. Nevertheless, for this last a /49

more detailed study of concentration has been carried out since the paramagnetic realm is more extensive ($0.89 \leq T \leq 1.07$), where T represents the ratio of atomic concentration of cobalt to that of gallium). On the other hand, the joint study of structural defects-gaps and substitutional cobalt which exist simultaneously within the CoGa alloy-and of magnetic properties has allowed us to clearly determine the nature of magnetic impurities which interfere with this compound. In the case of CoAl, such a study has not been able to be entirely accomplished. As we will see, the phenomena appeared within a very restricted realm of concentration above stoichiometry. From this fact, the relative precision on the concentration in defects is much lower.

For the assemblage of both compounds, experiments for transport properties and susceptibility at low field have demonstrated Kondo type behavior for low deviations from stoichiometry. This behavior is characterized by:

-a minimum of resistivity toward approximately 25°K [64];
-negative thermoelectrical force [64];
-negative magnetoresistance [65];
-negative paramagnetic temperature independent of the concentration in substituted cobalt atoms (c) [65].

Beyond these conclusions, a fine analysis of magnetization and magnetic susceptibility has been long planned. The authors have first sought to include in a single madel-diluted alloys and more concentrated alloys giving rise to ferromagnetic behavior-and to analyze uniformly-susceptibility on the one hand, magnetization at saturation within the ferromagnetic realm on the other hand, by using a single type moment whose concentration was assumed to be the concentration of substitutional cobalt. In the case of CoGa, where the concentrations are well known, they result in a strong concentration with a constant value of moment associated with these atoms, on the order of 6 to 7 μ_B, but at lower concentration, this value decreases [66] [67]. Indeed, Sellmyer and Kaplow [68] have demonstrated that the non-linear variation of magnetization at saturation as a function of the concentration in substituted cobalt, could be interpreted by attributing different values to the moments carried by isolated atoms, neighboring atom pairs, ... These authors find a very low value of the moment for isolated Co_B[1] atoms and for apirs, only clusters of three atoms having a noteworthy moment.

The situation has been clarified, at least in the realm of low concentration, by Amamou and Gautier [69] [70]. These authors have studied the CoGa compound by a magnetization technique in strong field, as we have done for the CoAl alloy. Their experimental results can be summarized in the following fashion:

i) an isolated cobalt atom on the gallium sub-lattice (B) is non-magnetic and does not contribute in significant fashion to magnetization;

[1]We will designate the extra transition atoms on the aluminum (or gallium) sub-lattice (B) by T_B. The sub-lattice of transition atoms will be designated by A.

ii) isolated triplets Co_B are magnetic, but the variation of magnetization as a function of the field and temperature of such clusters is close to that of magnetic pairs in the realm studied;

iii) isolated pairs of Co_B are magnetic solely when the corresponding atoms have their four neighboring sites A in common (first neighbors). Pairs of atoms Co_B second neighbors are nearly magnetic;

iv) clusters including 4 or more Co_B are magnetic;

v) finally, certain Co_A atoms (belonging to the cobalt sub-lattice) are nearly magnetic when they are located in the vicinity of isolated magnetic paris and isolated triplets.

With this interpretation, only Co_A atoms occurring in a particular environment and nearly magnetic portions have Kondo behavior, characterized by negative paramagnetic temperatures on the order of 10°K.

These results demonstrate that measurements of magnetization can be connected in quantitative fashion to the concentration of Co_B atoms. The formation of nearly-magnetic and magnetic impurities is interpreted with a model of local surroundings primarily making the cobalt atoms interfere on the gallium sites which leads us to associate different values of moments to each type of impurity. /50

In the case of CoAl, the situation has not been clarified up to here. The best established results are those of Sellmyer et al. [65] which with an analysis with a single type of moment [2] gives a value of 5.9 μ_B in the paramagnetic realm. These results are nevertheless doubtful since they assume that the concentration in gaps is negligible in comparison to the concentration in substituted cobalt and correspond besides to a realm where the deviation from stoichiometry is known with poor relative precision. We will nevertheless retain the measurements of Sellmyer et al., a negative and constant paramagnetic temperature which these authors have found equal to 28°K.

We finally note the results under low field (H<12 kOe) of Parthassarathi and Beck [71] concerning two samples of nominal concentration $Co_{0.5}Al_{0.5}$ and $Co_{0.48}Al_{0.52}$ which have been analyzed according to a law with two moments:

---

[2] In a model with a single type of magnetic moment, the initial susceptibility χ_o is written in the form: $\chi_o=\chi'+\frac{C_{CW}}{T-\theta}$ (1). χ represents the susceptibility of the matrix and non-magnetic impurities; C_{CW} and θ represent respectively the constant and Curie temperature of magnetic impurities. If c and μ are the concentration and magnetic moment of such impurities, the Curie constant is then written in the form: $C_{CW}=\frac{c\mu^2}{3k_B}$ (k_B is the Boltzmann constant). The magnetization M(H,T), when the impurities are saturated ($u H/k_B T>>1$), is written: $M(H,T)=M_o+\chi' H$ (2) with $M_o=c\mu$. The susceptibility χ', concentration c and moment μ of magnetic impurities can thus be deduced from equations (1) and (2).

$$M = \chi_0 H + \mu_1 c_1 B\left[\mu_1, \frac{H+\lambda_1 (M-\chi_0 H)}{T}\right] + \mu_2 c_2 B\left[\mu_2, \frac{H+\lambda_2 (M-\chi_0 H)}{T}\right]$$

with: $$B\left[\mu, \frac{H+\lambda (M-\chi_0 H)}{T}\right] = (\mu+1)\coth\left[(\mu+1)\frac{H+\lambda (M-\chi_0 H)}{T}\right] - \coth\left(\frac{H+\lambda (M-\chi_0 H)}{T}\right)$$

Such a description which introduces a very large number of adjustable parameters presents a low degree of confidence. Moreover, we observe several inconsistencies:
- λ_1 (molecular field for type 1 moments) is much stronger for the most diluted alloy;
- μ_2 (mean moment assoicated with clusters of large dimensions) is greater for the most diluted alloy;
- concentration c_1 is the same for both alloys.

An analogous analysis has been given by these authors for CoGa alloys which do not appear, even when we can judge them, in good agreement with the conclusions of Amamou (according to Parthassarathi and Beck, the isolated Co_B atoms were nearly magnetic).

β) Our Experimental Results

In order to study the CoAl system, we have undertaken measurements of specific heat under field between 1.2 and 20 K and susceptibility in low field between 4 and 300 K. The measurements have been carried out on four alloys, of which two present a concentration in cobalt slightly greater than the stoichiometric concentration (B and C), a third sample, designated A, being of slightly lower concentration; the fourth (D), being a little more concentrated than B and C, already presents at low temperature a large number of ferromagnetic clusters. These measurements have been completed by measurements of magnetization in strong field between 1.5 and 10 K for fields going up to 55 kOe for samples B and C, and through measurements of specific heat under field of 57 kOe between 1.2 and 8 K for sample C.

We will only give here estimated chemical concentrations, the mehtods of analysis not allowing us to attain this magnitude with all the precision required. These estimations are obtained from nominal concentrations at the start, corrected for a very low weight loss which we assume due solely to the evaporation of aluminum during production of the samples. Knowledge of the chemical concentration is insufficient in order to attain the concentration of aluminum sites occupied by cobalt atoms. This magnitude can be obtained from density measurements. Unfortunately, we have not been able to carry them out on a single sample so that it has been necessary to melt into the form of rods, bubbles being included in the specific heat sample. Measurement of the density for sample C gives a bracket for this concentration ($2-5\cdot10^{-3}$). /51

1) Measurements of Magnetization and Susceptibility

We first describe the general analysis of our results:
-at low temperatures $1.5 \leq T \leq 10$ K and at a given temperature T, M(H,T) is linear for fields lower than several hundred Oerstedts, then appeared a gradual approach to saturation (figure 43). The appearance /52
of this last is made even more rapidly when the cobalt concentration is high and when the temperature is low;
-at high temperature, the susceptibility (figures 44-45) ceases to decrease and tends toward a quasi-constant value, undoubtedly associated with the susceptibilty of the matrix and possible non-magnetic substitutional cobalt atoms.

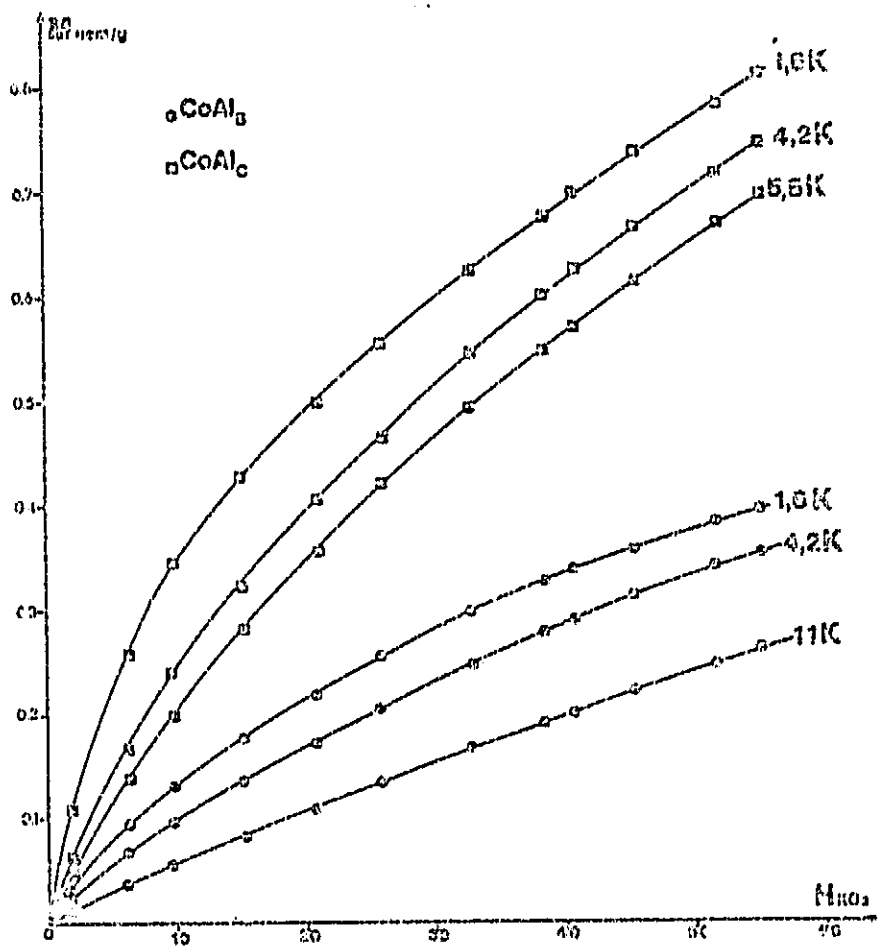

Figure 43. Magnetization as function of the magnetic field at several temperatures for alloys $CoAl_B$ and $CoAl_C$.

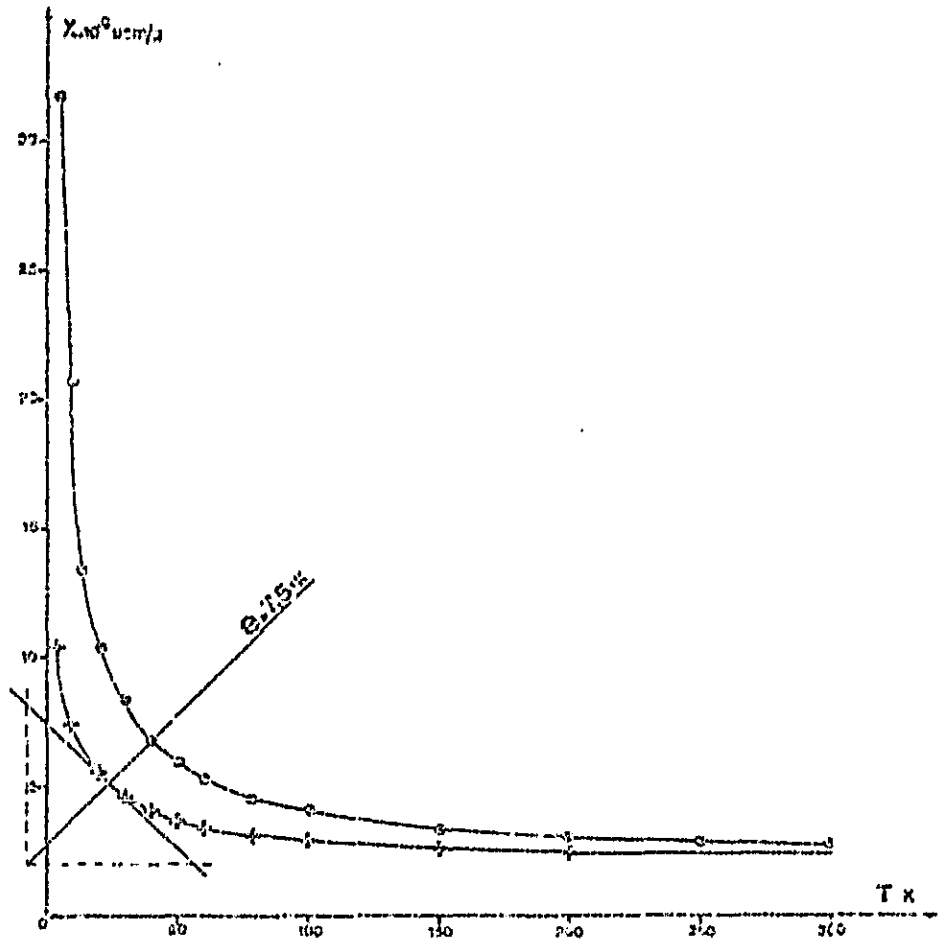

Figure 44. Variation of initial susceptibility χ_0 (•) for the $CoAl_C$ alloy as a function of the temperature. The curve (+) represents the variation as a function of the temperature of the susceptibility of the matrix (χ_m) and the Kondo contribution (χ').

In order to interpret the different terms which contribute to magnetization, we have used the method of Amamou [70] which appears to us more physical than that of Parthassarathi and Beck. However, the imprecision on the concentration of defects (extra cobalt atoms) has not allowed a detailled study of magnetization as a function of the concentration. Nevertheless, we demonstrate that our results are also interpreted in consistent fashion, for temperatures included between 1.5 and 300 K, by defining without ambiguity three terms:
-a term $\chi_m H$ very little dependent on the temperature, which represents the magnetization of aluminum atoms and non-magnetic cobalt atoms;
-a term proportional to the magnetic field $\chi'(t)H$ and varying according to $C'H/(T-\theta')$ for $T>>\theta'$. It is attributed to nearly magnetic cobalt atoms;
-finally, a term varying closely with H/T, $M_{mag}(H,T)$ which results

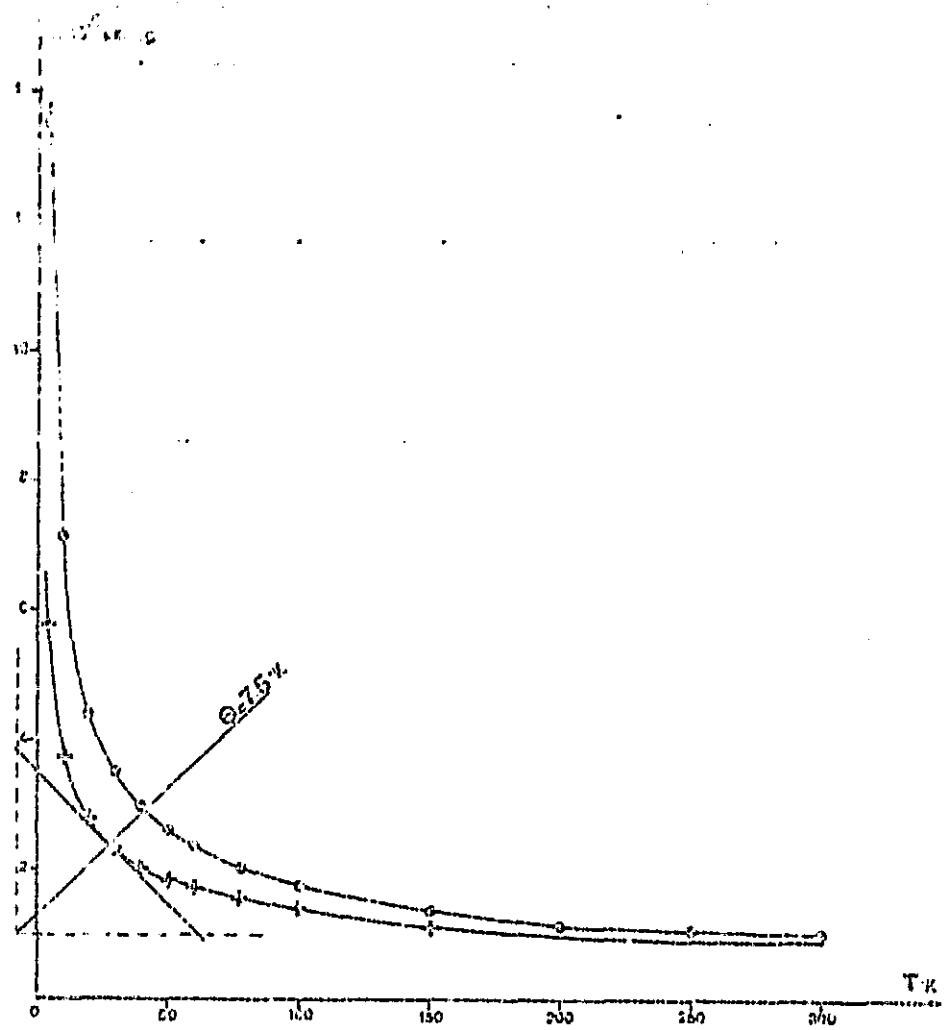

Figure 45. Variation of the initial susceptibility χ_0 (o) for the $CoAl_B$ alloy as a function of the temperature. The curve (+) represents the variation as a function of the temperature of the susceptibility of the matrix (χ_m) and the Kondo temperature (χ').

from the contribution of magnetic cobalt atoms whose characteristic temperatures are notably lower than 4.2 K.

The magnetization measured is then written in the form:

$$M(H,T)=\chi_m H+\chi'(T)H+M_{mag}(H,T)$$

In the vicinity of H=0, we can define an initial susceptibility:

$$\chi_0=\chi_m+\chi'(T)+\frac{C_{mag}}{T-\theta}$$

in which $\chi_m+\chi'(T)$ and $\frac{C_{mag}}{T-\theta}$ are defined by:

/54

$$\bullet\ \chi_m + \chi'(T) = \frac{\partial M(H,T)}{\partial H}\Big|_{H=\infty}$$

$$\bullet\ \frac{C_{mag}}{T-\theta} = \frac{\partial M(H,T)}{\partial H}\Big|_{H=0} - \frac{\partial M(H,T)}{\partial H}\Big|_{H=\infty}$$

term of magnetic clusters $M_{mag}(H,T)$ (figure 46) is not rigorously a function of H/T. This is why it has been analyzed according to the empirical model of Maley and Taylor [72] by introducing a characteristic temperature θ. The temperatures found are negative and very low (<1 K) and decrease when the concentration increases. Also, the value found for S increases when the concentration increases. Besides, and this despite the introduction of the temperature θ, magnetization does not follow exactly a Brillouin law. The term which we treat undoubtedly corresponds to an entire spectrum of different local configurations; magnetization should be written in complete rigor in the form of a sum of Brillouin functions whose weights vary with the concentration, each associated with a particular configuration. The values of moments which we calcualte are thus only mean values. The fact that θ decreases when c increases indicates that the Kondo temperature decreases with the dimensions of the defect with which it is associated;

-the separation between χ_m and $\chi'=\frac{C'}{T-\theta'}$ is made at high temperature after deduction of the term for clusters $\frac{C_{mag}}{T-\theta'}$ (figures 44-45). We find the same value of θ' for all the samples.

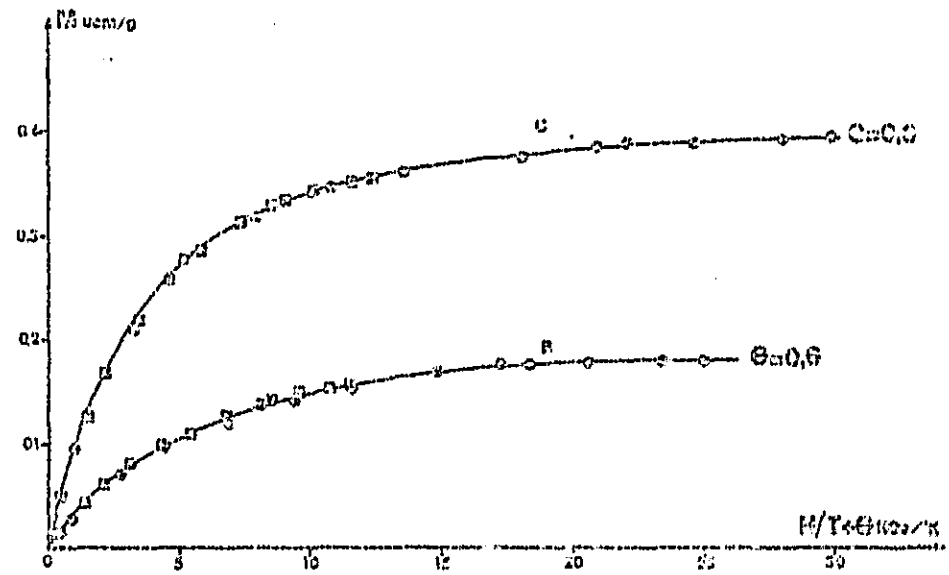

Figure 46. Magnetization as a function of $\frac{H}{T+\theta}$ of $CoAl_B$ and $CoAl_C$ alloys (the symbols • and ■ designate respectively the points originating from measurements with T=1.55 K and T=4.2 K.

The values of the different terms which we are going to determine are given in table 47 for samples B and C. .

TABLE 47. C': IN UEM K/MOLE; χ_{∞}: UEM/MOLE.

	Taux de[1] cobalt	C'	$c_1 p'^2$	c_1*	θ'	χ_m	Concentration[2] d'amas c_2	S amas[3]	θ amas[3]
A	40,5	$1,35\cdot10^{-3}$	$1,08\cdot10^{-2}$ **	-	7,5	$55\cdot10^{-6}$	-	-	
B	50,1	$4,18\cdot10^{-3}$	$3,35\cdot10^{-2}$	-	7,5	$86\cdot10^{-6}$	$3,18\cdot10^{-4}$	4	0,6
C	50,2	$8,37\cdot10^{-3}$	$6,7\cdot10^{-2}$	$2-5\cdot10^{-3}$	7,5	$170\cdot10^{-6}$	$4,34\cdot10^{-4}$	13/2	0,3
D	50,7 to 50,84	$5,01\cdot10^{-3}$ **	-	-	-	-	-	-	-

*The determination of c_1 has been obtained from a density measurement.

**It is possible to determine for this slightly sub-stoichiometric sample an estimation of $c_1 p'^2$ if we assume that the defects of greater order do not interfere.

**The Curie constant C' determined for the sample is relative to two types of defects (indeed for this sample, measurements with strong field and at low temperature have not been made).

Key: 1-Cobalt level;2-Concentration of c_2 clusters;3-Clusters.

At the inside of the bracket of concentration given earlier, the Curie constants found with the hypothesis where the nearly-magnetic term is associated with isolated cobalts, leads to acceptable values of S' (S'=2). On the contrary, defects of higher range would lead to abnormally high values of S'. The values retained for S' allow us to assume that the cobalt atoms substituted for aluminum atoms polarize their eight nearest neighbors in a manner similar to that observed with PdFe [73].

The preceding results call for several supplementary remarks:
a) the analysis which we have adopted for the susceptibility included a term very little dependent on the temperature which must not be neglected for relatively diluted samples. This term contributes approximately 75% to the susceptibility at ambient temperature of samples B and C.

Contrarily to that which we observe most often, this term is not independent of the concentration and appears to increase proportionaly to c_1; it thus appears that the susceptibility of the matrix was modified. This effect undoubtedly expresses a modification of the local susceptibility on the cobalt atoms near cobalt atoms in irregu-

lar sites (Co_B) and could be the result of the fact that the susceptibility of CoAl is already considerably reinforced (c.f. §II.4).

b) The paramagnetic temperature θ_p which we have found (7.5 K) is approximately three to four times lower than that which Sellmyer gives (28 K). Our value nevertheless appeared more consistent with the experiment, the difference with Sellmyer therefore originating aboveall from the introduction of the term χ_m which expresses for the assemblage the susceptibility of the matrix and not from experimental disagreement. We also observe that the law which we have taken for the susceptibility remains verified over a very extensive realm of temperature, while we would attain notable divergences for $T \simeq T_K$. This last point would merit an explanation.

c) The preceding results underline the difference between the CoAl and CoGa alloys: indeed, the isolated impurities formed by substitutional cobalt atoms are nearly-magnetic in the case of CoAl, while this type of impurity does not contribute in significant fashion to magnetization in the case of CoGa. For this last, the Kondo contribution originates from certain neighboring pairs of Co_B atoms or Co_A atoms at the periphery of magnetic clusters.

2) Specific Heat of CoAl Alloys

The results of magnetization of the preceding paragraph have demonstrated to us the existence of magnetic clusters of high moment. Before analyzing the results of specific heat of CoAl, we will thus recall the laws which govern the specific heat associated with an isolated magnetic moment of large quantum number S in the presence of an exterior field or a field of anisotropism.

The system constituted by a magnetic moment in the presence of a magnetic field H is represented by a regularly spaced assemblage of (2S+1) levels of $g\mu_B H$. For temperatures such that the population of the highest levels is negligible ($k_B T << (2S+1) g\mu_B H$), we can extend the 2S+1 levels to infinity without modifying the system. We then find ourselves in a system equivalent to a harmonic oscillator where the specific heat is described by a law of Einstein with a characteristic temperature θ_E equal to $g\mu_B H / k_B$. With the limit where $T >> \theta_E$ we find /56
the law of Dulong and Petit where the specific heat per moment is constant and equal to $3k_B$. As Schroder and Cheng [74] have demonstrated this result is found particularly in the case of magnetic clusters in the presence of a field of anisotropism when S is sufficiently large. We then observe a constant heat equal to nR, where n is the molar concentration of the moments considered, for the temperature interval: $g\mu_B H_A << k_B T << (2S+1) g\mu_B H_A$ where H_A is the field of anisotropsim. Typically the field of anisotropism for iron is approximately 700 G, which leads to an Einstein temperature on the order of 0.07 K. This result demonstrates that it is possible to observe experimentally a constant specific heat for a sufficiently large S, with a portion of the temperature interval explored (1.3-4 K).

Measurements of specific heat outside field have been carried out on the four samples. Conforming to the results obtained with the magnetizations, our analysis has been made according to the law:

$$C=\gamma T+\beta T^3(1+\beta' T^2)+f(T)\ ^1$$

where f(T) is a magnetic anomaly of low temperature which is the object of our study.

We have assumed that the specific heat of phonons did not vary for the four samples (β and β' constant). The results are reported in table 48 and are represented in figures 49-50 which clearly demonstrated for A, B and C:

-considerable increase, apparently proportional to the Curie constant C', that is to say to the concentration of nearly-magnetic defects, from the term of electronic specific heat; /57

-anomaly at low temperature corresponding to the term f(T) and increasing with the concentration.

	γ	β	β'
A	$2,2\cdot10^{-3}$	$15,5\cdot10^{-6}$	$2,7\cdot10^{-4}$
B	$3,4\cdot10^{-3}$	–	–
C	$4,8\cdot10^{-3}$	–	–
D	$4\cdot6\cdot10^{-3}$	–	–

Table 48. γ: J/K^2 mole; β: J/K^4 mole; β': K^{-2}.

The term f(T) presents a maximum for T=4°K; it must correspond to the sum of the terms of specific heat associated with isolated Kondo Co_B atoms and with magnetic clusters.

In order to attempt to separate with this anomaly the part of the Kondo term and that of the clusters, we have carried out on the sample C a measurement of specific heat under field (H=57 kOe).

First we will consider the terms of clusters:
-Under field, $g\mu_B H \simeq 7.5\ k_B$; thus toward 1.5 K the specific heat measured is $C=c_2R(1-0.85)$, where c_2 is the concentration of magnetic defects deduced from measurements of magnetization (curve 51). For 10 K, $C=c_2R$. The term of clusters has thus almost completely disappeared toward 1.5 K under field.

[1] The specific heat of phonons has been developed beyond the first term (βr^3) in order to include the results up to 20 K.

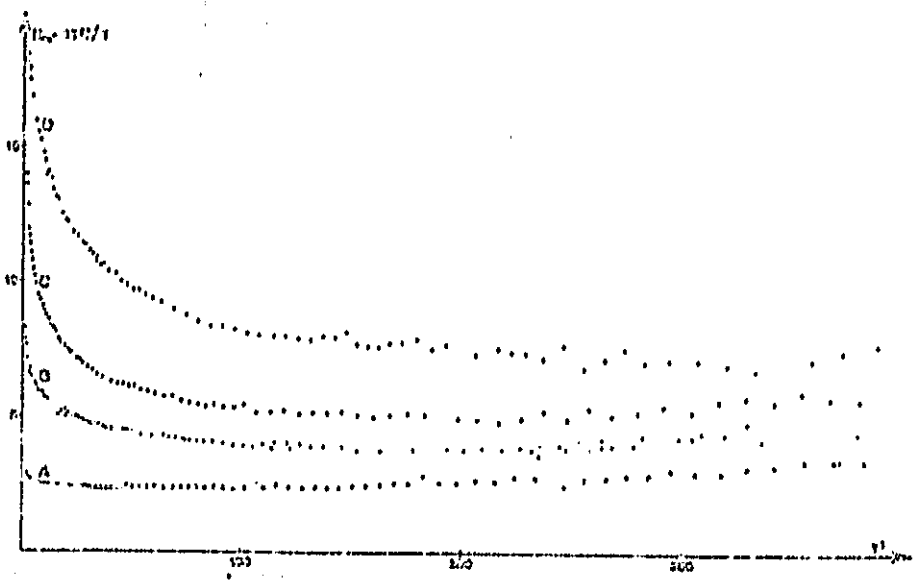

Figure 49. Specific heat of $Co_{1+x}Al_{1-x}$ alloys in mJ/K per mole CoAl, after deduction of an arbitrary term $14 \cdot 10^{-6} T^3$.

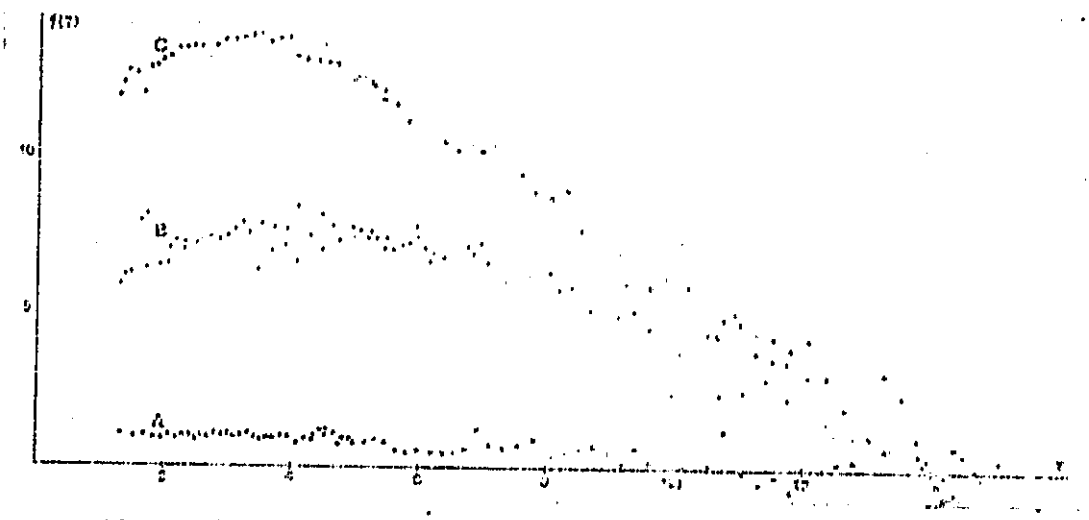

Figure 50. Magnetic specific heat f(T) in mJ/K per mole CoAl.

-Outside field, we are ensured, for probable values of the field of anisotropism H_A, that $g\mu_B H_A << k_B T$ in the entire temperature interval of the experiment. But $(2S+1)g\mu_B H_A >> k_B T$ is not verified for 10 K.

We thus observe:
1) The fact that f(T) was only reduced approximately 40% by admission of the field, proves well the existence of a notable Kondo term (curve 52).

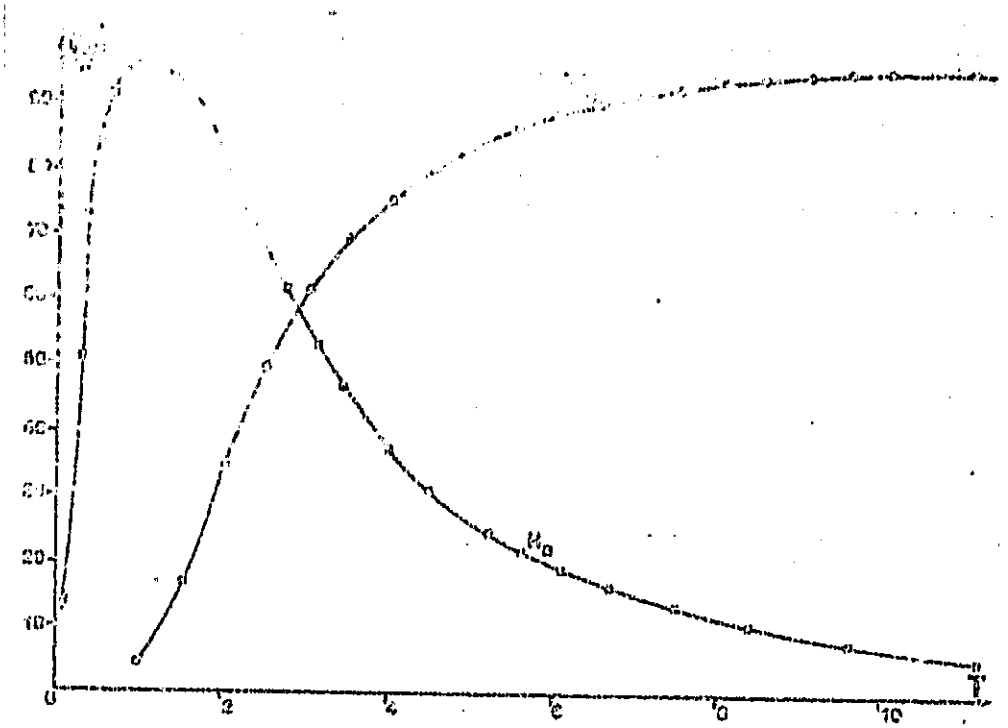

Figure 51. Magnetic specific heat of clusters for: H_a=5 kOe; H_e=57 kOe ($CoAl_C$ alloy).

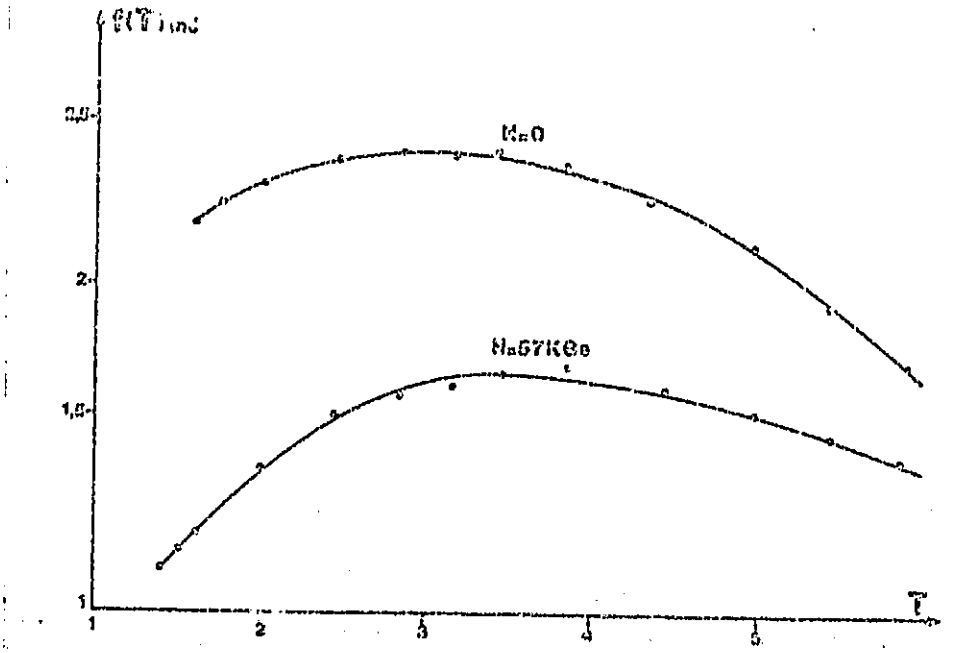

Figure 52. Variation as a function of the temperature for different fields of the magnetic term of the specific heat of the alloy $CoAl_C$.

2) The difference at 1.3 K between the values of the term of clusters under field and outside field is necessarily lower than 0.85 c_2R (this value is attained if the field of anisotropism is sufficiently high so that we have $(2S+1)g\mu_B H_A >> 1.3\ k_B$. Now the limit is less than approximately 50% with the deviation observed between the two manipulations (curve 53). This assumes that the Kondo specific heat varies slightly with the field or that the concentration of magnetic defects has been underestimated.

3) We observe that the maximum of the Kondo specific heat, obtained after deduction of the cluster term from values of f(T) under field, is surprisingly high (4 K). Indeed, the theory of Bloomfield and Hamann (c.f. §III.2.B) leads to a maximum toward $T_K/3$, being toward 0.5 K. In fact, this theory is relative to $S=\frac{1}{2}$ and can only give an approximative value of the maximum of magnetic specific heat. On the other hand, if as has been suggested by the preceding remark, the concentration of the clusters had been underestimated-this could have been due to non-homogeneity of the samples-it would be possible to reduce the temperature of its maximum by increasing the contribution of the clusters. Indeed, in the hypothesis where the Kondo term does not vary under field, we can estimate a concentration of clusters equal to $6.1 \cdot 10^{-4}$, which leads to a slightly lower Kondo temperature (3 K). The value thus deduced is intermediate between that given by the theory of Bloomfield and Hamann and that obtained by Selmyer..

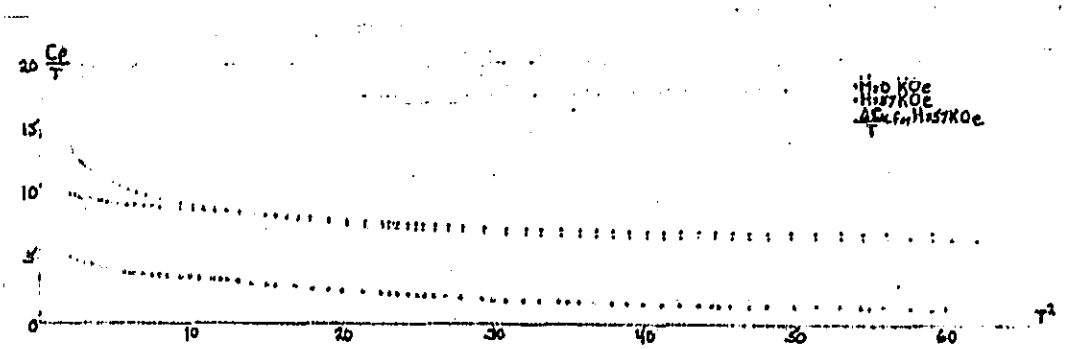

Figure 53. Variations as a function of the field of the specific heat of the $CoAl_C$ alloy. The curve (o) represents the variation under field of the Knodo contribution.

4) The difference toward 10 K is inversely related experimentally and its absolute value is limited in upper value by c_2R (the value c_2R being attained if we assume that at this temperature, the specific heat of clusters is eliminated in the absence of field ($k_BT >> (2S+1) g\mu_B H_A$). /59

From results under field, we can estimate the variation of entropy ΔS associated with the Kondo anomaly of low temperature. The

specific heat of the clusters under field [75] calculated from magnetization data is represented on figure 54 for alloy C. By drawing from curve 53 the terms $\gamma T+\beta T^3(1+\beta' T^3)+C_{cluster}$ (curve 55) (on this same curve we have reported the results corresponding to the hypothesis of a Kondo term not varying under field), we obtain the variation under field of the Kondo specific heat. Estimation of ΔS from this curve leads to $\Delta S=3.4\cdot10^{-3}R$. If we adopt for the concentration of nearly-magnetic defects (c_1) the value from table 47 ($c_1=2.8\cdot10^{-3}$) and for the spin of isolated cobalt atoms $S'=2$, we find $\Delta S=4.5\cdot10^{-3}R$, in good agreement with the result measured. This last point demonstrates that our results are interpreted very well with the hypothesis of Kondo behavior for nearly-magnetic isolated cobalt atoms. On the other hand, the curve obtained, with the hypothesis where the Kondo term does not vary under field, is very little different from that which we are going to describe (figure 55). This remark demonstrates the significance of the contribution of the Kondo term with the anomaly f(T) of low temperature. /60

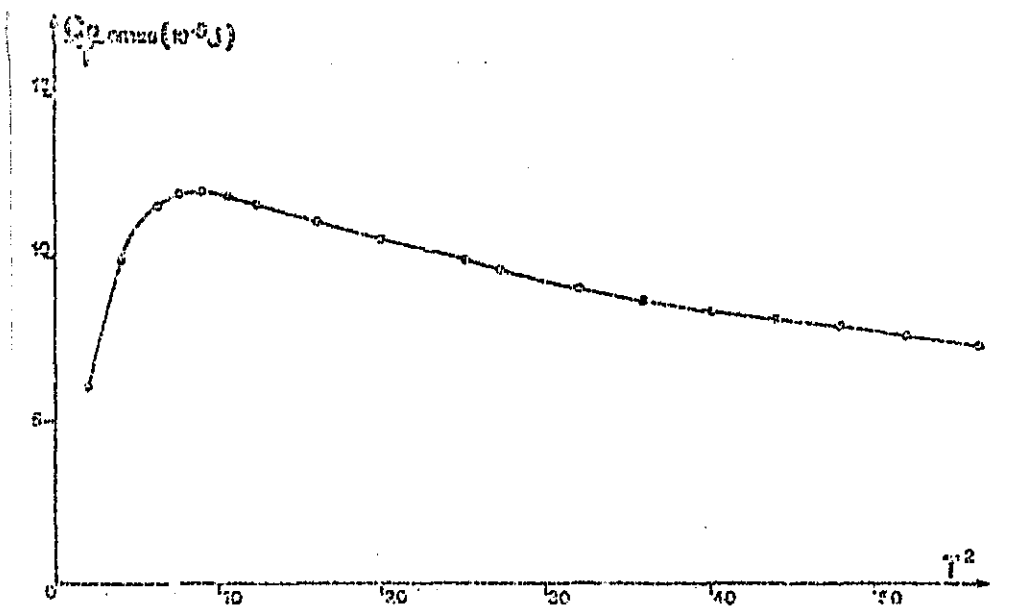

Figure 54. Variation as a function of T^2 of the specific heat of clusters for H=57 kOe.

We note that the increase of γ with the cobalt concentration Co_B is undoubtedly an effect of resonance type which we should be able to clearly demonstrate if the density of additional states associated with cobalt Co_B overlaps the Fermi level, at least for $T>T_K$, that is to say here between 10 and 20 K. The joint existence of this term and the Kondo term has not been clearly demonstrated up to now, either since alloys were too diluted (CuCR [76]), or experiments have not been conducted beyond T_K (CuFe [77]).

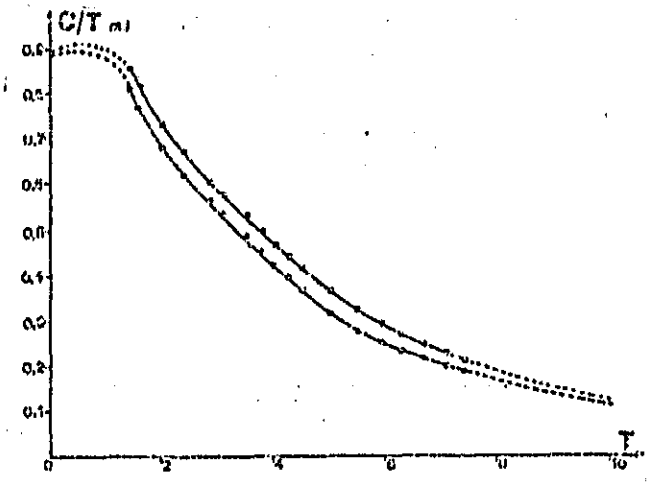

Figure 55. Estimation of ΔS from results under field. The curve ■ is deduced from magnetization results ($c_2=4.34\cdot10^{-4}$). The curve • has been graphed with the hypothesis where the Kondo term does not vary under field ($c_2=6.1\cdot10^{-4}$).

The value found is nevertheless very large ($\simeq$200 mJ/K^2 mole per unit of concentration). However, as we have also clearly demonstrated a reinforcement of the susceptibility of the matrix, it perhaps is necesssary to put together two effects: either that it is a question of an increase of the density of states distributed on the cobalt atoms close to Cl_B, or that we have reinforcement of the specific heat connected to effects of fluctuation of spins.

In conclusion, our study underlines the significance of effects of local surroundings when it is a question of explaining the magnetic properties of CoAl alloys. We have seen how the atoms in irregular crystallographic situation form localized moments within a non-magnetic matrix and how these moments formed interact with conduction electrons. We note that the Kondo effect has been observed up to concentrations on the order of 1%, while in normal matrices the concentration never exceeds 1‰ of impurity. This result is a result of the low distance between d-d interactions; we have to treat here a Kondo problem in a transition matrix where the mean free distance travelled of electrons is much lower than in a mormal matrix. An additional stage was the study, at stronger concentration, of the interaction between isolated Co_B atoms or between clusters in order to form a magnetic state and the investigation of the nature of this state.

III.5.B. Study of $Fe_{1+x}Al_{1-x}$ Alloys

α) Introduction

The study of the properties of transport and magnetic susceptibility in low field made on FeAl alloys in the vicinity of stoichiometry, demonstrate that the observed behaviors are different from those of the CoAl and CoGa alloys and that besides, they can not be interpreted in a Kondo model. The characteristics are the following [78]:

-no minimum of resistivity;
-a positive thermoelectric power;
-a negative magnetoresistance which increases in absolute value with temperature;
-a much more significant magnetic susceptibility than that observed for CoAl alloys (approximately a factor of 10).

At higher concentration ($52 \leq c \leq 67$, were c is the atomic concentration of iron in %) the experiements of Mossbauer effect [79] [80] demonstrate that the system is organized magnetically: the iron atoms in regular position are carriers of a very low moment (low value of hyperfine field) with the difference of iron substituted for aluminum which are carriers of a significant moment. Moreover, the experiments of susceptibility make appear a maximum as a function of the temperature and a paramagnetic temperature which varies linearly with the excess iron concentration [81]. It is a question, either as Huffman asserts, of an antiferromagnetic order, or, more likely, of a system dominated by R.K.K.Y. couplings of glass-magnetic type. As Sellmyer [78] indicates, the assemblage of experimental results is in agreement with this last hypothesis and probably implies antiferromagnetic coupling between the extra iron nearest neighbors (negative transfer integrals). /61

Concerning diluted alloys, however, fine analysis of the susceptibilities and magnetizations has not been made, either since the authors have used a model with a single type of moment, or since they have only carried out measurements in weak field or at high temperature. Sellmyer et al. [78] have analyzed their susceptibilities in the form: $\chi=\chi_0[1+\alpha\tau^2]+\frac{C}{\tau-\theta}$. The term of τ^2 of the band susceptibility is justified by the presence of a high Stoner coefficient in the matrix. The value of θ found appears strongly negative and independent of the concentration in the entire interval where no magnetic organization of the moments appeared, at least in the realm of temperature explored. Since it is not reasonable to believe that it could be a question of a Kondo temperature-this would be in contradiction with the transport properties observed and would make FeAl a more extensive system of magnetism than CoAl-we can believe that the concentration of substituted iron has not in fact varied in the interval of concentration considered, from the fact of atomic disordering and that θ is the expression of R.K.K.Y. coupling between impurities. These results merit verification, since the measurements have been made at 10 kOe and at low temperature, where the effects of saturation are already significant: neglecting them leads to underestimation of the susceptibility at low temperature and consequently displacement of θ toward negative values. We nevertheless take the results of Sellmyer et al., a value of 7.8 μ_B of the effective moment of the iron atoms substituted for aluminum in the paramagnetic state and a Pauli susceptibility of 10^{-3} uem/mole.

Beck and Okamoto [82] have analyzed their magnetization by including two types of moments:

$$M=x\mu_B(\mu,H[T-\theta_1]+(\chi_0+C/[T-\theta_2])H$$

The first term represents the contribution of clusters, whose concentration is $x=334\cdot10^{-6}$ and whose moment is large ($21\ \mu_B$). The second includes a Curie-Weiss term attributed to isolated substitutional iron. The estimated concentration of substituted iron is $6\cdot10^{-3}$ by making the hypothesis of a moment of $2.2\ \mu_B$ for the assemblage of magnetic iron atoms (isolated atoms and atoms belonging to clusters). This analysis leads to values $|\theta_2| < |\theta_1|$, which signifies that it is a question in the spirit of the authors of antiferromagnetic coupling and not Kondo effect. We observe as well the appearance at low concentration of clusters whose moment has a very high value, which according to the hypothesis of Okamoto and Beck would contain approximately half the Fe_B atoms and would be constituted of iron atoms coupled ferromagnetically, is in contradiction with the sign of coupling between nearest neighbor atoms of substituted iron (Fe_B) and more generally with the oscillating character of the interaction, at least to permit the chemical constitution (and not statistical) of clusters of iron atoms.

These same authors have studied between 1.5 and 4.2 K under zero exterior field the specific heat of several FeAl samples. They find a specific heat which follows in very satisfactory fashion a law of the form: $A+\gamma T$, the term of the phonons being negligible in this range of temperature by reason of high specific heats observed. The values of $A=Rx$ give a concentration of clusters of $500\cdot10^{-6}$, a number which compares well enough with that obtained through the results of magnetization ($334\cdot10^{-6}$). From the fact of the constancy of the magnetic specific heat, it is possible to know the order of magnitude of the field of anisotropism by referring to figure 56 which gives for $J=10$ the value of the specific heat as a function of the coefficient:

$$\beta=\frac{g\mu_B H_A}{k_B T}$$

H_A must be such that the values of β for $T=1.5$ and 4.2 frame the maximum of the curve. This gives for $H_A=120000$ Oe (±20%).

β) Our Measurement on the Alloys $Fe_{1+x}Al_{1-x}$

The study of these alloys is more delicate than that of $Co_{1+x}Al_{1-x}$ alloys from the fact of thermodynamic constants: on the one hand, extension of the side rich in aluminum of the β' phase is considerably more reduced than for CoAl; on the other hand, it appears that for FeAl there exists, besides the structural defects already considered (transition gaps, transition atoms substituted for aluminum) aluminum atoms substituted for iron, since in this case the atomic radii of the two constituents are very close. From the fact of these two constraints, it has not been possible to reduce as much as we would have desired the concentration in Fe_B atoms. Two alloys have nevertheless been studied (designated 3 and 6) after various thermal treatments (rough-cast (T), reheated (R), hardened from variable temperatures in a fashion to vary the concentration in Fe_B atoms (0)). This study has been carried out through combined measurements of magnetic susceptibility in weak field and through measurements of speci-

/62

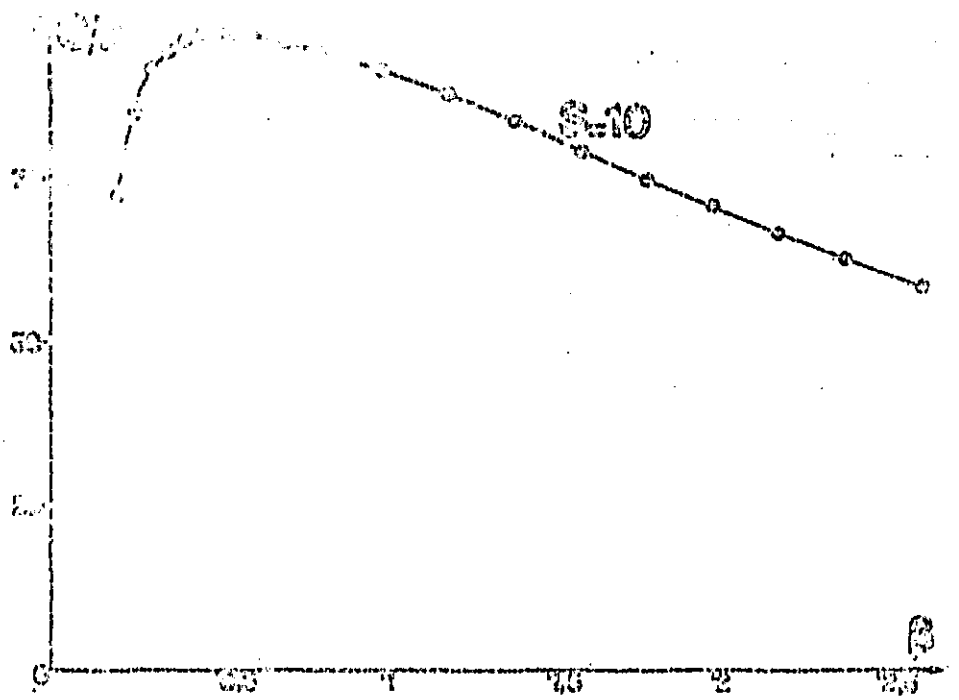

Figure 56. Variation of the specific heat of clusters for S=10 as a function of the coefficient $\beta = \frac{g \mu_B H_A}{k_B T}$

fic heat outside field, for the different samples. Moreover, this study has been completed by measurements of magnetization under strong field (H≈55 kOe) and specific heat under field (H=40-57 kOe) for the sample 3R. It has not been possible for us to measure the density of samples with sufficient precision in order to determine the concentration in Fe_B atoms, which would not appear to be justified. The values found are nevertheless sufficiently low so that it is necessary for us to admit that the magnetic defects described later and corresponding to a value of S on the order of 2 are attributable to isolated Fe_B atoms.

1) Susceptibility and Magnetization /63

General analysis of our results leads to the following observations:
-at low temperature ($1.5 \leq T \leq 10$ K), the curves M(H,T) (figure 57) are linear for fields lower than several hundred Oerstedts, then appeared to gradually approach saturation. This occurs even more rapidly when the temperature is low;
-at high temperature, the susceptibility (figure 58) ceases to decrease and tends toward a quasi-constant value, undoubtedly associated with the susceptibility of the matrix or with possible non-magnetic substitutional iron atoms.

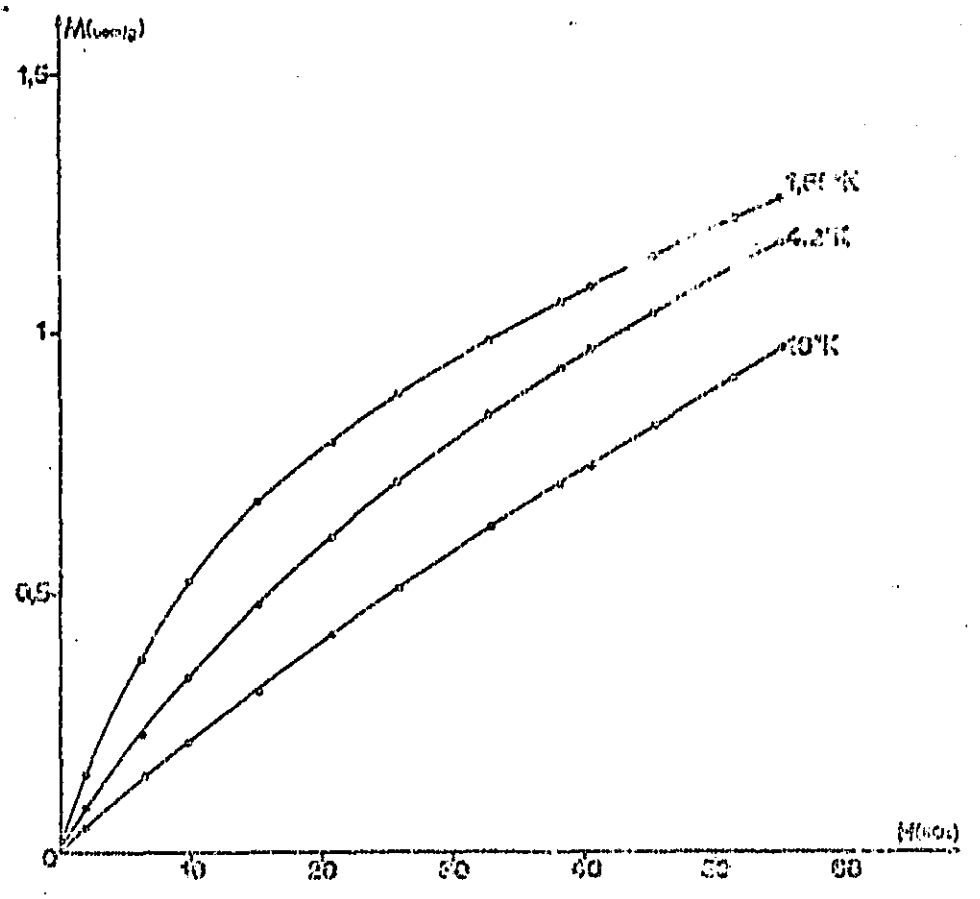

Figure 57. Magnetization of the FeAl 3R alloy as a function of field for several temperatures.

We have interpreted these different results as in paragraph III.5.A. Analysis leads us to distinguish two terms in magnetization and susceptibility:
-a term $\chi_m H$, very little dependent on the temperature, associated with the matrix;
-and a contribution of magnetic iron atoms finding themselves in a particular environment $M_{mag}(H/T)$.

The magnetization thus measured is of the form:

$$M(H,T)=\chi_m(T)H+mag^{(H/T)}$$

The $M_{mag}(H/T)$ component is saturated at 55 kOe and 1.5 K, although at this temperature, it has been possible to determine χ_m and consequently by difference: $M_{mag}(H/T)$. At higher temperatures (4.2 10 K) the magnetic contribution is not saturated, it is thus not possible to carry out the same procedure; we can nevertheless determine $\chi_m(4.2)$ and $\chi_m(10)$ if m_{mag} is still a single function of H/T. Figure 58 demonstrates that this analysis is possible. It leads to values of

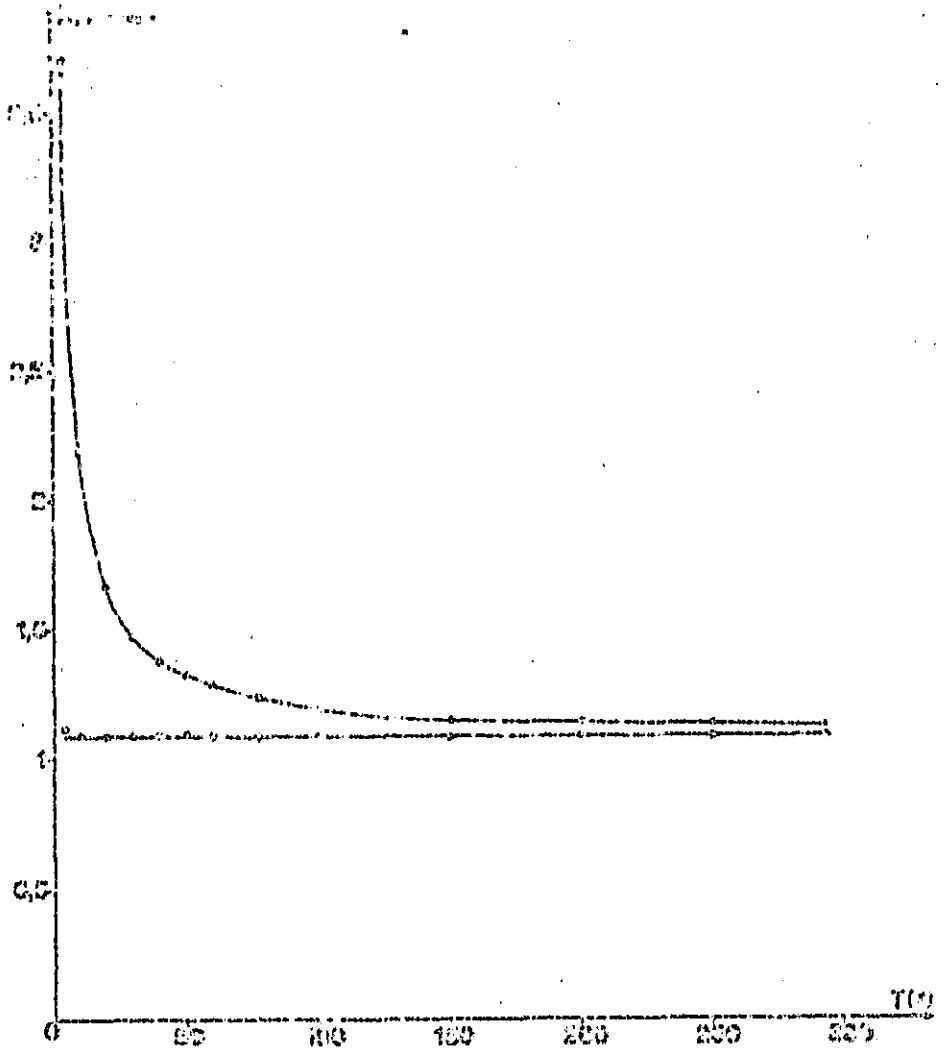

Figure 58. Variation of initial susceptibility (curve •) as a function of temperature for alloy 3R. Curve (o) represents the variation as a function of the susceptibility of the matrix.

χ_m (4.2) and χ_m (10) included between the values, themselves very close, of χ_m(1.55) and of susceptibility at ambient temperature. The very slow decrease of χ_m with temperature results from the high value of susceptibility of the matrix (c.f. §II.4.B). Indeed, the results of figure 59 demonstrate that M_{mag}(H/T) is not a Brillouin law. It is nevertheless possible to obtain good agreement by superimposing two Brillouin laws:

$$M_{mag}(H/T) = x_1 B_{S_1}\left(\frac{g\mu_B H}{k_B T}, S_1\right) + x_2 B_{S_2}\left(\frac{g\mu_0 H}{k_B T}, S_2\right)$$

where $x_2 = 3$ (or 6)x_1^2, that is to say with the hypothesis where x_1

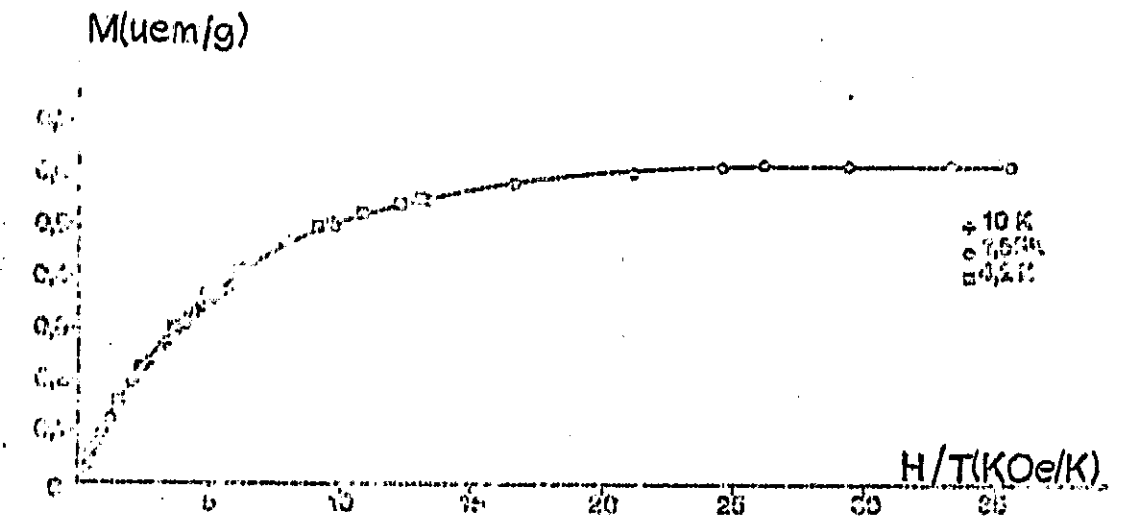

Figure 59. Magnetization as a function of H/T of the 3R alloy after deduction of the contribution of the matrix term.

Corresponds to a concentration of isolated Fe_B atoms and x_2 a concentration of pairs. Indeed, the form of the curve $M_{mag}(H/T)$, prescribed to take for S_1 values included between 2 and 3, this furnishes a bracket of values of x_1 around 10^{-3}; if, as the measurements of density demonstrate, the concentration in Fe_B is less than $5 \cdot 10^{-3}$, any other configuration would have a much lower probability of appearance: $<10^{-4}$ for pairs, $<10^{-6}$ for triplets, ..., numerical analysis led to the following values:

S_1	2	x_1	$2{,}19 \cdot 10^{-3}$	$3x_1^2 = 1{,}39 \cdot 10^{-5}$	x_2	24	first neighbor
			$2{,}09 \cdot 10^{-3}$	$6x_1^2 = 2{,}6 \cdot 10^{-5}$		18	second neighbor
	2,2		$1{,}375 \cdot 10^{-3}$	$2x_1^2 = 1{,}17 \cdot 10^{-5}$	S_2	25	first neighbor
			$1{,}92 \cdot 10^{-3}$	$6x_1^2 = 2{,}2 \cdot 10^{-5}$		18,2	second neighbor

The value of S_1 corresponds to a moment of 5 μ_B much greater than the usual value for metallic iron (2.2 μ_B). There is thus polarization of iron atoms of the matrix. This phenomenon has already been observed in the case of CoAl: we discover the same result, however with a value of S a little smaller and aboveall disappearance of the Kondo phenomenon. The difference is also considerable for pairs which give us this time very large values of S. By reason of the remarks made in the introductory paragraph, we can reasonably believe that these pairs are mostly pairs of second neighbors Fe_B (second and fourth line of the table following the value of S_1 adopted above.

2) Specific Heat of FeAl Alloys

The measurements of specific heat on sample 3 (rough-cast and reheated), sample 6 (rough-cast, reheated and hardened from 1000 and 150°C) are given on figures 60 and 61. The measurements as a function of the field (H=0, 40, 57 kOe) for sample 3R are given on figure 62. By referring to results of magnetization for this sample, it is possible to calculate the specific heat of clusters under field (H= 40, 57 kOe), the field of anisotropism being then weak in relation to the exterior field. Under zero exterior field, this specific heat can be quantified by parameters as a function of the field of anisotropism H_A. The analysis made by taking $S_1=2$ and $x_1=2.08\ 10^{-3}$ (magnetization value) are manifestly unsuitable: after deduction of the magnetic term, the specific heat does not follow the law $\gamma T+\beta T^3$ in the interval 1.4-2 K and it is not possible to find a value of the field of anisotropism H_A which gives reasonalbe agreement with the experimental results at H=0 and the law $C=\gamma T+\beta T^3+C_{cluster}$ L.B. (Law of Livingston and Bean for clusters, c.f. [75].

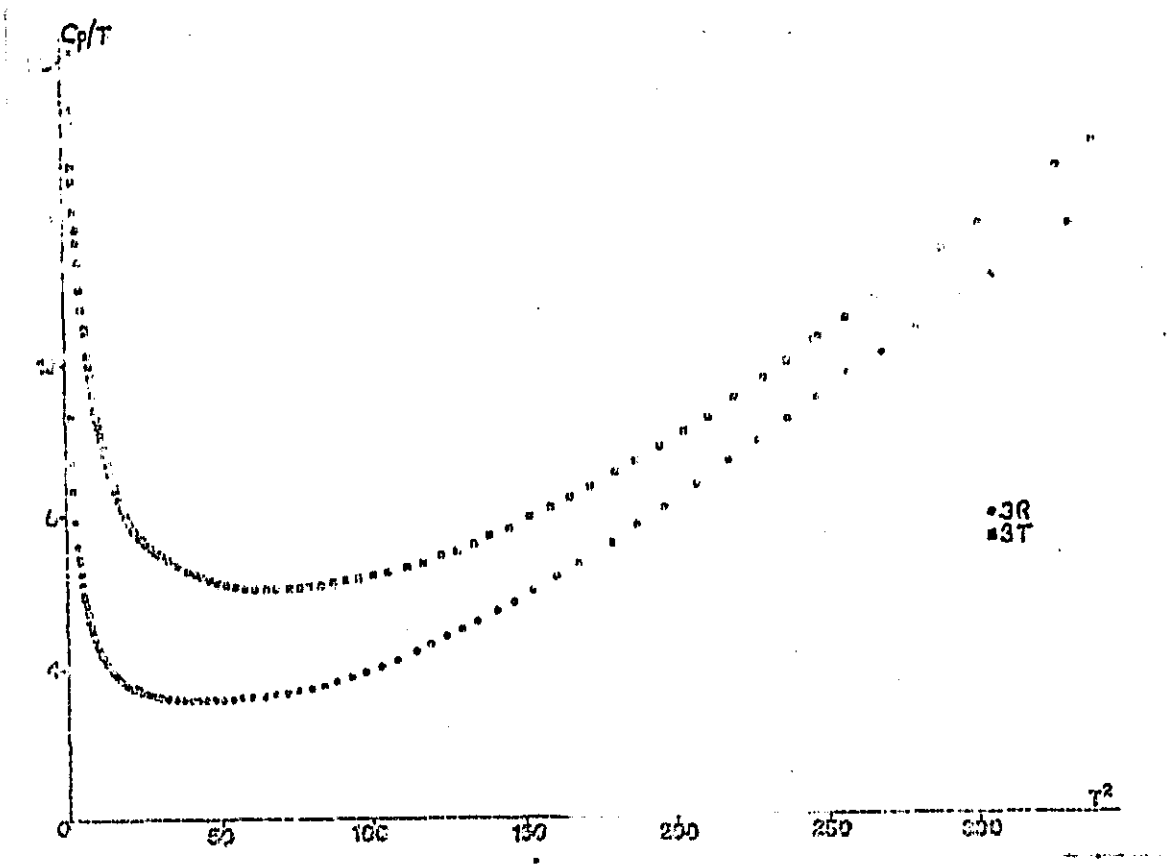

/66

Figure 60. Specific heat of $Fe_{1+x}Al_{1-x}$ alloys (3) in mJ/K mole FeAl, after deduction of an arbitrary term $\delta T+0.007\ T^3$.

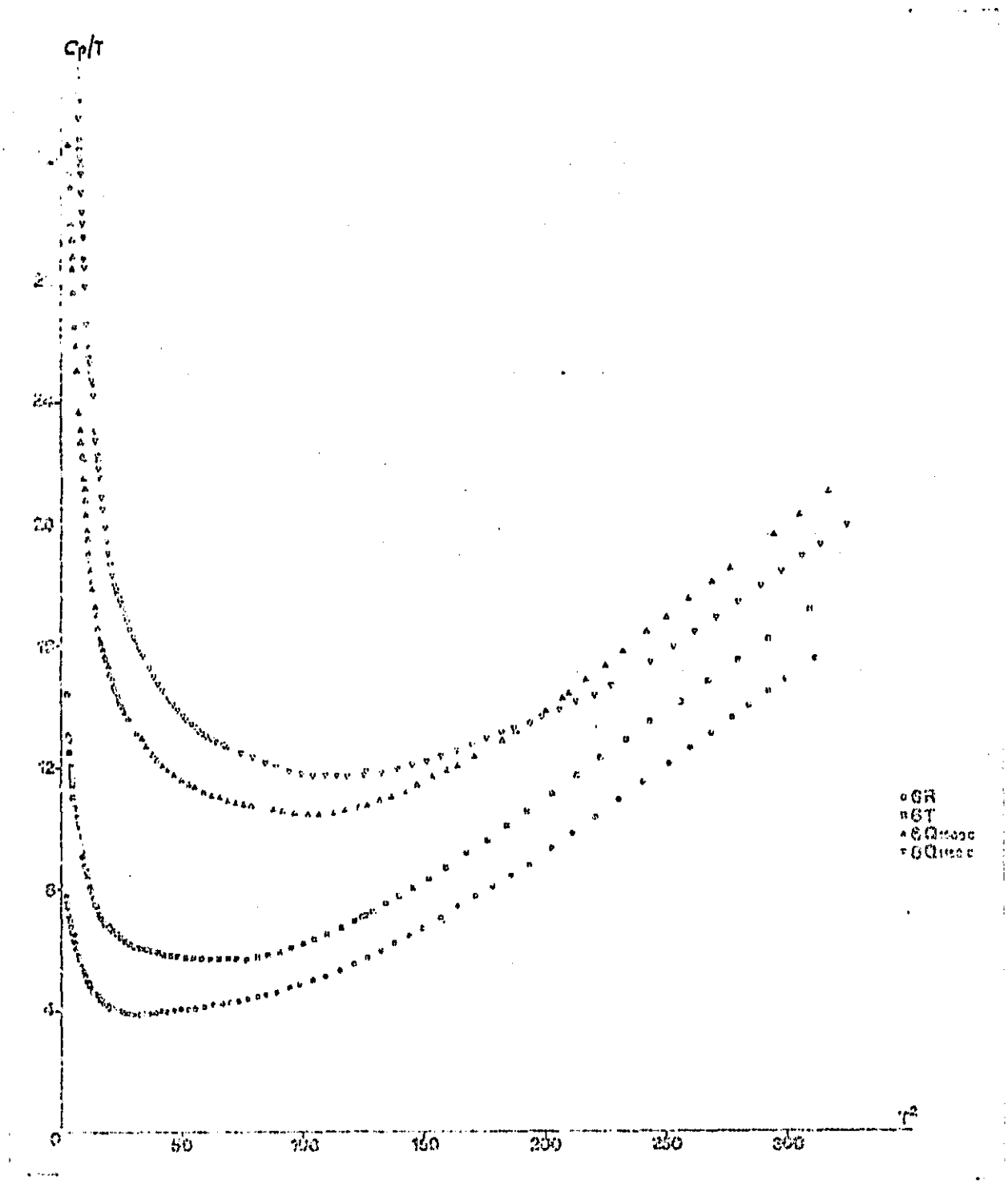

Figure 61. Specific heat of $Fe_{1+x}Al_{1-x}$ alloys (6) in mJ/K per mole FeAl, after deduction of an arbitrary term $\partial T+0.007\ T^3$.

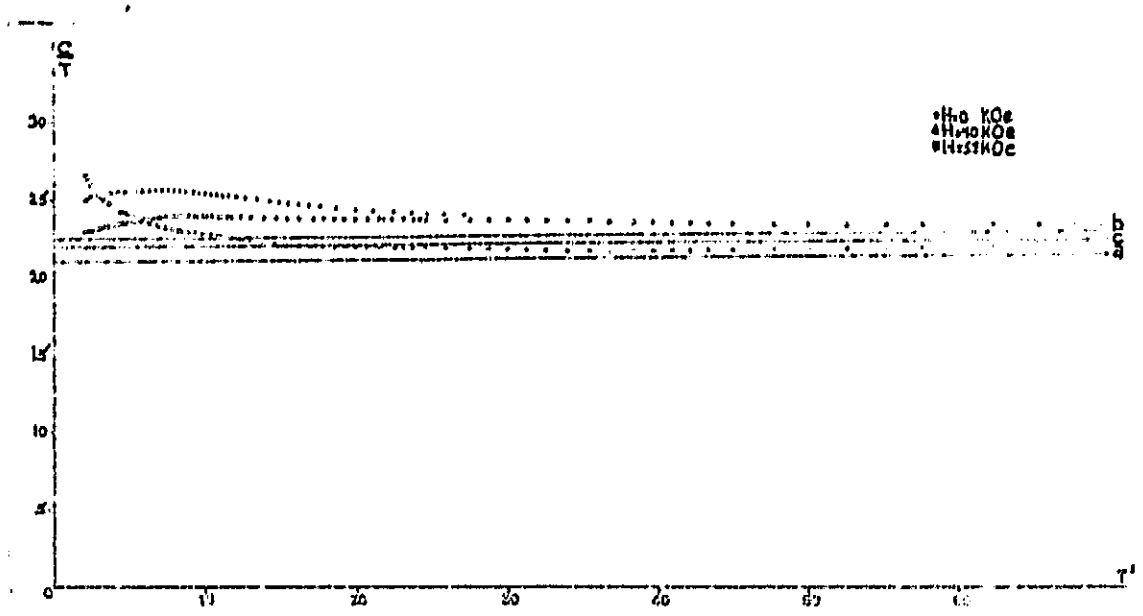

Figure 62. Specific heat of 3R alloy for several values of the field. The curves a, b, c represent respectively the contribution $T+T^3$ for the values 0, 40, 57 kOe of the field.

On the contrary, if we admit that the sample is not perfectly homogeneous and that we permit values of x_1 different from those found earlier, while keeping $S_1=2$, the agreement is excellent: we find for the three values of the field the same value of γ giving a comparable Debye temperature ($\theta_D=690$ K), but slightly greater than that of CoAl ($\theta_D=630$ K). However, measurements of elastic constants would be necessary in order to verify the values thus retained for the FeAl alloy. The values of γ are close, but very slightly different. These variations as a function of the field from the linear term of specific heat indicate perhaps a contribution of glass-magnetic type [83] connected with observations made on more concentrated alloys. An interpretation of these variations based on effects of fluctuation of spins appears on the contrary to be excluded, since it would lead to a decrease of γ according to the law:

$$\gamma = \gamma_0 \left[1 - 3\left(\frac{\mu_B H}{k_B T_{s.f.}}\right)^2\right]$$

($T_{s.f.}$ designates the temperature of fluctuation of spins) which was not observed. The optimum value of the field of anisotropsim is included between 12 and 15 kOe; it is on the same order as that which the analysis of Okamoto and Beck implicated.

The preceding calculations have been carried out on the 3R sample. The corresponding value of the field of anisotropism H_A (15 kOe) can be reused in order to analyze the specific heat outside field of other samples. Reasonable agreement is obtained for the least concentrated samples (6R and 6T) (curve 63); on the contrary, we observe

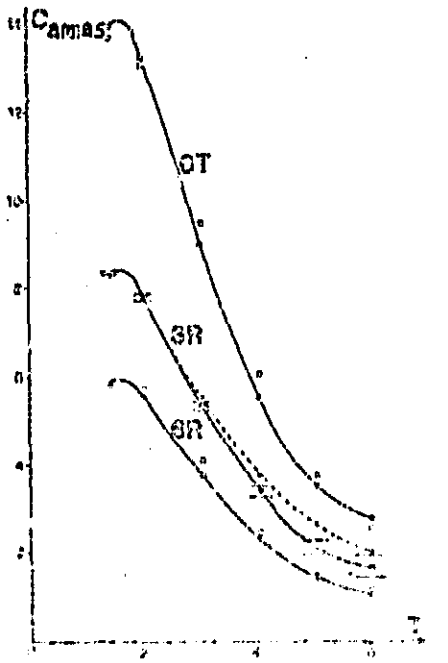

Figure 63. The solid curves represent the variation as a function of the temperature of the specific heat of clusters for the most diluted samples (6R, 3R, 6T). The dotted curve represents the specific heat of clusters calculated after [75] for a field of anisotropism of 15 kOe for sample 3R. The horizontal strokes represent the experimental error bars. The solid curves for 6R and 6T have been graphed with the hypothesis of a constant ratio between the concentrations of clusters in relation to sample 3R (points •). The squares (□) represent the experimental results.

for the other samples (3T, 60 1000 and 60 1150) a decrease of the specific heat as a function of temperature much slower than that calculated earlier for H_A=15 kOe and S=2. This result undoubtedly results from the progressive constitution of clusters of greater dimensions. Finally, we note the good agreement which appeared between the measurements of magnetization at slightly higher fields and the specific heats for sample 6R (table 64).

	γ (mJ/mole)	$\frac{\gamma_x}{\gamma_{3R}}$	χ_0 (uam/mole)	$\frac{\chi_{0x}}{\chi_{03R}}$
3R	20,82	1	$9,07 \cdot 10^{-4}$	1
6R	21,83	1,05	$9,89 \cdot 10^{-4}$	1,09
6T	23,7	1,13	--	--

Figure 64.

/69

Conclusion

The results which we have obtained for FeAl are considerably different from those which we have announced earlier for CoAl: indeed,

the extra isolated atoms are magnetic this time. The value of the moment associated with this type of defect is slightly higher than for CoAl and manifests notable polarization of the atoms of the matrix. This effect is in agreement with the high value of the Stoner coefficient given in paragraph II.4. The assemblage of results of specific heat under field and magnetization are in good agreement with this description; we also note the constitution of most significant moments organized around pairs of atoms of extra iron in position of second neighbors. The difference between CoAl and FeAl would certainly have been more marked at the level of the value of clusters of great dimension if the coupling between extra atoms ahd been of ferromagnetic type (as is the case with CoAl). The assemblage of our results is in very good agreement with the results found earllier on the matrices.

REFERENCES[1]

1. Connolly, J.W.D. and K.H. Johnson, NBS Third Material Research Symposium on Electronic Density of States, Nat. Bur. Standard, 1971, pp. 323. /70

2. Moruzzi, V.L., A.R. Williams and J.F. Janak, Phys. Rev. B. 10, 4856, (1974).

3. Wachtel, E., V. Linse, and V. Gerold, J. Phys. Chem. Solids 34, 1461 (1973).

4. Bashkatov, A.N., L.P. Zelenin, F.A. Sidorenko, and P.V. Gel'D, Fiz. metal. metalloved 31 (4), 719 (1971).

5. Dixon, M., F.E. Hoare, M. Holden, and D.E. Moody, Proc. R. Soc. A 285, 561 (1965).

6. Bower, D.J., E. Claridge, and I.S.T. Tsang, Phys. Status Solidi 29, 617 (1968).

7. Osborne, D.W., H.E. Flotow, and F. Schreiner, The Rev. of Scientific Instruments 36/2, 159 (1967).

8. Neuringer, L.J., A.J. Peflman, L.G. Rubin, and Y. Shapira, The Rev. Sci. Inst. 42,9 (1971).

9. Neuringer, L.J. and Y. Shapira, The Rev. Sci. Inst. 40, 1314 (1969).

10. Philipps, N.E., Sol. St. Sci. 2, 4 (1972).

11. Ducastelle, F., Note Technique,ONERA no. 3/1222 M (not published).

12. Kittel, C., Introduction to solid state physics, Dunrod.

13. Bozorth, Magnetism.

14. Ducastelle, F., Note technique,ONERA no. 3/121 MN (not published).

15. Mott, N.F., Proc. Phys. Soc. 47, 571 (1935).

16. Slater, J.C., Phys. Rev. 49, 537 (1936).

17. Ducastelle, F. and F. Cyrot-Lackmann, J. Phys. Chem. Sol. 32, 285 (1971).

18. Asdente, M. and J. Friedel, Phys. Rev. 124, 384 (1961).

19. Fletcher, G.C., Proc. Phys. Soc. London 65, 192 (1952).

[1]Numerous ideas which underlie this work have been taken from a general reference: "Electronic Properties of Metals and Alloys", Propriétés électroniques des Métaux et alliages, Ecole d'ete de Royan 1971, Masson and Cie, 1973.

20. See for example F. Gautier, "Electronic Properties of Metals and Alloys", Propriétés électroniques des métaux et alliages.

21. Heine, V., Phys. Rev. 153, 673 (1967).

22. Mueller, M., Phys. Rev. 153, 659 (1967).

23. Hodges, L., H. Ehrenreich, and N.D. Lang, Phys. Rev. 152, 505 (1966).

24. Mattheiss, L.F., Phys. Rev. 134/A, 970 (1964).

25. See Lederer, P., Paris Thesis (1967).

26. See Blandin, A., Paris Thesis (1961).

27. Hubbard, J., Proc. Roy. Soc. A 276, 289 (1963).

28. Stoner, E.C., Proc. Roy. Soc. A 165, 372 (1938).

29. Mott, N.F. and H. Jones, "The Theory of the Properties of Metals and Alloys", Dover Publications Inc., 1958.

30. Friedel, J., "Theory of Magnetism in Transition Metals", (W. Marshall, ed.), Academic Press, 1957, p. 283.

31. Soven, N.P., Phys. Rev. 156, 809 (1967).

32. Onodera, Y. and Y. Toyozawa, J. Phys. Soc. Japan 24, 341 (1968).

33. Velicky, B., S. Kirkpatrick, and H. Ehrenreich, Phys. Rev. 175, 747 (1968).

34. Tsukada, M., J. Phys. Soc. Japan 26, 684 (1969).

35. Brouers, F., F. Ducastelle, F. Gautier, and Van Der Rest, J. Phys. F.: Metal Phys. 3, 2120 (1973).

36. Jones.

37. Goodenough, J.B.,"Magnetism and the Chemical Bond", Interscience, New York, 1968.

38. Brodsky, M.B. and J.O. Brittain, J. Applied Phys. 40/9, 3615 (1969).

39. See for example "Amorphous Magnetism", Proceedings of the International Symposium on Amorphous Magnetism (H.O. Hooper and A.M. DeGraaf ed.), Plenum Press, New York, 1973.

40. Friedel, J., Phil. Mag. Sup. 3, 446 (1954).

41. Gautier, F. and P. Lenglart, Phys. Rev. 139/A, 705 (1965).

42. Friedel, J., J. Phys. 23, 501 (1962).

43. Tholence, J.L. and R. Tournier, Phys. Rev. 25, 13 (1970).

44. Frank, J.P., Proc. Roy. Soc. London A 263, 494 (1961).

45. Tripplett, B.B. and N.E. Phillips, Phys. Rev. Let. 27, 1001 (1971).

46. Bloomfield, P.E. and D.R. Hamann, Phys. Rev. 164, 856 (1967).

47. Kondo, J., Prog. Theore. Phys. (Kyoto) 32, 37 (1964).

48. Kurata and Yasuyuki, Prog. Theoret. Phys. (Kyoto) 43, 621 (1970).

49. Maley, M.P. and R.D. Taylor, Phys. Rev. B 1, 4213 (1970).

50. Coles, B.R., J.H. Waszink, and J. Loram, Proc. Int. Conf. Magn. Nottingham, 165 (1964).

51. Souletie, J., Grenoble Thesis, 1968.

52. Tournier, R. and A. Blandin, Phys. Rev. Letters 24, 397 (1970).

53. Tholence, J.L., Grenoble Thesis, 1973.

54. Cannella, V. and J.A. Mydosh, Phys. Rev. B 6, 4220 (1972).

55. Marshall, W., Phys. Rev. 118, 1519 (1960).

56. Adkins, K. and N. Rivier, J. Phys. 36/C4, 237 (1974). /71

57. Edwards, S.F. and P.W. Anderson, J. Phys. F. Metal. Phys.5, 965 (1975).

58. Kouvel, J.S., J. Phys. Chem. Sol. 24, 795 (1963); Kouvel, J.S. and J.B. Comly, Phys. Rev. 24, 598 (1970).

59. Chouteau, G., R. Tournier, and P. Mollard, J. Phys. 5/C4, 185 (1974).

60. See particularly: Crangle, J., Phil. Mag. 335 (1960); Nieuwenhuys, G.J., B.M. Boerstoel, J.J. Zwart, H.D. Dokter, and G.J. VanDenBerg, Phys. 62, 278 (1972), North Holland Publishing; Reference 29.

61. Chouteau, G., R. Fourneaux, and R. Tournier, Proc. L[illegible] XII, Academic Press, Japan, 1971, p. 788.

62. Trousdale, G. Longworth, and T.A. Kitchens, J. of Appl. Physics 38/3, 922 (1967).

63. Clark, P.E. and R.E. Meads, J. Phys. C Metal. Phys. 33, 308 (1970).

64. Aoki, T., J.O. Britain, and Y. Yamaguchi, 12th Int. Conf. Low. Temp. Phys. Kyoto, 1970, p. 763.

65. Sellmyer, D.J., G.R. Caskey, and J. Franz, J. Phys. Chem. Solids 33, 561 (1972).

66. Booth, J.G. and J.D. Marshall, Phys. Let. 32A/3, 149 (1970).

67. Berner, D., G. Geibel, V. Gerold, and E. Wachtele, J. Phys. Chem. Solids 38, 221 (1975); Wachtel, E., V. Linse, and V. Gerold, J. Phys. Chem. Solids 34, 1461 (1973).

68. Sellmyer, D.J. and R. Kaplow, Phys. Let. 36A/5, 349 (1971).

69. Amamou, A. and F. Gautier, J. Phys. F: Metalphys. 4, 563 (1974)

70. Alamou, A., Strasbourg Thesis, 1975.

71. Parthasarathi, A. and P.A. Beck, Solid State Communications 18, 211 (1976).

72. Maley, M.P. and R.D. Taylor, Phys. Rev. B 1, 4213 (1970).

73. Craig, P.P., D.E. Wagle, W.A. Steyert, and R.D. Taylor, Phys. Rev. 9, 12 (1962).

74. Schroder, K. and C.H. Cheng, J. of Applied Physics 31/12, 2154 (1960).

75. Livingston, J.D. and C.P. Bean, J. of Applied Physics 32/10, 1964 (1961).

76. Triplett, B.B. and N.E. Philipps, Proc. LTP 12, Tokyo, 1970.

77. Franck, J.P., F.D. Manchester, and D.L. Martin, Proc. Roy. Soc. 263A, 494 (1962).

78. Caskey, G.R., J.M. Franz, and D.J. Sellmyer, J. Phys. Chem. Solids 34, 1179 (1973).

79. Frankel, R.B., D.J. Sellmyer, and N.A. Blum, Phys. Lett. 33A, 13 (1970).

80. Huffman, G.P., J. of Applied Phys. 42/4, 1606 (1971).

81. Höhl, M., Z. Metalkunde 51, 85 (1960).

82. Okamoto, H. and P.A. Beck, Monatshefte für Chemie 103, 907 (1972).

83. Caudron, R., Strasbourg Thesis, 1975.